



POLITECNICO
MILANO 1863

SCUOLA DI INGEGNERIA INDUSTRIALE
E DELL'INFORMAZIONE

Dual Energy X-ray Absorptiometry: a mini Health Technology Assessment for innovation in technology within Santagostino Medical Centre

TESI DI LAUREA MAGISTRALE IN
BIOMEDICAL ENGINEERING

Author: **Piertobia Laporta**

Student ID: 970482

Advisor: Anna Maria Bianchi, PhD

Co-advisor: Mirco Baroni

Academic Year: 2021-22

Abstract

This thesis project is the main part of my personal contribution given during the internship carried out in the Department of Clinical Engineering at Santagostino medical centre, started in February 2022 and currently ongoing. The thesis work represents a final milestone for my Master of Science degree in Biomedical Engineering (Clinical Engineering track) at Politecnico di Milano.

Centro Medico Santagostino was founded in 2009 with the objective to cover the growing needs of a large catchment area of patients: high quality medical services combined with the possibility to have an easy access to the available services thanks to fair prices. To date CMS counts 32 centres, the highest majority of them located in Milan and its hinterland: in the meanwhile, an increasing interest is pushing toward new openings located in Rome and Bologna. The pillars for value generation in Santagostino are represented by a weighted sum that accounts for innovation, short-time accessibility, transparency based on real data and, last but not least, the care toward the final user of any medical service here in Santagostino: the CMS clinics offer the possibility of performing medical examination over 73 different branches.

For the purpose of this project, it has been carried out a Health Technology Assessment for the evaluation of the clinical effectiveness of an innovative Dual Energy X-ray Absorptometer, considered as a standard typology of examination for the diagnosis of osteoporosis and other endocrinologic diseases. Finally, a Multi Criteria Decision Analysis has been performed in order to attribute a score to the technologies that were under the assessment. With the choice of the new machine, a subsequent on-site installation and technology configuration in "Panfilo Castaldi" centre was taken out. Of course, with the objective to permit an optimization of wasting time and associated costs related to the company, it was scheduled an operating plan before the installation of the new DEXA technology. Moreover, a training of the technical and medical personnel was carried out to ensure a correct workflow for the exam execution, and consequently a production of a valuable report. Physicians, also, were trained with the aim to provide guidelines on the correct use of threshold values for the discrimination among different physio pathological conditions.

Osteoporosis is an emerging medical and socioeconomic threat characterised by a systemic impairment of bone mass, strength, and microarchitecture, which increases the propensity of fragility fractures. It affects more than 75 million people in Europe, Japan and the USA, and causes more than 2.3 million fractures annually in Europe and the USA alone. Osteoporosis does not only cause

II

fractures, it also causes people to become bedridden with secondary complications that may be life threatening in the elderly. Assessment of bone mass, mostly termed as Bone Mineral Density (BMD) is the standard method for the definition of a diagnostic approach for an osteoporotic fracture risk evaluation. An expert panel of the World Health Organization (WHO) recommended thresholds to divide among different categories of patient at risk of osteoporosis and proposed the DXA examination at the hip as the standard technology for the evaluation of an osteoporotic condition.

Specialists in endocrinology, supported by the clinical opinion of the CMS health director, have presented, as a project for the new clinical offering for 2022, the intention to introduce newer technologies in the field of densitometry. The clinical requirement to be satisfied were concerned about the introduction of innovative software for the execution of textural measurements, in order to acquire information not only about bone quantity, but also regarding bone quality microarchitecture and applied loads. For these reasons, software integration was considered as a target tool to be adopted in this innovation. Textural parameters such as BMD and TBS provide useful information about bone quantity and bone quality, respectively, but detailed information about geometry and load definition are still missing. Recently, it has been developed a bone FEM analysis on DXA images named Bone Strain Index (BSI), in order to take into account bone strength features in the prediction of a fracture risk. Bone Strain Index automatically calculates strains and stresses in a bone segment, starting from a specific loading condition, defined specifically for each patient. It is based on finite element algorithms usually used in engineering applications.

A Mini HTA was carried out in order to perform an assessment of the consequences after the introduction of the new technology from different points of view: being a complete private reality that is experiencing a swift growth, it was necessary to undertake a short timeframe and a limited resources analysis. In particular technical (TEC), clinical effectiveness (EFF), organizational (ORG) and economic domains (ECO) were analyzed in order to produce indications for the final decision-making process.

The use of DALYs or QALYs as outcomes within cost-utility analyses to determine the health status presents some limitations: for the aims of this project, generic summary measures on only the clinical improvement with respect to a standard technology may be overly simplistic and reductionist and may not be capturing all of the benefits of this intervention, since other aspects related to TEC and ORG domains should be taken into account. That's why multi-criteria decision analysis (MCDA) method aimed to facilitate the identification of the best possible solution. A pseudo Best-Worst Scaling method was used for our purposes. Therefore, the target solution was in this way identified as the Hologic proposal, with its Horizon Ci technology.

Apart from the technical aspects, the skills that were needed to actualize this project from the managerial, operative and economic point of view were never acquired before in my professional experience. Being the owner of a project means to have the responsibility to guide the entire workflow towards an effective, efficient and valuable management: the description of the clinical and technical features, to be presented then to the clinical audience, has been only one of the responsibilities for a global satisfaction. In fact, a precise time-based schedule of all the activities was necessary in order then to combine all the actors take took part in this process: the preventive communication with internal and external figures of CMS allowed to actualize the project without many bottlenecks, prone to happen in case of an incorrect management of the preoperative activities to be prepared.

After the acceptance of the economic offer, it was requested a schedule for the on-site installation, configuration and training of the Technical personnel days. In this final part, it was actualized all the operative plan previously scheduled. Program included the On-site installation of the new health technology, BMD and TBS calibration, configuration of the machine and testing. Also, a daily agenda was opened during the installation days for allowing technical personnel training. Finally, it was scheduled a webinar with CMS specialists in the field of radiology and endocrinology, with the aim to inform them about the correct use of BMD, TBS and BSI threshold according to official guidelines, in order to interpret in a standardized manner any real case study under examination.

Key-words: Clinical Engineering, Bone Densitometry, X-ray imaging, Dual-Energy X-ray absorptiometry, DEXA, Osteoporosis, Vertebral Fracture, Bone Micro-Architecture, Bone Mineral Density, Trabecular Bone Score, Bone Strain Index, Health Technology Assessment, mini HTA, Multi Criteria Decision Analysis.

Abstract

Questo Progetto tesi rappresenta la parte principale del mio contributo personale dato durante il tirocinio svolto nel Dipartimento di Ingegneria Clinica, presso il Centro Medico Santagostino (CMS), iniziato nel febbraio 2022 e tutt'ora in corso. Questo lavoro di tesi costituisce l'ultima pietra miliare per il mio percorso di Laurea Magistrale in Ingegneria Biomedica (ramo Ingegneria Clinica) al Politecnico di Milano.

Il Centro Medico Santagostino fu fondato nel 2009 con l'obiettivo di coprire le necessità crescenti di un ampio bacino di pazienti: servizi medici di qualità combinati con la possibilità di averne accesso grazie a prezzi calmierati. Ad oggi CMS conta di 32 centri, la maggior parte di essi presenti sul territorio di Milano e hinterland: nel mentre, un interesse crescente continua a spingere verso le nuove aperture di Roma e Bologna. I pilastri per la generazione del valore all'interno del Santagostino sono rappresentati da una somma pesata che tiene in considerazione di innovazione, accessibilità in tempi ridotti, trasparenza basata su dati reali e, ultimo ma non ultimo, la cura verso l'utente finale riguardo ogni prestazione erogata qui al Santagostino: CMS offre la possibilità di eseguire prestazioni mediche per oltre 73 specialità.

Per gli obiettivi di questo progetto, è stato condotto un Health Technology Assessment (HTA) per la valutazione dell'efficacia clinica di una nuova macchina per Assorbimetria a raggi X a doppia energia, considerato come una tipologia di esame standard per la diagnosi di osteoporosi e altre malattie endocrinologiche. In ultimo, è stata condotta una Multi-Criteria Decision Analysis (MCDA) con l'obiettivo di attribuire un punteggio alle tecnologie che erano sotto esame. Con la scelta della nuova macchina, sono state effettuate operazioni di installazione e configurazione presso il centro di "Panfilo Castaldi". Ovviamente, con l'obiettivo di permettere un'ottimizzazione dei tempi e dei costi associati per la compagnia, è stato schedulato un piano operativo prima dell'installazione della nuova tecnologia DEXA. Inoltre, è stata condotta una formazione sul personale tecnico e medico per far sì che la procedura di esecuzione esame venisse effettuata secondo un workflow corretto, al fine di produrre un report di valore per la refertazione medica. Inoltre, sono stati formati anche gli specialisti, con l'obiettivo di fornir loro linee guida per un corretto utilizzo di valori soglia per il discernere tra differenti condizioni fisio-patologiche associate ai diversi soggetti sotto esame.

L'osteoporosi è una minaccia emergente dal punto di vista medico e socioeconomico, caratterizzata da uno squilibrio sistemico di variabili come

massa, forza, e microarchitettura associate al tessuto osseo, con un conseguente incremento del rischio di fratture da fragilità. La malattia colpisce più di 75 milioni di persone in Europa, Giappone e USA, e causa più di 2.3 milioni di fratture in un anno in Europa e Stati Uniti soltanto. L'osteoporosi non causa solo danni da fratture, ma provoca l'allettamento del paziente, con conseguente insorgenza di complicazioni secondarie che potrebbero essere dannose durante la vecchiaia. La valutazione della massa ossea, quindi il calcolo della Bone Mineral Density (BMD), rappresenta un metodo standard per la definizione di un approccio diagnostico ai fini della valutazione del rischio di frattura da osteoporosi.

Un panel di esperti della World Health Organization (WHO) ha reso disponibili i valori soglia per la suddivisione tra diverse categorie di pazienti a rischio di osteoporosi, e ha identificato l'esame DEXA all'anca come la tecnologia standard per la valutazione di una condizione osteoporotica.

Specialisti in endocrinologia, supportati dall'opinione clinica del direttore sanitaria del centro medico, hanno presentato, come progetto per la Nuova Offerta clinica del 2022, l'intenzione di introdurre tecnologie ancora più innovative nel mondo della densitometria ossea. Il requisito clinico da soddisfare era improntato sull'introduzione di software innovativi per il calcolo di parametri di texture dell'immagine, in modo tale da acquisire informazioni non solo sulla quantità di osso, ma sulla qualità della microarchitettura ossea, e sugli sforzi meccanici applicati. Per queste ragioni, l'integrazione software è stata considerata come lo strumento di target da adottare con questa innovazione tecnologica. Parametri di texture come BMD e TBS forniscono informazioni utili riguardo qualità e quantità dell'osso, mancando però di specificazioni riguardo geometria e carichi applicati sull'osso. Recentemente, è stata sviluppata un'analisi ad elementi finiti applicata all'immagine DEXA, il cui software è chiamato Bone Strain Index (BSI), per far sì che vengano prese in considerazione variabili di sforzo nella predizione del rischio di frattura. BSI calcola automaticamente sforzi e deformazioni nel segmento osseo, a partire da una condizione specifica di carico, definita univocamente per ogni paziente. Il software è basato su algoritmi di FEM utilizzati spesso per applicazioni ingegneristiche.

E' stato condotto mini HTA per effettuare una valutazione delle conseguenze dopo l'introduzione della nuova tecnologia, sotto diversi punti di vista: essendo completamente una realtà privata che vive un percorso di rapida crescita, è stato necessario effettuare un'analisi con time window e risorse limitati. In particolare, i domini riguardanti l'aspetto tecnico (TEC), l'efficacia clinica (EFF), l'organizzazione (ORG) e l'analisi economica (ECO) sono stati analizzati al fine di produrre indicazioni per un processo di Decision Making finale.

L'utilizzo di QALY o DALY come outcome nell'analisi costo utilità per determinare lo status di salute presentano alcune limitazioni: per lo scopo del progetto, misure generiche basate esclusivamente sul miglioramento clinico rispetto alla tecnologia standard potrebbero essere troppo semplicistiche e riduttive, non potrebbero catturare tutti gli effetti dell'intervento. Aspetti legati alla tecnologia o all'organizzazione potrebbero non essere presi in considerazione. Ecco perché un MCDA è un metodo che facilita l'identificazione della migliore possibile soluzione. Uno pseudo metodo di Best-Worst scaling è stato usato per gli obiettivi del progetto. Pertanto, la soluzione target è stata identificata nella proposta di Hologic, con la sua tecnologia Horizon Ci.

Oltre agli aspetti tecnici, le competenze necessarie per realizzare questo progetto dal punto di vista gestionale, operativo ed economico non erano mai state acquisite prima nella mia esperienza professionale. Essere l'Owner di un progetto significa avere la responsabilità di guidare l'intero flusso di lavoro verso una gestione efficace, efficiente e di valore: la descrizione delle caratteristiche cliniche e tecniche, da presentare poi al pubblico clinico, è stata solo una delle responsabilità per una soddisfazione globale. È stata infatti necessaria una precisa programmazione temporale di tutte le attività per poter poi combinare tutti gli attori che hanno preso parte a questo processo: la comunicazione preventiva con le figure interne ed esterne al CMS ha permesso di realizzare il progetto senza molti intoppi, che potevano verificarsi in caso di una non corretta gestione delle attività preoperatorie da preparare.

Dopo l'accettazione dell'offerta economica, è stato richiesto un calendario per le giornate di installazione, configurazione e formazione del personale tecnico in loco. In questa parte finale, è stato attualizzato tutto il piano operativo precedentemente programmato. Il programma prevedeva l'installazione in loco della nuova tecnologia sanitaria, la calibrazione del BMD e del TBS, la configurazione della macchina e il collaudo. Inoltre, durante i giorni di installazione è stata aperta un'agenda giornaliera per consentire la formazione del personale tecnico. Infine, è stato programmato un webinar con specialisti CMS nel campo della radiologia e dell'endocrinologia, con l'obiettivo di informarli sul corretto utilizzo delle soglie BMD, TBS e BSI secondo le linee guida ufficiali, al fine di interpretare in modo standardizzato qualsiasi caso clinico reale in esame.

Parole chiave: Ingegneria Clinica, Densitometria Ossea, Radiologia, Dual Energy X-ray absorptiometry, DEXA, Osteoporosi, Frattura Vertebrale, Microarchitettura Ossea, Bone Mineral Density, Trabecular Bone Score, Bone Strain Index, Health Technology Assessment, mini HTA, Multi Criteria Decision Analysis.

Summary

ABSTRACT	I
----------------	---

ABSTRACT	IV
----------------	----

1. INTRODUCTION: TECHNOLOGY INNOVATION AND REPLACEMENT - CLINICAL ENGINEERING WITHIN SANTAGOSTINO MEDICAL CENTRE	1
---	----------

1.1. SANTAGOSTINO MEDICAL CENTRE	1
1.2. ROLE OF THE DEPARTMENT OF CLINICAL ENGINEERING (DCE) FOR SANTAGOSTINO 6	
1.3. INNOVATION AND REPLACEMENT FOR SANTAGOSTINO	9
1.4. DUAL X-RAY ABSORPTIOMETRY INTRODUCTION	10

2. DUAL X-RAY ABSORPTIOMETRY: STATE OF THE ART	13
---	-----------

2.1. X-RAY AND IMAGE GENERATION	14
2.1.1. X-RAY GENERATION	14
2.1.2. INTERACTION WITH MATTER	18
2.1.3. X-RAY DETECTION AND IMAGE GENERATION	22
2.1.3.1 Analog and digital detectors	22
2.1.3.2 Reconstruction from projections with fan beam geometry	26
2.1.3.4 DEXA: Dual energy X-ray and Image generation	29
2.2. CLINICAL USE	32
2.2.1. SCREENING FOR PATIENTS: INCLUSION CRITERIA FOR DXA	32
2.2.1.1 Osteopenia and osteoporosis: epidemiology	33
2.2.1.2 Risk factors	37
2.2.1.3 Skeletal sites	39
2.2.2. BONE MINERAL DENSITY	42
2.2.3. TRABECULAR BONE SCORE	45
2.2.3.1 International Commission Of Clinical Densitometry Iscd: Tbs	51
2.2.4. BONE STRAIN INDEX	51

3. MINI HEALTH TECHNOLOGY ASSESSMENT: MULTIDISCIPLINARY EVALUATION OF CONSEQUENCES AFTER REPLACEMENT	57
---	-----------

3.1. TECHNOLOGY BENCHMARKING	57
3.2. DESCRIPTION AND TECHNICAL CHARACTERISTICS OF THE TECHNOLOGIES (TEC) ...	60
3.2.1. FDX VISIONARY DR, 3D DXA SCAN	61
3.2.2. LUNAR PRODIGY PRO, TBS	64
3.2.3. HORIZON CI, TBS & BSI	68
3.3. CLINICAL EFFECTIVENESS (EFF)	74
3.4. ORGANIZATION (ORG)	76

3.5.	ECONOMIC ANALYSIS (ECO)	79
4.	MULTI CRITERIA DECISION ANALYSIS	82
4.1.	RECEIPT OF OFFERS & ASSESSMENT: HTA (EFF, TEC) REPORT PREPARATION	82
4.2.	MULTI CRITERIA DECISION ANALYSIS: INTERNAL OFFER ACCEPTANCE	84
5.	INSTALLATION, CONFIGURATION & TRAINING	95
5.1.	OPERATING PLAN.....	95
5.1.1.	ON-SITE INSPECTION FOR FACILITY SUITABILITY	95
5.1.2.	COORDINATION BEFORE INSTALLATION	98
5.2.	INSTALLATION	99
5.3.	CONFIGURATION & TESTING	101
5.4.	TRAINING	103
5.5.	GENERAL FEEDBACKS	108
6.	CONCLUSION AND FUTURE DEVELOPMENTS.....	111
6.1.	CONCLUSION.....	111
6.2.	LIMITATIONS.....	112
6.3.	OUTLOOKS.....	113
6.4.	ACKNOWLEDGMENTS.....	114
7.	BIBLIOGRAPHY	116
	LIST OF FIGURES.....	124
	LIST OF GRAPHS.....	128
	LIST OF TABLES	130

1. Introduction: Technology Innovation and Replacement - Clinical Engineering within Santagostino medical centre

1.1. Santagostino Medical Centre

Santagostino Medical Centre, the Company in which the internship experience was carried forward, was founded in 2009 with the objective to cover the growing needs of a large catchment area of patients: high quality medical services combined with the possibility to have an easy access to the available services thanks to fair prices, offering also the coverage of areas uncovered by the National Health System (NHS) – dentistry, psychotherapy, speech therapy and other categories – where the access is mostly private, and where costs couldn't be easily sustainable due to higher average prices[1].

In Santagostino Medical Centre, from now on called CMS for sake of simplicity, the pillars for the supply of medical services are represented by:

- Care of the final users, with the objective to guarantee not only high-quality services at affordable prices, but mostly to respond to the relational necessities of the patients, encouraging so the construction of a fair doctor-patient relationship based on listening and trust.
- Transparency, at all levels – every strategic and operative choice is based on data-based objectivity – as expressed in [1, p. 7].
- Accessibility, in terms of costs, service offered and location: the aim here is polyvalent, meaning that the patient has to view the advantages, covered not only by fair prices, but also the possibility to have access to a large variety of services offered, either than what he's looking for. The advantage to reach the clinic in a short time will also be accounted, being the CMS a developing network of health clinics.
- Innovation, trying always to generate value for the society and for the enterprise.

CMS differs from other realities in the surrounding area since it's placed in the market as a complete private entity, competing with other enterprises that presents the same business model: advantages and disadvantages of this choice are listed below.

Firstly, a complete private reality allows to take decisions without any constraint related to tenders, that are a common practice inside a public or in an accredited private company. The direct consequence of this aspect is related to a reduction in the operating time related to any multi criteria decision analysis for the purchase, the installation or the activation of a new medical service.

As cited in [2] private sector companies are often assumed more progressive in exploiting digital media: CMS's ET department exploits power and flexibility of digital technologies for a variety of scopes, such as monitoring of ambulatory and waiting room environmental parameters for preventive maintenance, online monitoring of medical devices functionality.

Of course, the authorization to medical practice must be regulated in a rigid way, sometimes more with respect to the public sector: Agenzie di Tutela della Salute (ATS) is a health protection agency established with the regional law of 11-th August 2015 [3], that imposes strict constrains before providing the authorization to medical practice, and that provides also eventual variations with respect to an internal operating plan.

It must be said that CMS, despite being a health clinic that offers over 73 different branches, it doesn't handle with more complex realities, such as hospitalization, first aid or intensive care.

CMS was born as a start-up in 2009, promoted by OltreVenture, an impact investing company founded by Luciano Balbo and Lorenzo Allevi. In 2020 L-GAM, an investment firm founded in 2013 by Ferdinando Grimaldi, became the major shareholder of the company.

To date CMS counts 32 centres, the highest majority of them located in Milan and its hinterland, while one centre is currently placed in Bologna.



Figure 2: Distribution of CMS centres in the Lombardy region [1]



Figure 1: Distribution of CMS centres in Italy [1]

CMS is trying to look towards other urban realities: as an example, Roma Cavour centre, in Rome, is the first clinic, to date, that took its first steps in a complete different urban environment, with its legal and administrative constraints. Currently ongoing, CMS is working on new apertures in Rome, trying to respond to the needs of patients that have access to one of the worst public health apparatuses of the Italian landscape, as expressed in [4].

As a proof, below in Figure 3 it is represented the ranking of regional performance in Italy, provided by C.R.E.A. [5]

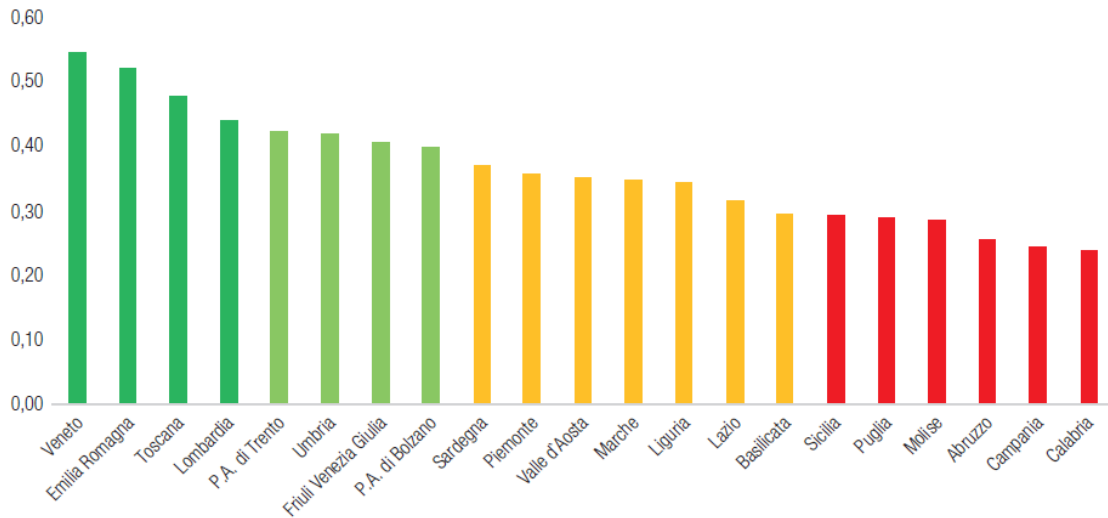


Figure 3: Ranking of regional performance [5]

As stated in [1], CMS was awarded as growth champion in 2022: this acknowledgment was given by Istituto Tedesco di Qualità e Finanza (IQTF), a German Institute that conducts market surveys aimed at analyzing the economic and qualitative aspect of companies active in various sectors. [6]

One of the strengths of CMS is based on the optimization of the efficiency and the effectiveness of any internal process, in terms of time and a variety of different cost sources: this is reflected into an average price of the performances that is attenuated by an improvement in the planning and operative management of any given internal task. Also, the time for the supply of the medical service is taken into account, in order to book time slots, whose time duration is optimized, and so to have the possibility to fill-in specialists agendas in a complete manner, generating value for all the players in this market.

As defined in the CMS mission, Santagostino aims to grant the best medical quality while respecting the timing needs of his users.



LA NOSTRA MISSION

“

Il Santagostino ascolta, capisce e prende in carico i bisogni di salute di tutti.

Offre servizi di alta qualità, accessibili e diffusi, nel rispetto dei tempi dei suoi utenti. I suoi specialisti indagano e intervengono sulle cause di malesseri e malattie per proporre soluzioni efficaci e integrate.

Il Santagostino rende eccezionale l'esperienza di ogni utente creando fiducia, consapevolezza, salute e benessere.

Un'esperienza che diventa incontro.

”

Figure 4: CMS's mission [1].

Taking into account not only the economic aspect, on the other hand the clinical quality delivered to patients is ensured by the presence of a clinical quality control organization, based on different entities: the presence of a medical leader for each medical specialty and the existence of a digital record system, used as storage environment for collecting different typologies of information referred to the CMS patients. The reason why patients' data are stored is manifold, but firstly it should be done a distinction between the different typologies of data collected: the data associated to the patient registry and the radiologic images acquired. The former ones are regulated by the General Data Protection Regulation GDPR [7], that guarantees the correct data management in appropriate structures, with regulated access to the operators of these data. For what concern the storage of the radiologic images, the regulation instead is given by [8], that in articles 3, 4 and 5 reports the following principles:

- Article 3, Principle of Justification: the dose exposition has to be preliminarily justified, taking into account specific objectives of the exposition and the patient characteristics.
- Article 4, Principle of Optimization: the dose exposition for radiologic scopes has to maintain the lowest achievable level, compatible with the achievement of the required diagnostic information.
- Article 5, Responsibility: the dose exposition is performed by the technical specialist based on the reasoned request of the prescriber.

The existence of a digital record system allows to comply with the regulation provided by the Legislative Decree 26 May 2000, n. 187[8]: in case of a request of the prescriber to perform a dose exposition on a patient, if the information

regarding an historic image acquired in the past is adherent with the current status of the patient, it would be useless to perform another exposition for the same anatomic area.

The [1] also reports the distribution of patients, divided by sex and age, in particular:

- The 60% of the overall patients population is women;
- The largest catchment area of patients, in terms of age, is between 19-45 years (54%), followed by people aged 46-65 (26%), while the remaining 20% is composed by patients whose age is lower than 18 years or higher than 66.

The reason why of this distribution is given by the fact that some medical specialties, such as gynecology or obstetrics, show a public average waiting time much longer with respect to the private sector: as stated in the Executive Summary published by the Lombardy Region in 2018 [9], the longest waiting time is associated to the time to perform an echography (59 days), followed by the time to have access to a CT (39 days) or an MRI (24 days). In CMS instead it is possible, usually, to get a first access in only three days.

For what concerns instead the distribution of the population grouped by age, the lower numerosity of patients, that are younger than 18 or older than 65, is related to the fact that a group of this category of patients is entitled to have the exemption from payment of the ticket [10].

1.2. Role of the Department of Clinical Engineering (DCE) for Santagostino

As cited in [11], engineers were first encouraged to enter in the clinical scene during the late 1960s to cope with the rapid proliferation of the medical equipment for diagnosis and therapy in an hospital-based setting. The need for this figure was born with the aim to provide scientific and technological knowledge, developed through engineering education within the health-care environment in support of clinical activities. Moreover, the rapid technology developments experienced during the past years have necessarily required a qualified figure dedicated to the management of these devices, for all their lifecycle period, from their acquisition to their dismissal.

The expansive perspectives of this developing market, and the importance assumed by the technology, have required the establishment of different directives related to the medical devices, due to their inherent technology for the diagnosis, therapy and rehabilitation. In particular, the European Union produced three different directives related to the use of a medical device:

- Directive UE 93/42 [12], recently modified by the 07/47 directive [13], concerning the field of design and realization of a medical device, from now on it will be mentioned a MD.
- Directive UE 90/385 on active implantable devices [14].
- Directive on in-vitro MD [15].

The Associazione Italiana Ingegneria Clinica (AIIC), that was born in 1993 in Milan with the institutional purpose of protect the figure of the Clinical Engineer, defines the Clinical Engineer as “[...] un professionista che partecipa alla cura della salute garantendo un uso sicuro, appropriato ed economico delle tecnologie nei servizi sanitari “ [16].

The inherent activities related to a Department of Clinical Engineering (DCE), from now on called also DCE, can be manifold, and that requires an integration with different figures:

- Health Technology Assessment (HTA) and planning for the introduction of new medical technologies: a clinical engineer is required for the technical and economic assessment with the aim of the establishment of a new medical device in an hospital-based setting.
- Management of the maintenance of the medical devices included in an hospital-based setting, and subsequent activities.
- Periodic safety and functional inspections.
- Safety and clinical risk management: any manufacturer of MD has to be compliant with the aforementioned normative in order to obtain the CE marking, and in particular he has to produce a document related to the risk analysis for the destination of the designed use. A DCE will have to consult this documentation in order to ensure the compliance with the previously mentioned regulations.
- Training and education of the technical and medical personnel in order to ensure the correct and safe use of the medical device throughout the entire product lifecycle: it is therefore necessary a technical supervisor that is constantly working in cooperation with the MD operators, from the

product implementation until its dismissal. Its presence allows to grant audience to personal feedbacks related to the use of the technology.

- Regulatory design of the host structures in which there'll be placed the MDs.
- Clinical informatics and Information Technology: as cited in [17]"[...] Healthcare technologies are increasingly becoming digitalized. As patients move around the healthcare ecosystem, their electronic health records must be available, discoverable, and understandable". The CMS health clinics network distribution primarily implies that digital records of the patient, starting from patient personal data until the collection of radiographic images, must be acquired from local hosts and must be sent to a central node, from which it is possible to use the obtained information for multiple purposes. A clinical engineer has a central role inside this domain: he will ensure the correct management of healthcare data exchange, with modelling standards [18]that permit a precise and error-free sharing of a so sensitive typology of data.
- Software development and procedures for the improvement of the efficiency of the medical device assistance, in case of damages or errors. As an example, the IC department has just realized a new archive on the entire medical equipment using stickers equipped with RFID technology, through which it is possible to consult the list of procedures of maintenance in case of primary assistance. In case of problem preservation, the user is allowed to open an assistance ticket. The strong advantage is that, thanks to the information acquired during the construction of the archive, all the fields related to the description of the instrumentation will be automatically compiled, in order to reduce human compilation errors, reduce wasting time and improve the efficiency of the maintenance operations.

As a consequence of the distinctive network of the CMS, the planning and management of the interventions on biomedical devices is a crucial point for eputation and economy, since a failure or a delay in restoring the functionality of the equipment would lead to loss of revenues and patient retention.



Figure 5: Diathermocoagulator equipped with RFID technology

1.3. Innovation and replacement for Santagostino

Organizational and equipment changes are more likely to succeed when health care professionals, of different academic experience, have the opportunity to communicate, share ideas and collaborate to generate additional value. CMS in fact houses a medical team of 1150 physicians, of different medical specialities, that in scheduled webinars and internal meetings have the possibility to express opinions about the introduction of new medical offers: also, they can generate value, proposing the introduction of an innovation in the healthcare technology. Of course, the new offering occurrence is related to projects that are economically and technically feasible, and that's why a Health Technology Assessment (HTA) process is required.

HTA is a field of scientific research to inform policy and clinical decision making about the introduction and diffusion of health technologies. HTA is a multidisciplinary field that addresses the health impacts of technology, considering its specific healthcare context as well as available alternatives.

Contextual factors addressed by HTA include economic, organizational, social, and ethical impacts. [19]

As declared in the aforementioned definition, in the assessment phase there'll be analysed all the aspects of interest for the adoption of the health technology, most of them related to the strategic and technical fields, taking as a constraint the part related to the amount of the investment required and potential revenue that the new offering could generate, for both the patient and enterprise. Complexity and aspects related to environmental and space constraints will be analysed, as well as market supply and potential competitors in the surrounding area.

The perpetual growth of CMS is an aspect that, despite advantages and disadvantages related to the expansion of the health clinics network, pushes towards the constant innovation, in order to keep onboard highly innovative clinical offer, being so competitive with respect to all the other market players. Not only, the innovation brought towards newer centres will bring with it also all the other health clinics, since a coherent and homogeneous clinical offer will be always proposed to the patient: this will facilitate the correct lifecycle of the health technology, ensuring a correct and time-sensitive replacement of the entire medical equipment.

1.4. Dual X-ray Absorptiometry introduction

To date innovation was carried forward in all the specialities, with particular regard with respect to the field of radiology. Biomedical images are used for both diagnostic and therapeutic purposes: CMS exploits both of them to generate value. Patients can present a medical prescription for the irradiation with the purpose of an external medical intervention, and more: the dose exposition can be inherent inside a treatment plan of the patient, with the aim to build a surgical programme for particular typologies of intervention, such as Ronchosurgery for the treatment of the obstructive sleep apnoea or Ultrasound-guided emptying of soft tissue cysts.

CMS currently possess a medical equipment for biomedical images that counts:

- Forty-four technologies for diagnostic biomedical images, such as Magnetic Resonance (MR) or Computerized Tomography (CT) machines.
- Sixty-eight Ultrasound Scanners (US) for the generation of echo or echo-colour images.

- Three Dual-Energy X-Ray Absorptiometry (DXA or DEXA) machines.
- One Optical Coherence Topographer (OCT) for the diagnosis of eventual glaucoma or retinal pathologies. [20]
- Two Video-Dermatoscopes (VD) for the diagnosis of diagnosis of pigmented skin lesions [21]

Among all, specialists in endocrinology, supported by the clinical opinion of the CMS health director, have presented, as a project for the clinical offering for 2022, the intention to introduce newer technologies in the field of densitometry. Bone density scanning, also called DXA or bone densitometry, allows to visualize the bone structure and, most importantly, provides a quantitative measurement of the Bone Mineral Density (BMD) [22] and fractural risk assessment (FRAX) [23], which can facilitate the early diagnosis and treatment of several pathological condition. Osteopenia and osteoporosis are systemic skeletal disorders, the most common metabolic disease.[24]

From January 2016 it was installed the GE-Bravo DEXA scanner in “Repubblica” centre, located in 6, St. Panfilo Castaldi, Milan.



Figure 6: R7 ambulatory in “Panfilo Castaldi”, GE-Bravo positioning

The machine was installed without being purchased: CMS activated a service contract with the supplier of the technology, whose costs were associated to a percentage of the cost of the examination, with a minimum monthly pay-out. In 2021, some clauses of the established contract were modified, in terms of incorporation of the in charge technical personnel, resulting in a reduction of the monthly payment percentage. The intention to internalize this typology of

examination, with the presentation of the proposal by internal physicians to include additional diagnosis tools, such as Trabecular Bone Score (TBS) [25] , brought to the establishment of the project for the replacement of this machine: during its course it has been performed a Mini Health Technology Assessment for the evaluation of the clinical, economic and organizational impact of the acquisition of a new technology with respect to the standard care. The overall process of internalization was divided into the part devoted to the assessment of all the valuable comparators that are competing in the same market segment, with the analysis of technical, economic, payment, warranty and maintenance specifications: the objective was to identify the most cost-effective solutions among all the proposals that were considered. Afterwards, the production of a brief report that was describing the cost-effectiveness of the different proposals allowed to bring toward the appraisal phase. Physicians in the field of endocrinology and radiology, by reading the produced document, contributed for the realization of future operative recommendations, such as the identification of the most effective solution. Ultimately, the collaboration with the Administrative, Operative and Facility departments let to investigate also on not clinical parameters, already discussed with medical doctors, such as cost of the purchase, modality of payment, electrical and structural adequacy, and operative blocks of agendas for that type of examination, since the technology took time for its replacement.

Once it was installed and configured for the communication with the CMS Picture Archiving and Communication System (PACS) [26], training on technical and medical personnel was performed, in order to ensure a safe, correct use of the machine for the exam execution.

Also it was dispensed to the medical personnel the information reporting guidelines for the correct use of threshold values for the discrimination among different pathological conditions, with the aim to generate a correct clinical and statistical-based medical report.

2. Dual X-ray absorptiometry: State of the Art

In this Chapter it will be reported the background on principles of X-ray and image generation, with a particular attention to fan beam projection geometry scanners. In Section 2.1 there'll be analysed the clinical use of the Dual-Energy X-Ray Absorptiometry: it will be reported the category of patients on which it will be administered DXA examination, with particular remark to the most common and diffused metabolic diseases that can be diagnosed with this health technology. Official Positions of the International Society for Clinical Densitometry (ISCD), 2019 will be presented, with the recommendations for the Bone Mineral Density (BMD) Testing. There'll be analysed the State of the Art of the Trabecular Bone Score (TBS) in section 2.2.3, described in [27] as a grey-level texture measurement, based on the exploitation of experimental variograms of 2D-projection images acquired at spinal level: this additional tool will provide further information about the 3D characteristics of bone microarchitecture, in order to increase, together with BMD measurements, the prediction of osteoporotic fractures overall and vertebral fractures alone. [27].

Beyond Bone Mineral Density (BMD), Bone Strain Index (BSI) will be described in Section 2.2.4. BSI is a new-DXA-derived index based on Finite Element Analysis (FEA) of greyscale of density distribution measured on spine and femoral scan. This additional tool provides information about the bone strength based on density distribution, bone geometry and loadings, and it differs from BMD and TBS, which are variables all based on the quantification of bone mass and distribution averaged over the scanned region. [28]

2.1. X-ray and image generation

2.1.1. X-ray generation

Ionizing radiation can be generally considered any form of radiation exposure that will produce subatomic ionization event. The ionizing radiation can be in the form of electromagnetic radiation (EMR) or particles; however, it must have a sufficient energy to cause ionization in the target molecule [29]. Ionizing radiation feature:

- High frequency (beyond 10^{16} Hz).
- Small wavelengths (lower than 10^{-8} m).

Classical physics states that every time a charged particle is accelerated, energy is released as electromagnetic waves. Therefore, when a charged particle is either deflected from its linear path or varies its velocity, it irradiates radiative energy proportionally to its acceleration. The production of EMR, more precisely X-ray radiation, exploits the acceleration of negative charged particles, such as electrons.

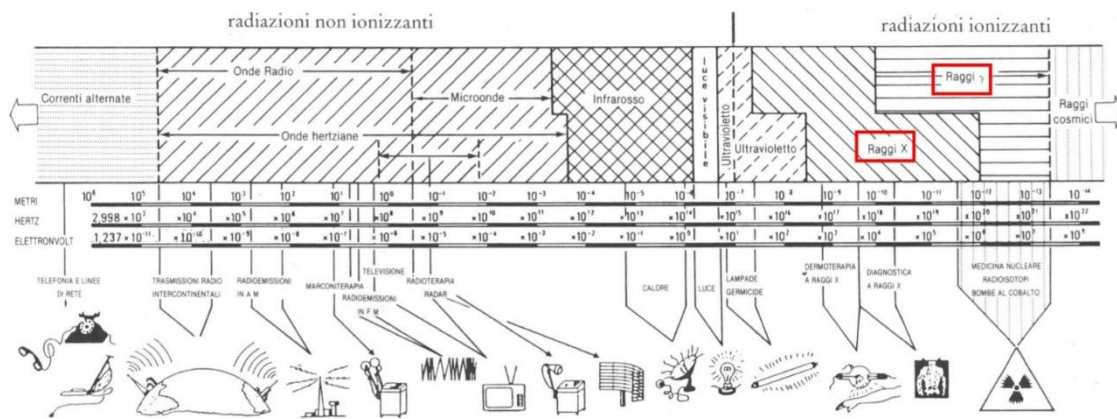


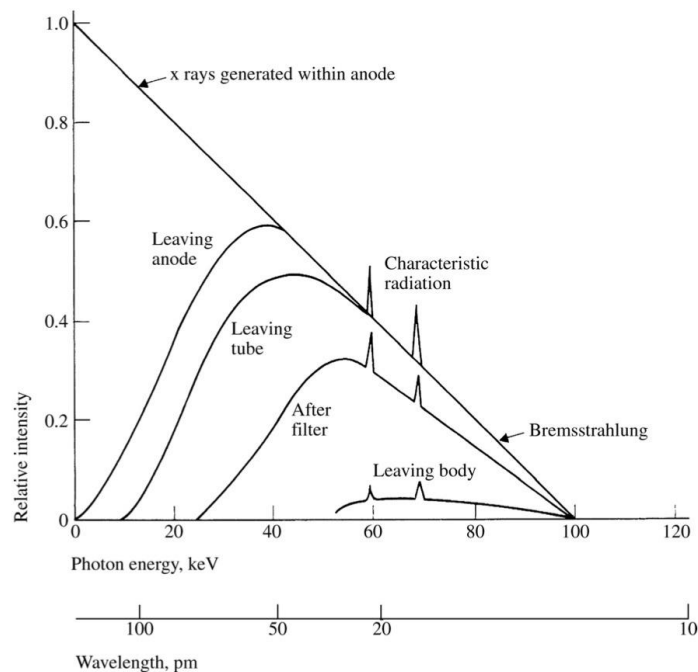
Figure 7: The Electromagnetic (EM) Spectrum

Ionizing X-ray photons can be subdivided into:

- Bremsstrahlung X-rays (continuum energy spectrum), generated by charged particle acceleration (deceleration). A Bremsstrahlung radiation is produced when an electron changes its velocity following the Columbian interaction with the atomic nucleus. The emission is larger more energetic is the electron and larger is atomic number (Z) of the absorbing electrons.

The energy emitted as X-rays has a continuous spectrum from 0 to E_{\max} (the kinetic energy of the incoming electron, in the case it is fully absorbed in the interaction).

- Characteristic X-rays (discrete energy spectrum), generated by transitions of electrons bound to atomic shells (K, L, M etc.). The energy of the electron accelerated by the electric field will hit internal atomic energetic shells, producing the emission of an electron belonging to that shell. Consequently, an electron of the next energetic level, will take the place of the ejected one. During this process, it will be produced a photon of definite energy, equal to the difference between the two energy levels.



Graph 1: X-ray spectrum using a tungsten anode. Low-energy X-rays are absorbed by the components of the X-ray tube itself. Characteristic radiation lines from anode occur at approximately at 60 and 70 KeV.

Since more than 120 years, Bremsstrahlung from X-ray tube has been the workhorse of medical diagnostics [30]. X-ray segments in diagnostic systems consists of an X-ray tube housing assembly, comprising the vacuum electronics of an X-ray tube and means for radiation shielding, cooling, electrical insulation and mechanical interfacing.

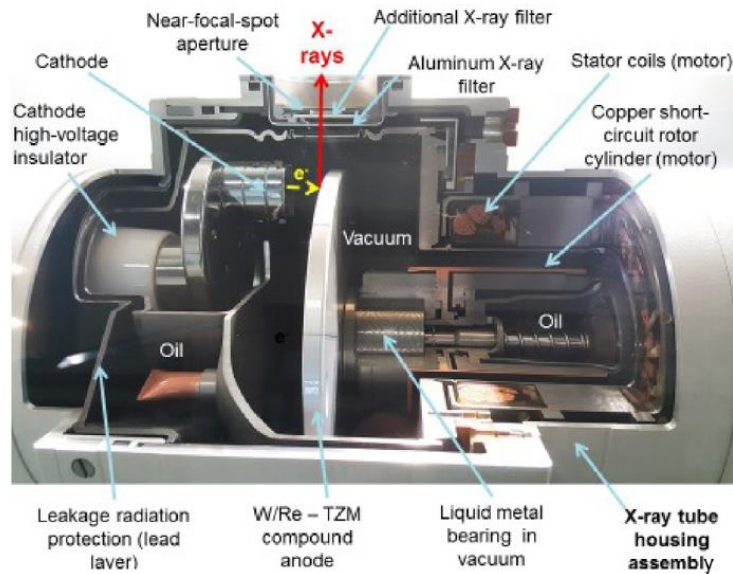


Figure 9: Cut view of an X-ray tube assembly

At first, a heated coil of Tungsten wire, in the negative charged cathode, releases electrons into the vacuum space of the tube by thermionic emission. An electric field between anode and cathode accelerates the electrons. The total applied voltage defines the energy that will possess accelerated electrons, thus defining the X-ray spectrum bandwidth. It is worth to mention that in physics, an electronvolt (eV) is the measure of an amount of kinetic energy gained by a single electron, accelerating from rest through an electric potential difference of one volt in vacuum.[31] On the other hand, a rotating anode is positively charged: accelerated electrons will hit the anode in rotation, thus generating the X-ray radiation. The anode is put in rotation in order to reduce the heating effects induced by the impinging electrons.

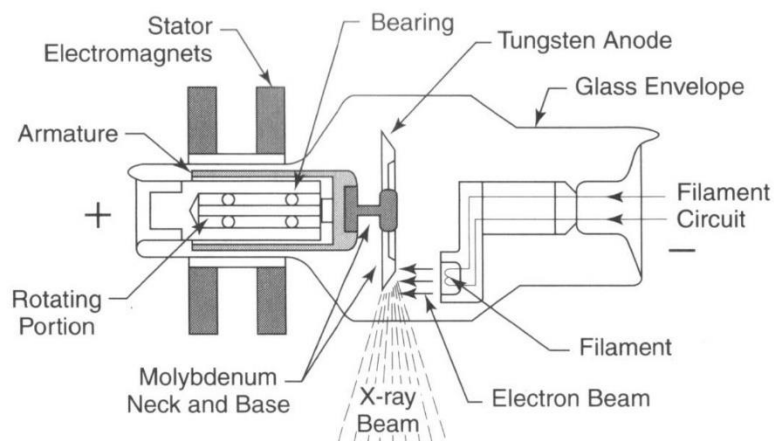


Figure 8: Simplified X-ray tube with a rotating anode and a heated filament

The spectrum of the x-ray beam ejected from the x-ray tube contains useless components that have to be filtered out: the lowest energy X-rays are absorbed in the anode metal and the tube glass envelope. As visible in Figure 10, an Al filter further reduces the low-energy X-rays that do not pass through the body and would just increase the secondary radiation, thus increasing the patient dose. Moreover, the beam is shaped thanks to the use of collimators, in order to focus the beam towards the target. In this way, only high energetic photons will be capable of penetrating the body and contributing to the image generation. After the interaction with matter, it's needed to collect the primary radiation and eliminate the contribution of the scattered, or secondary one. The collection of the primary radiation occurs at the detector, placed at the opposite side of the source location: this convey is facilitated thanks to the use of a collimation grid, having channels approximately oriented as the ideal direction of the exiting beam. Here represented, a synthetic schematic of the x-ray pathway crossing the patient, toward the detector. [32]

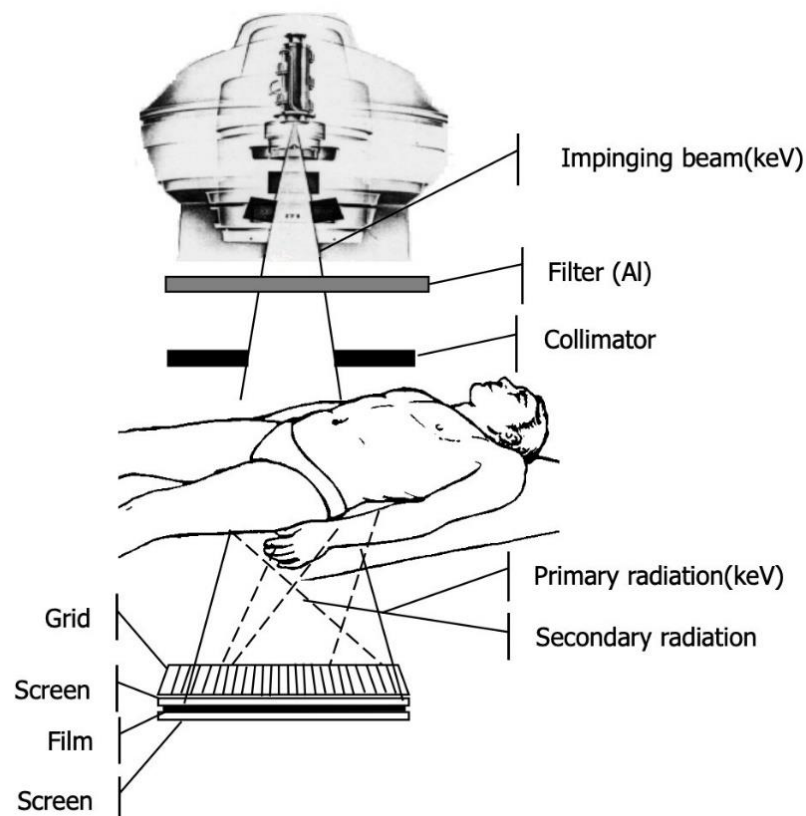


Figure 10: Schematic of the X-ray pathway crossing the patient, towards the detector

2.1.2. Interaction with matter

Interaction of generated X-ray photons with matter is material and energy dependent. In the energy range of medical imaging, that varies approximately from 50-150 KeV for diagnostic imaging and from 3-10 MeV in the case of therapeutic irradiation, there're three types of interactions with the biological matter:

- Interaction with atomic electrons.
- Interaction with nucleons.
- Interaction with electric fields associated to atomic electrons and atomic nuclei.

As a matter of that, X-ray radiation can experience, respectively, complete absorption, inelastic or elastic scattering. The process of image generation is a consequence of a reduction in the radiation intensity passing through an object, usually referred as attenuation. The attenuation phenomena can be related to different causes, such as reduced photon counts, changes in the x-ray direction or energy attenuation. As expressed in the Beer-Lambert law [33], in case of passing through a heterogeneous object and considering a linear projection profile:

$$I = I_0 \exp\left(-\int_0^L \mu(x) dl\right)$$

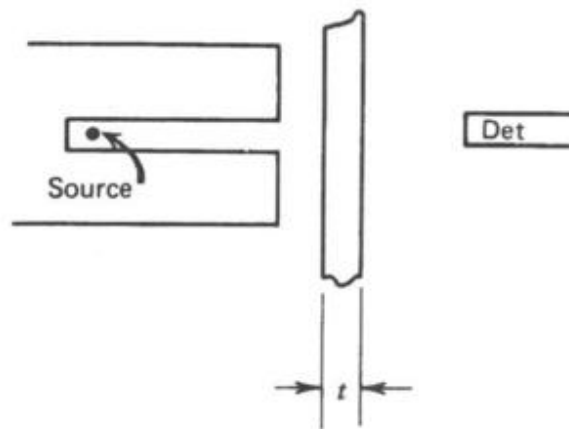
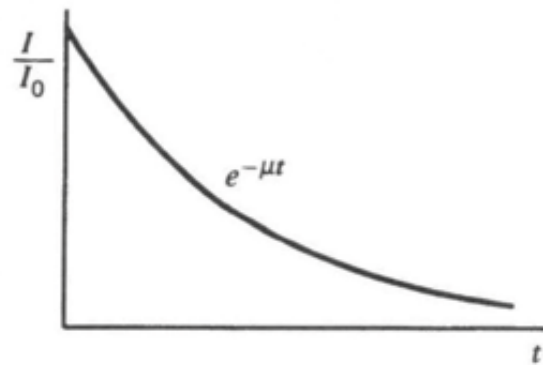


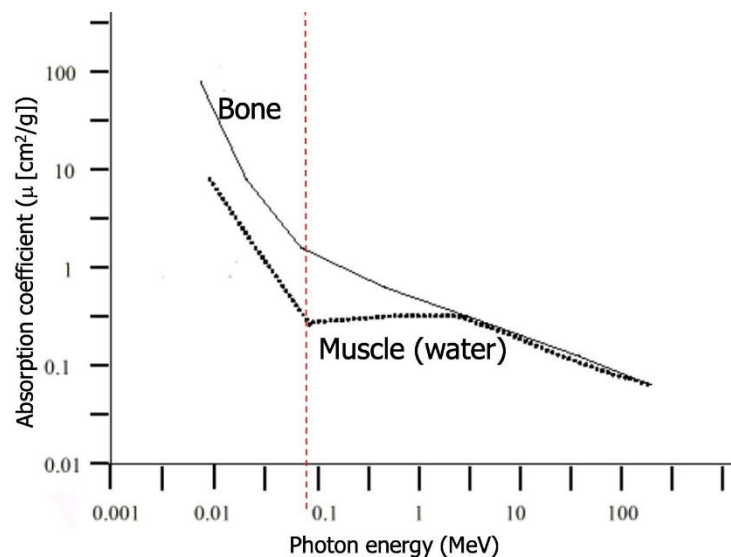
Figure 11: X-ray from source to detector



Graph 2: Graph of the Beer-Lambert law as a function of t variable

The ejected energy I is function of the initial energy I_0 , the attenuation coefficient μ , specific of the material under examination, and the depth x travelled by the ray.

Absorption coefficient varies as a function of the beam energy, moreover, in biological tissues, we found peak differentiation at 50-70 KeV, as visible in the graph below, in order to generate the highest image contrast possible.



Graph 3: Attenuation coefficient variation as a function of energy and tissue type

As expressed in Section 2.2.1, after the interaction with hard and soft tissues, it's needed to collect the primary radiation and eliminate the contribution of the secondary one. Sources of secondary radiation during highly energetic photon interaction with matter, in the field of diagnostic imaging are:

- The Photoelectric effect, in which the incoming photon possess an energy close to the binding energy of an electron of the target atom. The incident photon gives up its entire energy to an electron, called photoelectron or secondary radiation, that then is ejected from the atom with an energy equal to the initial energy of the impinging photon. The residual atom is left in an excited state, since the emitted electron left a free orbital vacancy, filled by less bound (and more energetic) electrons from external orbitals. Characteristic X-rays are emitted during this atomic de-excitation.

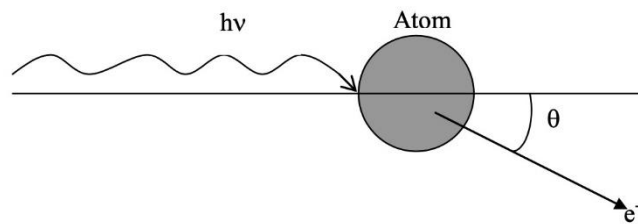


Figure 12: Schematic view of the photoelectric effect

- Compton scattering is the most dominant interaction mechanism in tissue-like materials. It describes photon scattering interactions with atomic electron: this effect is most probable at energies higher than the target electron binding energy. As a result of the collision, the striking X-ray photon ejects an electron from the atom, and it's deflected, or scattered, through an angle θ with partial loss of initial energy. The reduced amount of energy possessed now by the x-ray has been transmitted to the so-called Compton electron [33].

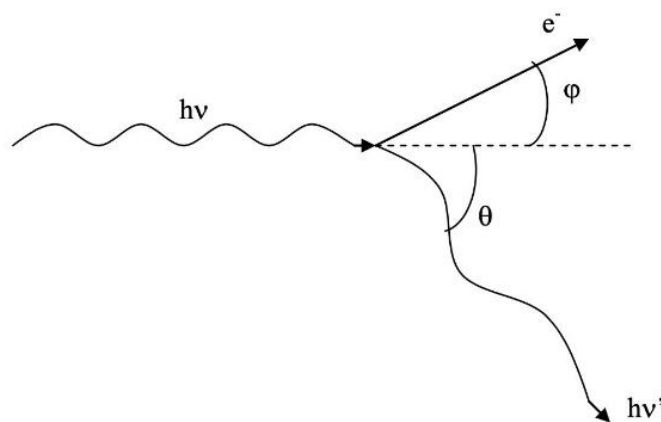
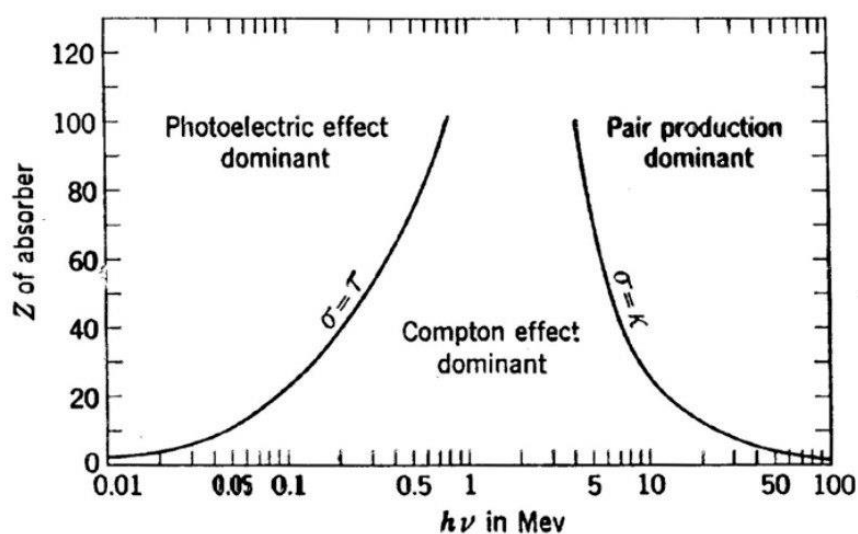


Figure 13: Schematic view of the Compton effect

- Rayleigh scattering is more probable at low energies, consequently at energies lower with respect to the binding energy of an atomic electron. In this process, the energetic photons are scattered by the atomic electrons and the surrounding atoms, neither ionized nor excited. No ejection occurs: the excess energy from the receiving electron is transmitted into an electromagnetic photon, with a different direction. For medical imaging purposes, the contribution of the Rayleigh can be considered negligible compared to other secondary radiation.



Graph 4: Schematic view of the Compton effect

As described in this section, different energetic photons can experience different types of interaction with tissue-like matter. As visible in Graph 4, the probability of occurrence of Photoelectric, Compton and Pair production effects as a function of the impinging photon energy and the target atomic number. In Graph 4 it can be noted that at higher energies pair production effect will be dominant: it won't be analysed in detail since its effect is much higher in the field of therapeutic imaging. Typical ranges for diagnostic imaging vary from 50 KeV up to 511 KeV, while for therapeutic imaging the energy range starts from values usually higher than 1 MeV, up to approximately 10 MeV for medical purposes.

2.1.3. X-ray detection and image generation

2.1.3.1 Analog and digital detectors

Imaging diagnostics can be divided into two main categories, depending on the type of signal processing performed after reaching the detector. The nature of the detector will drive this distinction into:

- Analog detectors.
- Direct and indirect conversion digital detectors.

For what concern analog image detector of an X-ray unit, it's composed by three components: X-ray film, intensifying screen and a light-proof housing (cassette) [34]. X-ray film is made of a thin polyester film and a thin layer of a photographic emulsion. A schema of the X-ray film structure is given in Figure 14. The emulsion is covered with protected polymeric layers: the photosensitive element in this representation are silver halide microcrystals. Quanta of X-rays transfer their energy as soon as they reach the silver halide crystals: if the incident X-ray photon possess a sufficient energy, when hitting a crystal electron, it can be transferred from the valence band to the conduction band, with the possibility to move freely inside the silver crystal. The electron moves until it reaches the place of crystal structure distortion, where it's "trapped". Trapped electrons will cause attraction of positively charged silver ions, which further leads to the origin of a metallic silver atom in that particular place [34]. The amount of developed metallic silver atoms in a given position will determine the amount of blackening of the real image in a given point.

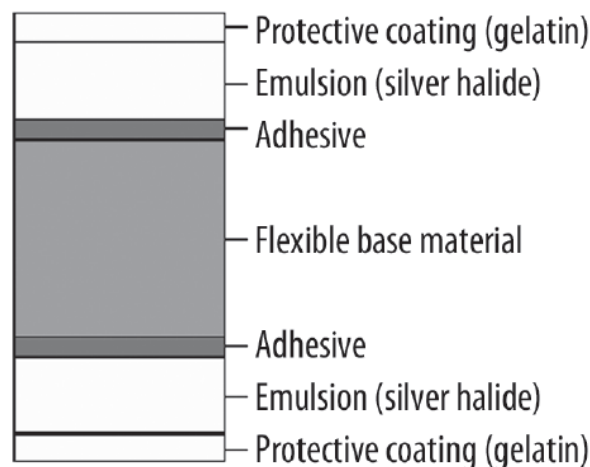


Figure 14: Cross-sectional diagram of the X-ray film

Active digital detector can perform direct or indirect conversion: for direct conversion it's intended that, in the same material, it occurs both photon absorption and electrical conversion. The energy of the incoming photon is converted in a given quantity of electric charge, that then is collected at an output electrode of the detector. Detectors, which consist of photoconductors, such as amorphous silicon or selenium. The photoconductor is a material where the conductivity is sensitive to the amount of received radiation. When an X-ray is absorbed by the photoconductor it allows the generation of an electron hole pair. By applying a voltage difference between top and bottom plates of the sensor, the negative created charge flows in the upper direction toward the upper plate, while holes are pushed towards the bottom one. The bottom electrode is the upper plate of a capacitor. The holes are collected by the capacitor plates, and their presence will allow for voltage signal generation. If we activate the gate line corresponding to the TFT switch, a connection among the signalling capacitor and the data line occurs. On the bottom side a schematic diagram of cross-sectional structure of a direct-conversion X-ray imager.

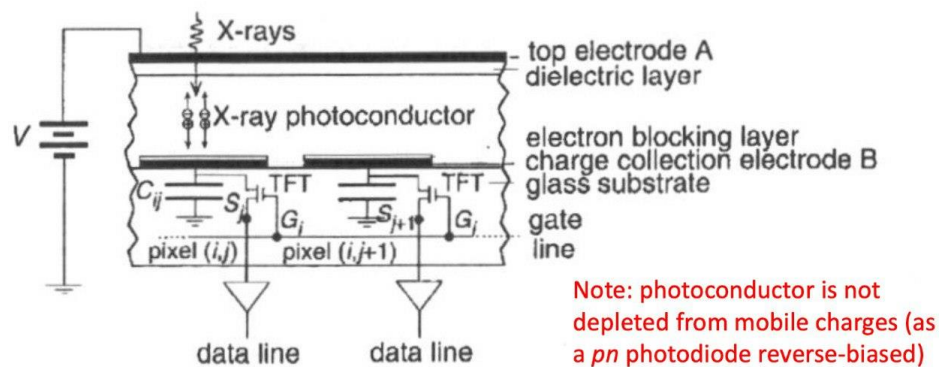


Figure 15: Simplified schematic diagram of a cross-sectional structure of two pixels of a-Se X-ray image detector

In the case of indirect conversion detectors, the process of charge generation follows two different stages: the energy of an incoming X-ray photon is firstly absorbed and converted into visible light by scintillators. The obtained light will be then converted into electric charge by photodetectors. The advantage related to the use of a two stage detector is given by the fact that its components can be chosen freely depending on the needs required, while direct conversion detectors present thicknesses constrained by the intrinsic lower detection efficiency of the Si. For this way, photodetectors can be of various types, such as photodiodes or

photomultiplier tubes. It will be described the process of charge generation with a sensor composed by a scintillation material, coupled with an array of photodiodes for the conversion of light into electric charge. The scintillation process is based on molecule excitation, passing through different energetic levels, from ground state to vibrational states, when an energetic photon arrives at the molecule. The electron kicked out by the radiation excites the surrounding molecules allowing them also to pass from ground to excited state. The process of de-excitation from a vibrational state releases an optical photon through fluorescence phenomena. Below depicted the representation of the energetic levels of an organic scintillating molecule.

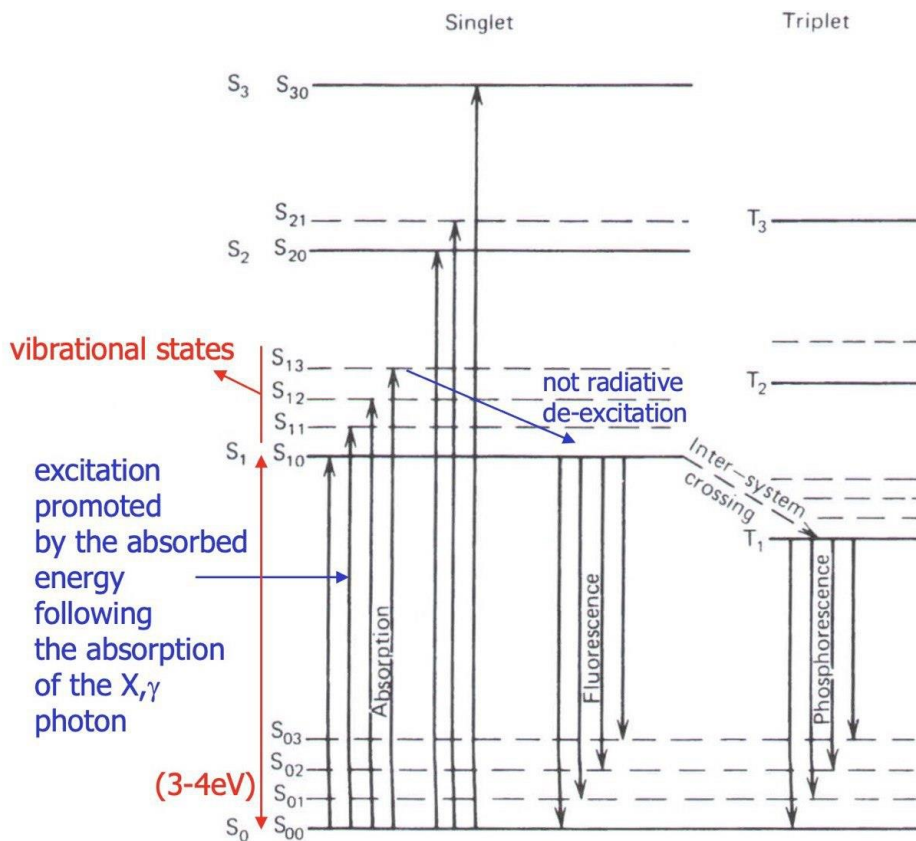


Figure 16: Energy levels of an organic scintillation molecule

Visible light generation is an intermediate step before electrical charge generation: an array of photodiodes, each one specific for a single pixel of the image, always in reverse bias mode [35] "deplete" the entire volume of the detector from mobile charges, in order to make it active for the creation of the

electric signal generated by the absorption of an optical photon coming from the scintillation crystal.

Because the p-type material is now connected to the negative side of the applied voltage, the holes in the p-type material are pulled away from the junction; similarly, because the n-type region is connected to the positive side, electrons will also be pulled away from the junction. Therefore, the depletion layer widens, and does so increasingly with increasing reverse-bias voltage. This increases the voltage barrier causing a high resistance to current flow. The strength of the depletion layer increases as the reverse-bias voltage increases. Once the electric field intensity increases beyond a critical level, the PN junction depletion layer breaks-down and current starts to flow. In figure 17 it's given a representation of the increased depletion region for the reverse biased mode with respect to the forward mode, followed by a schematic diagram of a PN reverse biased junction, Figure 18.

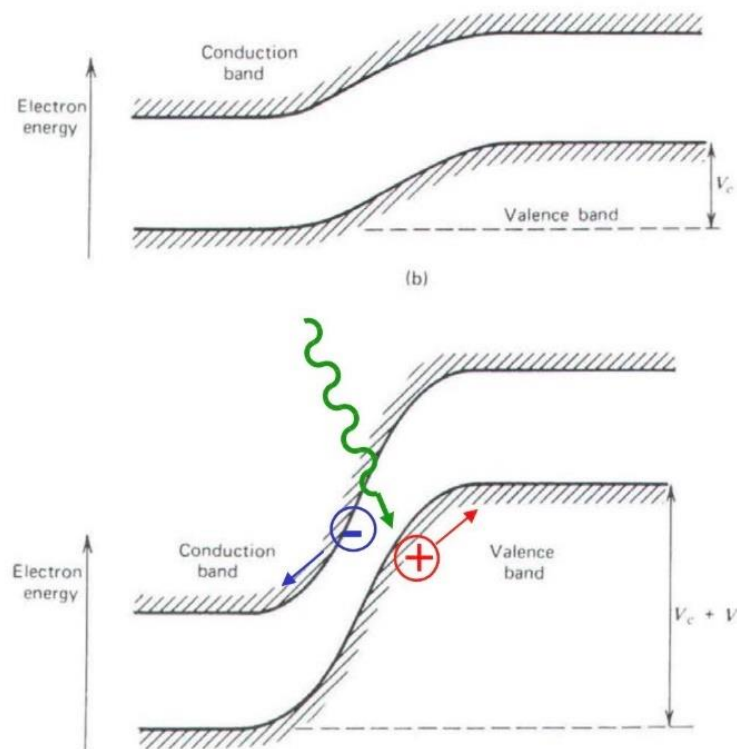


Figure 17: Electronic potential in forward and reverse bias mode

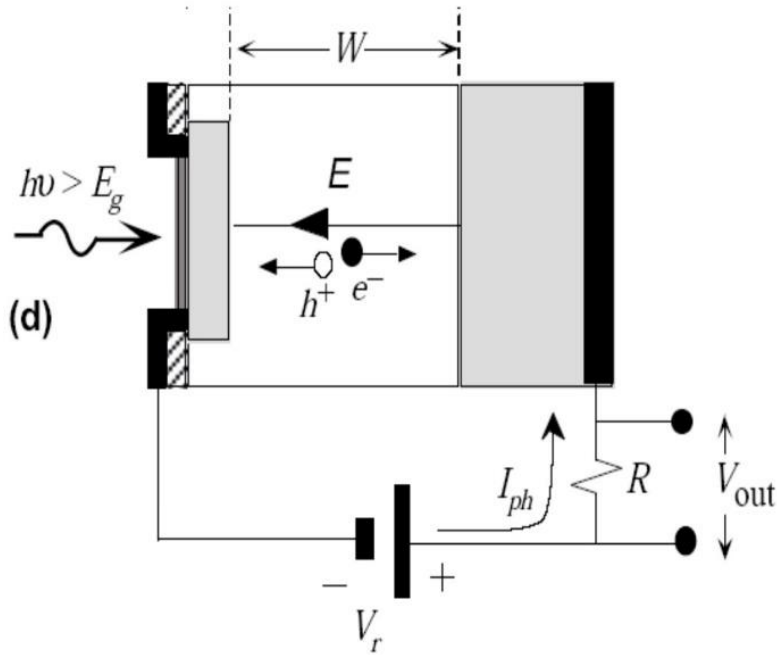


Figure 18: Functioning of a reverse biased photodiode

2.1.3.2 Reconstruction from projections with fan beam geometry

The electronics of single detection element, for the conversion of an energetic photon into an electric charge, can compose a single unit of multichannel detector shaped in arch or linear mode beyond patient positioning, with respect to the X-ray source. The process of the image generation from a radiation source signal is given by the possibility to acquire projections, generated with a given geometry, that contain the information related to the amount of intensity attenuation it experienced travelling the source to detector distance. The logarithm of the Beer's law formula yields the integral of the attenuation along the ray, which is the projection value:

$$I = I_0 \exp^{-\int_0^L \mu(x) dl}$$

$$p_L = \int_0^L \mu(x) dl$$

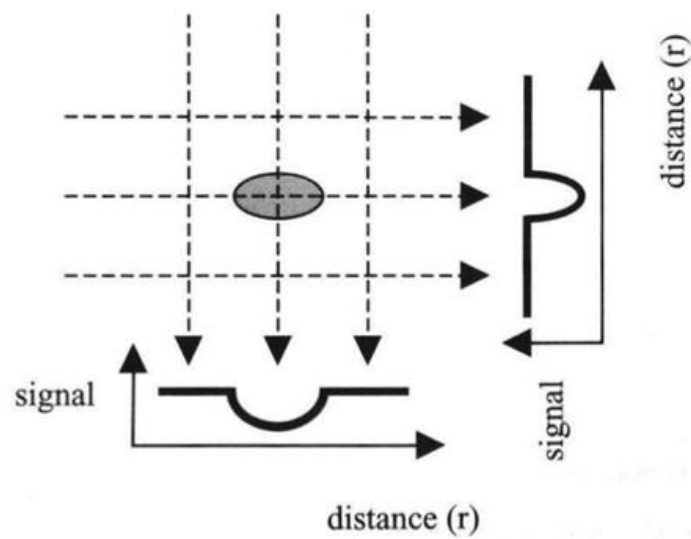


Figure 19: Two sets of linear projections, whose final intensity correspond to value p_L

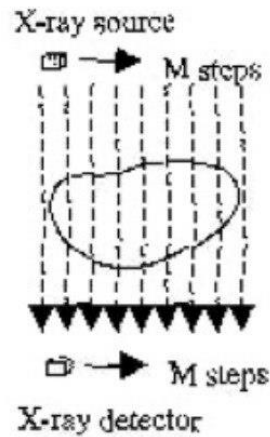


Figure 20: A single set of linear projections acquired in the transversal plane

Projections rays are defined by the unit vector in the t direction, orthogonal with respect to the projection ray r :

$$\hat{\xi}_{\vartheta} = \left| \frac{\cos(\vartheta)}{\sin(\vartheta)} \right|$$

Any point $r = \begin{pmatrix} x \\ y \end{pmatrix}$ on the projection ray will have constant displacement, so the scalar product among the projection ray and the t direction is kept to zero.

$$\hat{\xi}_{\vartheta} \cdot r = t \Leftrightarrow x \cos(\vartheta) + y \sin(\vartheta) - t = 0$$

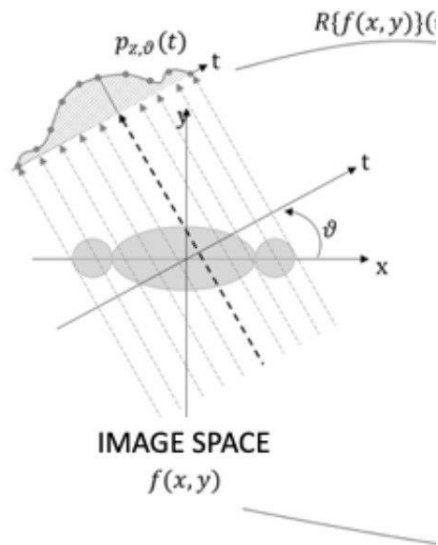


Figure 21: Parameters of a projection ray: angular and linear displacement ϑ and t

Newer generations of scanner systems project the X-ray beam in other fashions with respect to the classical parallel beam geometry: fan beam or cone beam geometries are nowadays exploited [36].

For the purposes of this project, it will be described only the FB configuration with corresponding equations, for which it exists an exact analytical solution, both for the arch detector and the linear detector. A visual representation of the source positioning, source to detector X-ray propagation is provided in Figure 20.

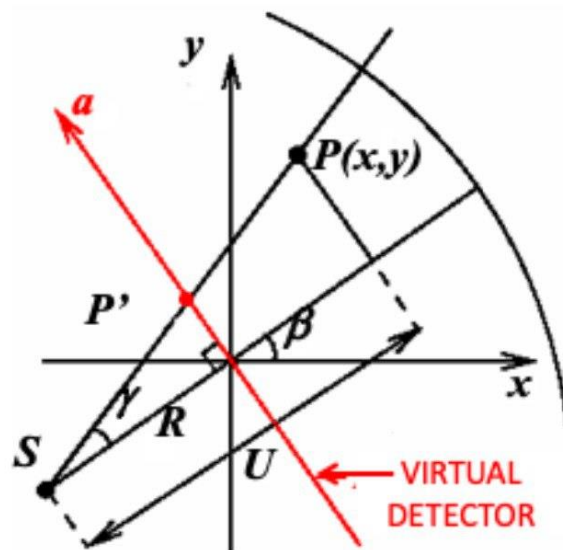


Figure 22: Fan beam geometry representation

For sake of simplicity, detector coordinates and equations refer to a detector virtually positioned across the isocentre of the scanner, as visible by the red arrow in Fig. 22. The coordinates of a fan-beam projection ray are the angular position β of the source (point S, alias the focal spot of the X-ray tube), and the angle of displacement from the central ray γ . With linear detectors, the latter is more conveniently substituted by the displacement of the when hitting the virtual detector, and so $a = R \tan \gamma$. The angular and linear displacement coordinates of the parallel beam geometry can be found as:

$$\vartheta = \beta + \gamma = \beta \arctan\left(\frac{a}{R}\right)$$

$$t = R \sin \gamma = R \sin\left(\arctan\frac{a}{R}\right)$$

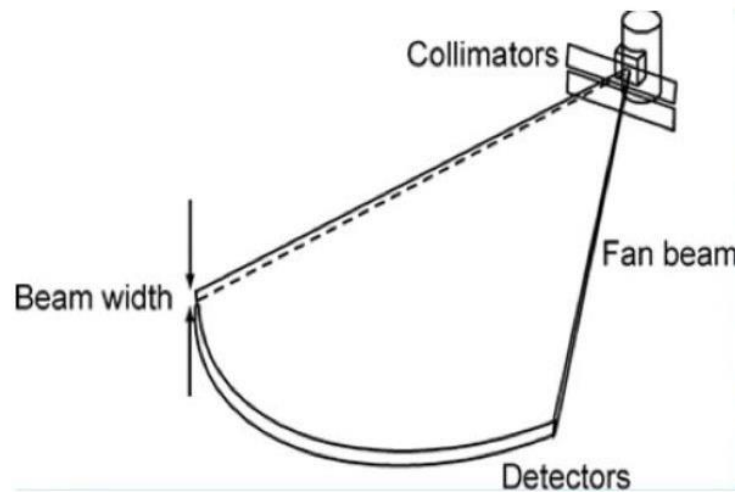
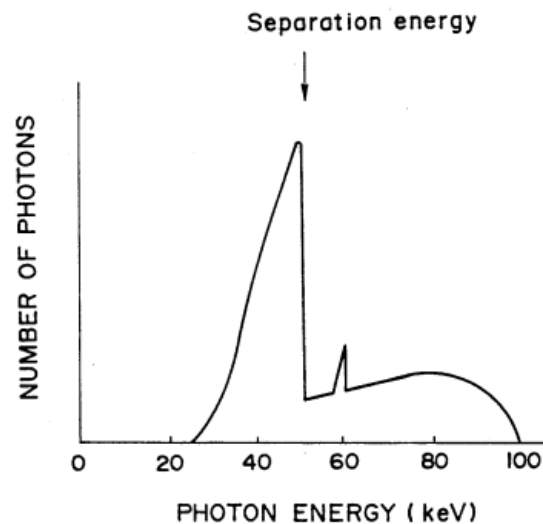


Figure 23 Single slice acquired with fan-beam geometry

2.1.3.4 DEXA: Dual energy X-ray and Image generation

As described in [37], Dual X-ray absorptiometry has undergone many transformations over the past decades. Absorptiometry refers to the imaging modality that estimates the bone mass and soft tissue mass, by the measurement of the amount of radiation attenuation by the skeleton or soft tissue, while an energy beam is transmitted through a subject. From the early 1960s, single photon absorptiometry (with single energy source) was established, followed by

the use of two different energetic levels, Dual photon absorptiometry (DPA), in the 1980s. The two modalities uses a radionuclide source, mainly Gd sources, for the generation of gamma rays, while in Dual X-ray absorptiometry (DXA), a low current X-ray radiation replaces the gadolinium. The use of an X-ray source instead of Gd allows for the generation of higher photon flux with a smaller diameter of the source: as a consequence, higher image resolution, better precision and lower patient exposition to secondary radiation, with faster scanning times. For these reasons, DPA nowadays has been almost completely replaced by the DXA technology. The composition of a DXA scanner include an X-ray tube and a K-edge filter [38]: the latter component allows for the generation of two predetermined energy spectra of the emitted X-ray radiation. Graph 5 shows the X-ray spectrum obtained after X-rays have passed through a K-edge filter made of gadolinium possessing a thickness of 100 μm .



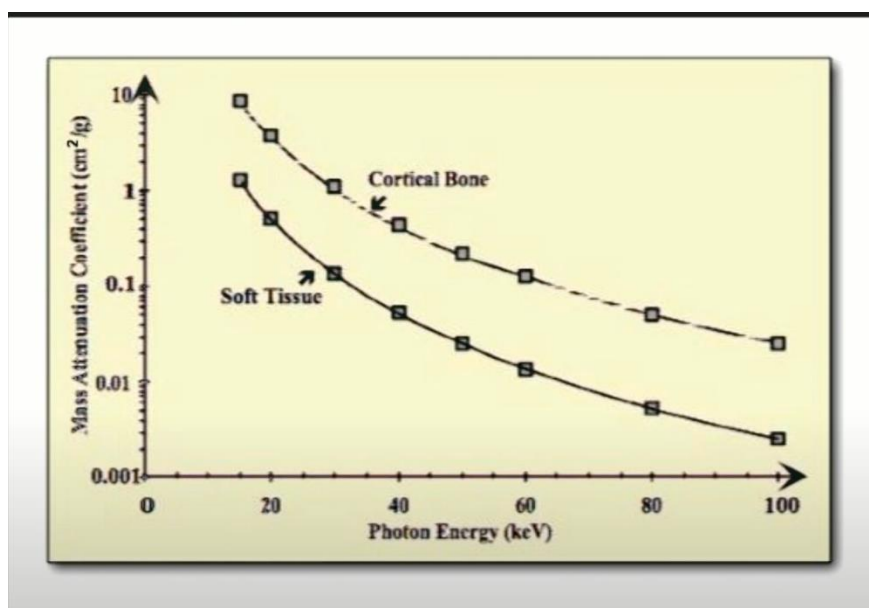
Graph 5: Spectrum of X-rays after gadolinium K-edge filter

It can be seen that the energy spectrum of X-rays is separated into two different energetic regions at a K-absorption edge of Gd at 50.2 KeV.

When a characteristic X-ray is absorbed into the X-ray detector, an output pulse signal accurately representing the energy of an incident photon can be obtained. The output intensity is related to its photon energy: when the energy spectrum of X-rays has been separated by the K-edge filter there'll be generated two categories of effective energy, and so two different classes of pulse signals. An

effective energy of the peak before the separation energy is 45 KeV, while an effective energy of the peak at the side higher than the separation energy is 80 KeV, but it can be measured an effective energy signal up to ranges of 150 KeV.

Dual-Energy X-ray absorptiometry uses subtraction of multiple scans to obtain estimates of the Bone Mineral Density (BMD) and fat content. A soft tissue absorption image is subtracted from a higher energy bone image in order to estimate bone density with a high degree of accuracy. In Graph 6 are visible the typical mass attenuation coefficient curves of soft and cortical bone tissues as compared to photon energy, measured in KeV. It can be noted that at 40 and 60 KeV the absolute and relative values of the two curves change. DEXA scanners exploit this difference in absolute and relative values to calculate DXA images. The acquired image will be then used for the calculation of Bone Mineral Density, allowing also for the diagnose of an osteoporotic risk condition with the measurement of textural parameters. See Section 2.2.2 for further description on BMD.



Graph 6: Mass attenuation coefficient of a soft and cortical tissue

A typical DEXA scan acquisition consists of more than 10.000 individual measurement points (pixels), each one containing both spatial and consequent bone density information related to the intensity of the arrival photons in that specific unit. Examples of 2D images acquired with DEXA scan are visible in Figure 26.

2.2. Clinical use

2.2.1. Screening for patients: inclusion criteria for DXA

Bone density testing is a screening exam that is prescribed under the guidance of specific physio-pathological conditions of a given subject. Bone density testing, as expressed in [39], is strongly recommended in case of:

- Have a prevalence for the development of osteoporotic fracture events due to personal or maternal history.
- Smoking addiction.
- Post-menopausal women not taking oestrogen.
- Post-menopausal women who is very tall or thin.
- Men with clinical conditions associated to bone loss, such as rheumatoid arthritis, chronic kidney or liver diseases.
- Use medications that are known to cause bone loss, including corticosteroids or high-dose thyroid replacement drugs.
- Have type 1 diabetes.
- Have a parathyroid condition, such as hyperthyroidism.
- Have a parathyroid condition, such as hyperparathyroidism.

In Italy, the Quality Department of the Ministry of Health released “Individuazione dei criteri di accesso alla Densitometri Ossea, an attachment of the Legislative Decree 29 november 2001 about the “Definizione dei livelli essenziali di assistenza”. [40]. There’re defined inclusion criteria for the access to the DXA as a screening examination. For the access to the bone densitometry examination, *High Risk Factors* and *Low Risk Factors* are taken into account.

High Risk Factors are defined in the following.

- 1) For female and male subjects of all ages:
 - a) Previous fragility fractures or radiologic confirmation of a vertebral fracture.
 - b) Radiologic diagnosis of osteoporosis.
 - c) Chronic therapies (On-going or scheduled).
 - d) Pathologies at risk of Osteoporosis, like endocrine diseases with significant bone remodelling (hyperthyroidism, hyperparathyroidism)

- 2) Limited to menopausal women:
 - a) Maternal family history of osteoporotic fracture under the age of 75 years
 - b) Menopause before 45 years old.
 - c) Underweight condition: body mass index $\leq 19 \text{ kg/m}^2$.

The densitometry examination is also indicated in presence of the following inclusion criteria:

Low Risk Factors (3 or more) for menopausal women.

- 1) Age higher of 65 years old.
- 2) Family history of severe osteoporosis.
- 3) More than 6 months of premenopausal amenorrhea.
- 4) Inadequate calcium integration.
- 5) Vitamin D deficiency.
- 6) Smoking addiction [>20 cigarettes/day].
- 7) Alcohol abuse [>60 g/day].

Low Risk Factors (3 or more) for men older than 65 years old.

- 1) Family history of severe osteoporosis.
- 2) Underweight condition: body mass index $\leq 19 \text{ kg/m}^2$.
- 3) Inadequate calcium integration.
- 4) Vitamin D deficiency.
- 5) Smoking addiction [>20 cigarettes/day].
- 6) Alcohol abuse [>60 g/day].

2.2.1.1 Osteopenia and osteoporosis: epidemiology

As expressed in [41] "Osteoporosis is an emerging medical and socioeconomic threat characterised by a systemic impairment of bone mass, strength, and microarchitecture, which increases the propensity of fragility fractures". As a background, it will be provided also the definition of Osteoporosis given by the World Health Organization (WHO) [6]: "Osteoporosis is an established and well-defined disease that affects more than 75 million people in Europe, Japan and the USA, and causes more than 2.3 million fractures annually in Europe and the USA alone. The lifetime risk for hip, vertebral and forearm (wrist) fractures has been estimated to be approximately 40%, similar to that for coronary heart disease.

Osteoporosis does not only cause fractures, it also causes people to become bedridden with secondary complications that may be life threatening in the elderly. Since osteoporosis also causes back pain and loss of height, prevention of the disease and its associated fractures is essential for maintaining health, quality of life, and independence among the elderly.” Osteopenia, instead, is a term to define bone density that is not normal but also not as low as osteoporosis. By definition from the World Health Organization osteopenia is defined by bone densitometry as a T score -1 to -2.5 [42]. Women with bone density levels more than 2.5 standard deviations (SD) below the young adult reference population mean are considered to have osteoporosis. In a recorded sample in the USA, 17% of postmenopausal Caucasian women experience osteoporosis, compared to 12% of Hispanic-American women and only 8% of African-American women. [43] published a metanalysis where there were analyzed 40 studies (31 related to Asia, 5 studies related to Europe and 4 related to America), with a total sample size of 79.127 people. The overall prevalence of osteoporosis in the elder in the world was reported to be 21.7% (95% confidence interval: 18.8–25%), while the prevalence divided by sex was divided into 35.3 % for women% (95% confidence interval: 27.9–43.4%), 12.5% for men (95% confidence interval: 9.3–16.7%). Also, results shown that the highest prevalence of osteoporosis in the elders was reported in Asia, 24.3% overall (95% confidence interval: 20.9–28.1%). Furthermore, as fracture incidence is typically higher in countries with a more northerly latitude (Fig. 24), vitamin D status may be implicated.

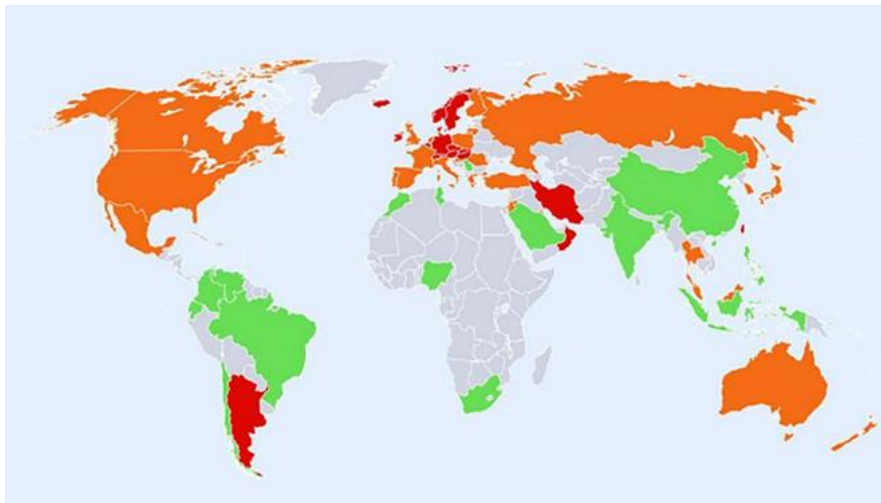
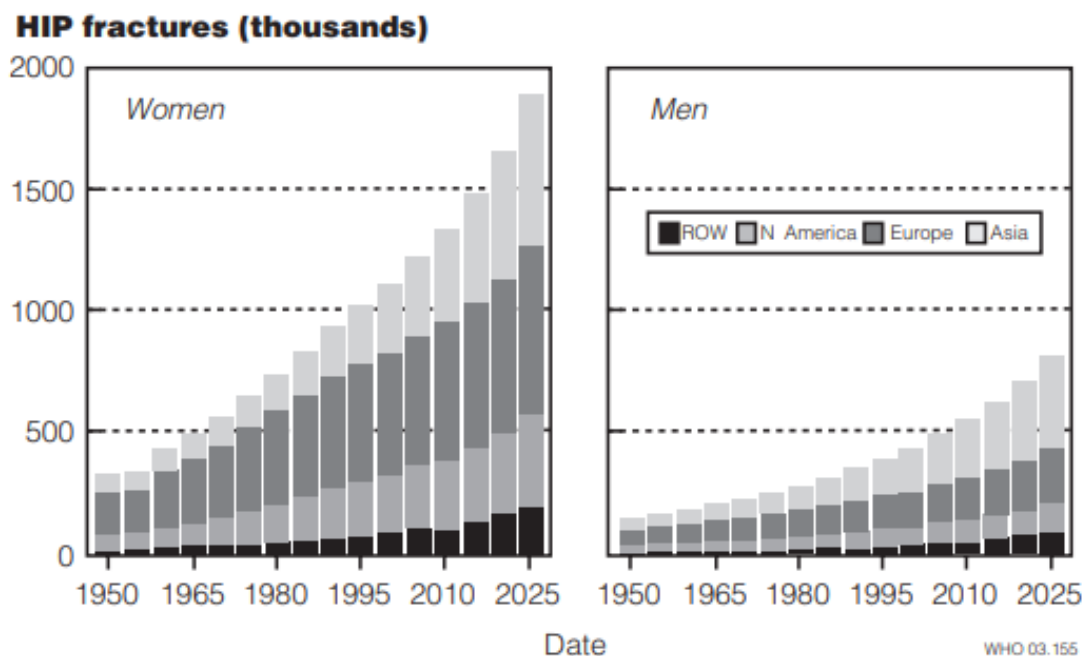


Figure 24: Hip fracture rates for men and women combined in different countries of the world, categorized by risk. Countries are coded red (annual incidence $>250/100\ 000$), orange ($150\text{--}250/100\ 000$) or green ($<150/100\ 000$) where estimates are available

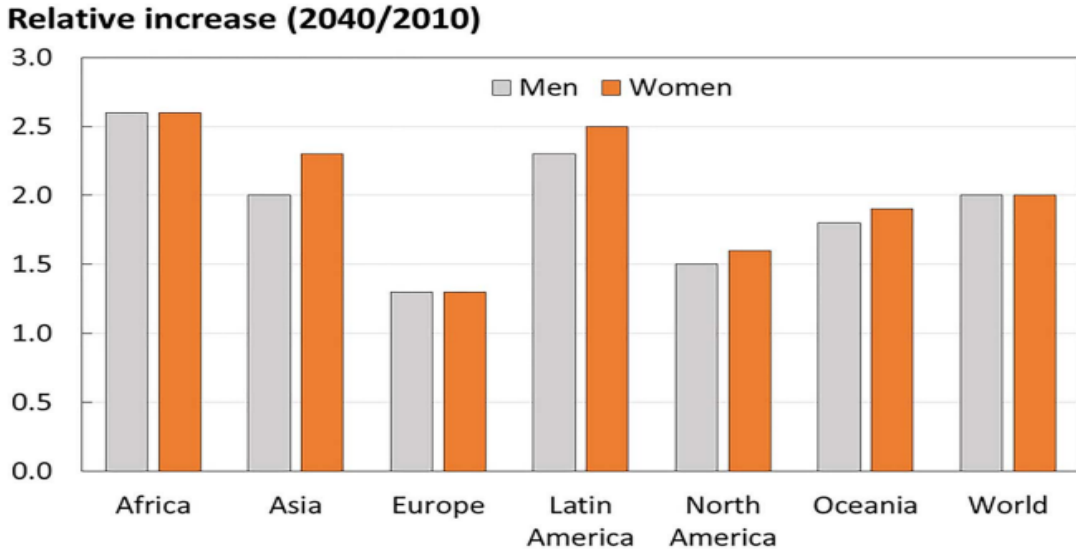
An estimated 1.7 million hip fractures occurred throughout the world in 1990. Since both world population and life expectancy are increasing, that number is expected to rise to 6.3 million by 2050.[6]



Graph 7: Estimates of the number of hip fractures between 1950 and 2025 by gender and region

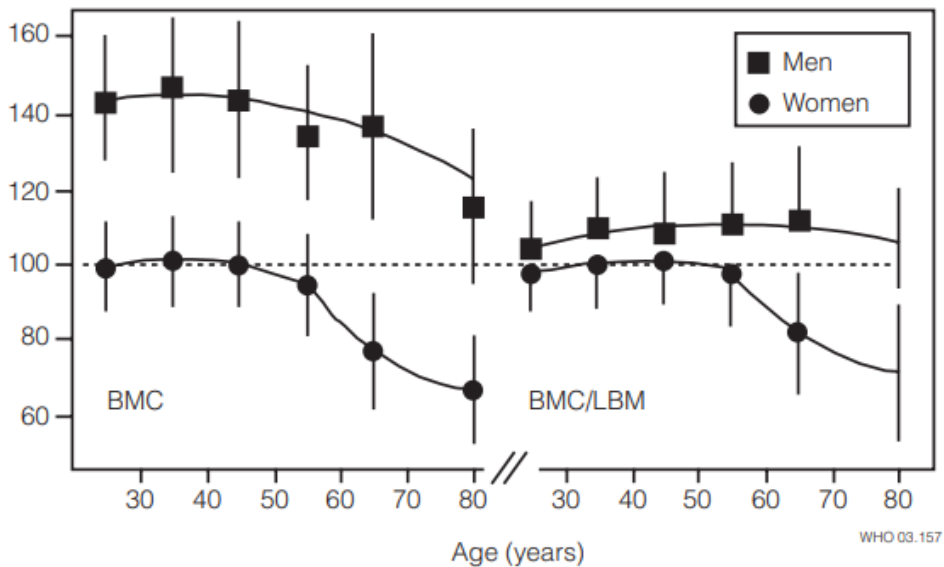
Worldwide, the proportion of individuals living to older age is increasing rapidly, with the United Nations predicting that by 2050 all major areas of the world, with the exception of Africa, will have approximately a quarter of their populations aged above 60 years.³⁴ This ageing population demographic will likely have a significant impact on the number of hip fractures, with a conservative estimate being an increase from 1.66 million in 1990 to 6.26 million in 2050. [44]

The number of individuals at high fracture risk worldwide is also projected to increase, the largest relative increases predicted for Africa, as visible in Graph 8. The fracture risk associated with more developed countries is going has stabilized over the last two decades (Graph 8).



Graph 8: Number of men and women at high fracture risk in 2040 relative to 2010, by world region

Osteoporosis is three times more common in women with respect to men, partly because women have a lower peak bone mass, as visible in Graph 9, and partly because of the hormonal changes that occur during menopause.



Graph 9: Bone Mineral Content (BMC) as a function of age in men and women

The economic burden of osteoporosis-related fracture is significant, costing approximately \$17.9 and £4 billion per annum in the USA and UK, respectively (Table 1 summarizes fracture impact across the European Union).[44]

	Hip	Spine	Wrist
Lifetime risk in women (%)	23	29	21
Lifetime risk in men (%)	11	14	5
Cases/year	620 000	810 000	574 000
Hospitalization (%)	100	2-10	5
Relative survival	0.83	0.82	1.00
Costs: All sites combined ~ €37 billion			

Table 1 : Impact of osteoporosis-related fracture across Europe.

2.2.1.2 Risk factors

Although risk factors for osteoporotic fracture have been identified, risk factors for different fractures may differ. As an example, an early menopause stage represents a high-risk factor for vertebral fractures, but not for hip fractures. Risk factors may be causally related or indirect also. For what concern the former one, they can be associated with personal modification, environmental or therapeutic manipulation, while also indirect risk factors may be useful in determining individuals at high risk.

Trauma

Fractures occur when skeletal loads, whether from trauma or the activities of daily living, exceed the breaking strength of bone. The annual risk of falling increases from about 20% in women aged 35-49 to nearly 50% in women aged 85 years and over, and is 33% in elderly man [6]. Although experimental hazard apply a role in every accidental fall, up to half the falls among the elderly are associated with organic dysfunction, including diminished perceptions of the lower extremities and postural control, gait abnormalities, muscular weakness, decreased reflexes or poor vision.

Low Bone Density

Risk factors for low bone density include inadequate peak bone mass and excessive bone loss. In addition to the accelerated bone loss that occurs at the

menopause, bone loss results also from age-related factors, such as reduced calcium absorption and secondary hyperparathyroidism.

Previous fracture

The occurrence of one osteoporotic fracture may increase the risk of further future fractures. Both in men and women, who have suffered a distal fracture of the forearm, the risk of subsequent proximal femur or spine fractures is almost doubled. [6]

Genetics

Up to 50% of the variance in peak bone mass and some aspects of bone architecture and geometry relevant to bone strength may be determined genetically. A family history of fragility fracture, and particularly of hip fracture, can be used in the risk assessment of patients. [6]

Nutrition

Risk factors associated to nutrition influence bone mass, age-related bone loss and fracture risk. Calcium and vitamin D are of particular interest since their deficiency can be potentially correctable. In a meta-analysis of 33 studies, an association between higher calcium intake and higher bone mass was found in post-menopausal women.[45]. For what concern vitamin D deficiency, it is common in elderly population in many regions of the world, especially in northern latitude countries, as visible in Fig. 24. Lesser degrees of vitamin D deficiency are associated to an increase of the PTH production [46], resulting in increased bone turnover and bone loss in absence of any significant mineralization defect.

Physical inactivity

Immobility is another important cause of bone loss. Enforced immobility in healthy volunteers decreases the bone mineral mass, as do motor deficits due to neurological disorders such as hemiplegia or paraplegia. Bone mineral mass also decreases during space flights due to absence of gravity effect, that takes a crucial role in bone remodelling phenomena. [6]

Cigarette smoking

Cigarette smoking reduces BMD as a result. In [47] it is shown that, after adjusting for potential confounding variables, the participants under analysis

who were current smokers had a Bone Mineral Density that was 7.3 % (95% CI 0.4%-14.2%) lower than participants who had never smoked.

Alcohol consumption

Studies on people dependent on alcohol have suggested that high levels of alcohol consumption could be harmful for bones, possibly as a result, inter alia, of protein and calcium metabolism, mobility, gonadal function and a direct toxic effect on osteoblast. However, a moderate alcohol consumption has not consistently been associated with increased risk of fracture or reduced bone density. [6]

Body mass index

Low body mass index is associated with lower peak bone mass, and an adverse influence on bone loss. This may be the consequence of reduced peripheral oestrogen production by adipose tissue among thin women: in fact, excessive leanness is also a risk factor for hip and vertebral fracture.

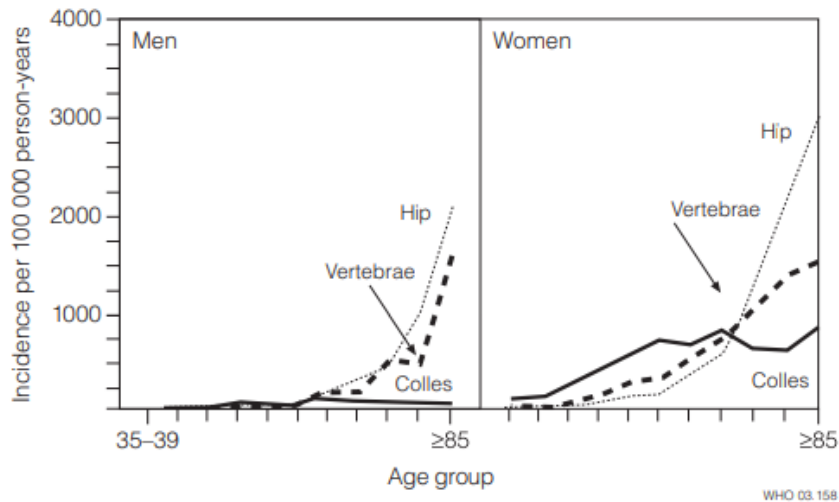
Sex hormone deficiency

Primary hypogonadism in both sexes is associated with low bone mass, and decline in oestrogen production at the menopause is the most important factor contributing to osteoporosis in later life. [6]

2.2.1.3 Skeletal sites

Common sites for osteoporotic fracture are the spine, hip and distal forearm. Hip fractures are the most detrimental osteoporotic fractures, and the majority of them follow a fall from the standing position. There are two main types of hip fractures: intracapsular (cervical or femoral neck fractures) and extracapsular (lateral or trochanteric). [6]

These types of fracture are always painful: for this way they require hospitalization. These 2 groups of hip fractures differ both in their natural history and also in their associated treatment. Trochanteric fractures are more characteristically osteoporotic, and the increase in age and sex specific risk of hip fractures is greater in trochanteric fractures with respect to cervical ones. As visible in Graph 10, the incidence rates of hip fractures increase dramatically in both sexes with age, reaching almost the 3% of cases of fractures considering Caucasian women aged 85 years or more.



Graph 10: Age-specific incidence rates of hip, vertebral and forearm fracture

Talking about the second category of osteoporotic fractures, as reported in [48], vertebral fractures are the most common type of osteoporotic fracture and are associated with substantial morbidity and decreased survival. Women with osteoporotic vertebral fractures have an increased risk of subsequent vertebral fractures and experience reduced health related quality of life (HRQOL) [49], both in short long-term perspective. As included in [48], the Canadian Multicentre Osteoporosis Study declared that 21.5% of men and 23.5% of women aged more than 50 years possess at least one vertebral deformation. Despite the high prevalence of vertebral fracture, more than two thirds of the cases remain undiagnosed. Care gaps in vertebral fracture diagnosis may result from radiologists, which usually focus their attention on the patient's illness rather than skeletal comorbidities. Asymptomatic (morphometric) and symptomatic vertebral fracture can be diagnosed using the Genant semiquantitative method[50], as described in the Figure below.

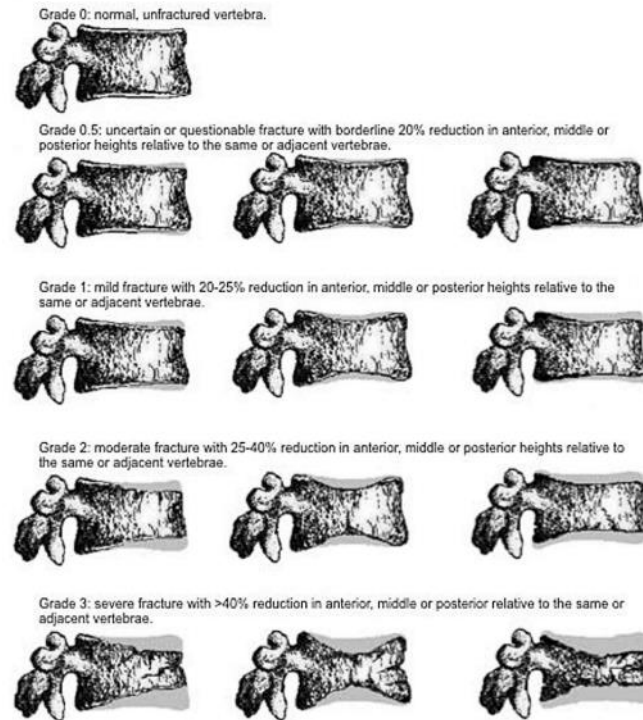


Figure 25: Classification of vertebral fractures by the Genant semiquantitative method

From the pattern drawn as a function of age, the forearm fracture instead differs from the vertebral and hip fractures, as visible in Graph 10. It's stated in [6], that the rates reported in many studies possess an incidence that increases linearly in white women between 40 and 65 years and then stabilize. The reason for the presence of this plateau for female incidence in some countries remains unknown, but it may be related to change in the modalities of falling with advancing age.

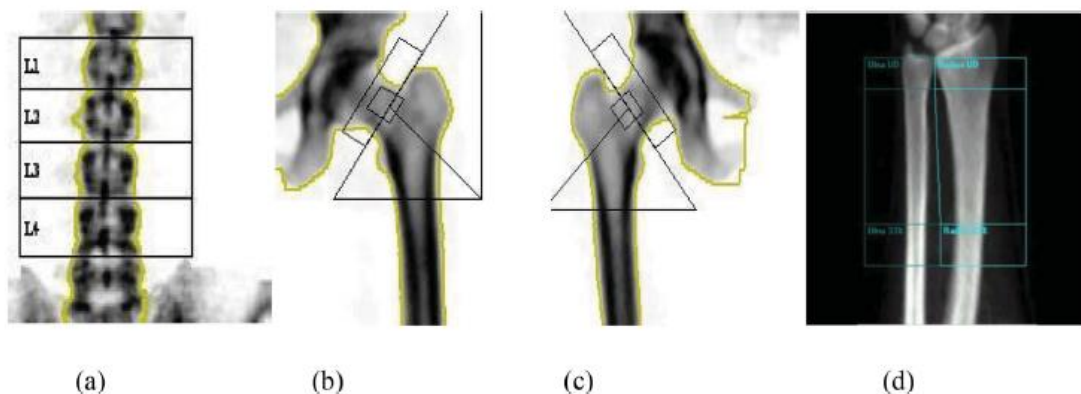


Figure 26: DEXA scan image (a) spine with vertebrae numbering (b) right femur (c) left femur (d) forearm

2.2.2. Bone Mineral Density

Assessment of bone mass, mostly termed as Bone Mineral Density (BMD) is the standard method for the definition of a diagnostic approach for an osteoporotic fracture risk evaluation. An osteoporotic condition could potentially be evaluated in different modalities: strong evidence supported the perception that defining a BMD-threshold, which could take into account most of the patients with fracture, could be a reasonable and easy-to use approach to diagnose osteoporosis [51].

In 1994, an expert panel of the World Health Organization (WHO) recommended thresholds to divide among different categories of patient at risk of osteoporosis and proposed the DXA examination at the hip as the standard technology for the evaluation of an osteoporotic condition [51]. “Dual X-ray absorptiometry was used for measurement of BMD, bone mineral content (BMC), and the projected area of the lumbar vertebrae”[52]

In the study of [52], it was presented a model for the calculation of the apparent volumetric bone mineral density (BMD_{vol}), since DXA scanning is projected to give as output 2D images, not volume reconstruction: therefore, indirect measurements are required (Figure 27). In this study, it was tested the validity of the proposed model with the use of magnetic resonance imaging (MRI) for the measurement of the vertebral dimension. As a result, the precision error (coefficient of variation, CV) of the method for the measurement of the vertebral volume, based on three consecutive measurements on ten subjects, was 1.0%.

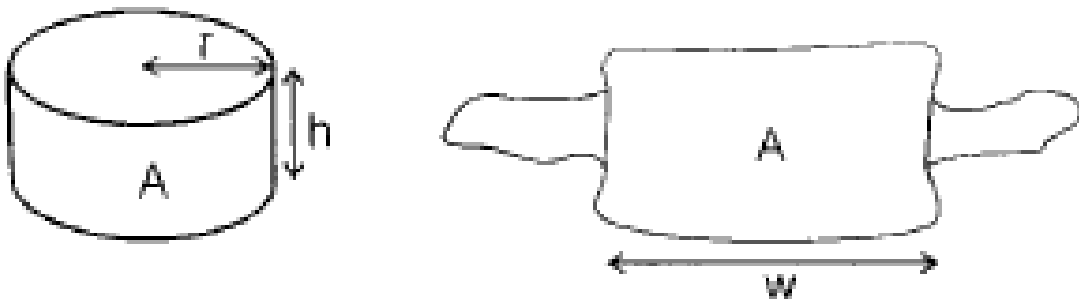


Figure 27: Model for the calculation of volumetric bone mineral density (BMD_{vol}) using DXA data

The lumbar body was assumed to have a cylindrical shape: the volume of the cylinder and (BMD_{vol}) were calculated as follows:

$$Vol = \pi r^2 h = \pi (w / 2)^2 (A / w)$$

$$BMD_V = BMC / Vol = BMD_A [4 / (\pi w)]$$

Where w = mean width of the vertebral body and A = mean area of vertebral body.

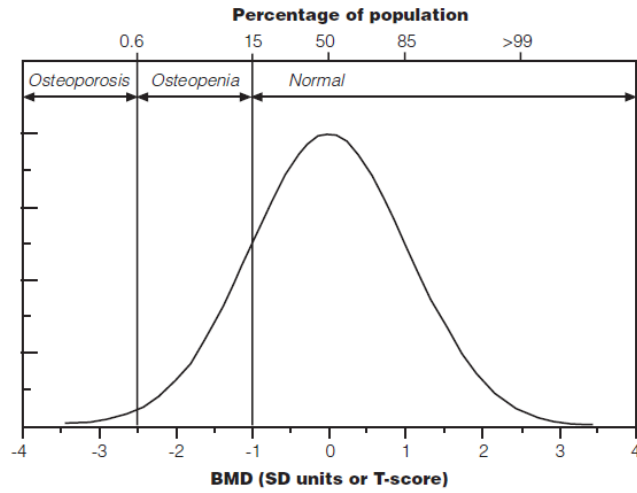
As declared in ('WHO Technical Report Series 921 prevention and management of osteoporosis report of a WHO Scientific Group', no date), the distribution of bone mineral content or density in young healthy adults is approximately normal irrespective the measurement technique used. With this distribution, individual bone values can be compared in relation to a reference young healthy population database value (NHANES III data, for femoral neck and total hip) [53], in standard deviation units. This reduces the differences in instruments calibration. Standard deviation units in relation to the young healthy population are called T-scores. The Z-score is another interpretation that describes how much the individual BMD differs from the mean value expected for age and sex [54]: however, it is important to note that it cannot be used to diagnose osteoporosis [51].

T-score of the BMD is then calculated by taking the difference among the patient's measured BMD and the mean BMD of the young normal population, and then by dividing this difference with the standard deviation (SD) of the BMD of the young normal population. The Z-score is similarly calculated, by comparing the patient with his/her age matched group.[54]

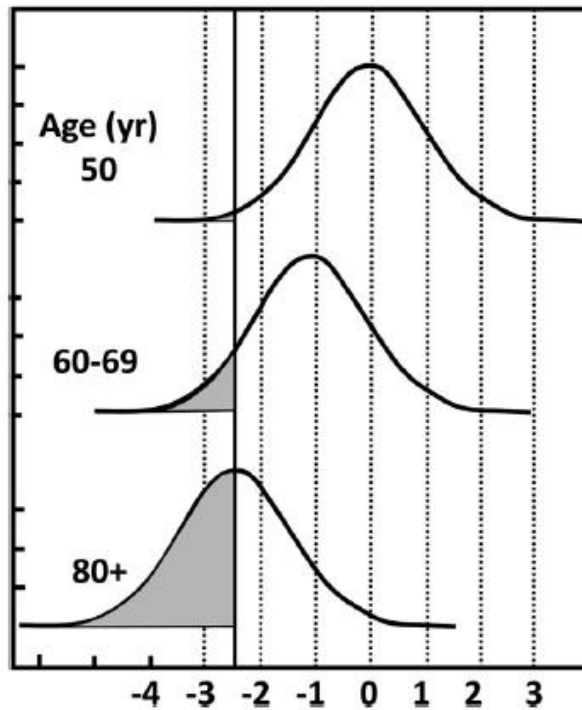
$$T - score = \frac{\lambda - \mu}{\sigma}$$

$$Z - score = \frac{\lambda - \beta}{\alpha}$$

Where λ = Patient's measured BMD, μ = Mean BMD of young normal population, σ = SD of BMD of young normal population, β = Mean BMD of age-matched group, α = SD of BMD of age-matched group.



Graph 11: Distribution of BMD in young healthy women aged 30-40 years



Graph 12: Increasing prevalence of osteoporosis with increasing age when using WHO criteria for diagnosis of osteoporosis

According to ('WHO Technical Report Series 921 prevention and management of osteoporosis Report of a WHO Scientific Group', no date) the following four general diagnostic categories for women have been proposed:

- *Normal*. A BMD value within 1 SD of the young adult reference mean (T-score ≥ -1).
- *Low bone mass (osteopenia)*. A BMD whose value is between -1 SD and -2.5 SD with respect to the young adult mean.
- *Osteoporosis*. A BMD value lower or equal to -2.5 SD with respect to the young adult mean.
- *Severe osteoporosis (established osteoporosis)*. A BMD value lower or equal to -2.5 SD with respect to the young adult mean, but in this case in presence of one or more fragility fractures.

Here below, a summarizing table for Caucasian women:

Category	Definition
Normal	A value for BMD or bone mineral content (BMC) within 1 SD of the young adult reference mean.
Low bone mass (osteopenia)	A value for BMD or BMC more than 1SD below the young adult mean but <2.5 SD below this value.
Osteoporosis	A value for BMD or BMC 2.5 SD or more below the young adult mean.
Severe osteoporosis (established osteoporosis)	A value for BMD or BMC 2.5 SD or more below the young adult mean in the presence of one or more fragility fractures.

Table 2: WHO diagnostic categories for osteoporosis.

2.2.3. Trabecular Bone Score

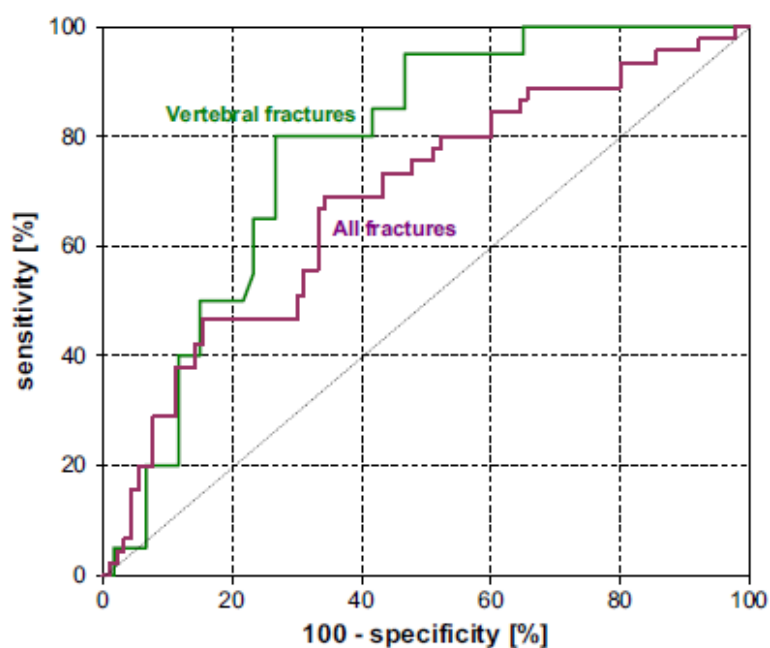
The diagnosis of osteoporosis with DXA suffers from the lack of any evaluation of the 3D microarchitecture of bone tissue, which constitutes an important component of bone strength[55]. To meet the need for a clinical tool capable of assessing bone microarchitecture, the Trabecular Bone Score (TBS) was developed. As cited in [56], TBS has emerged as “[...] a novel grey-level texture measurement that uses experimental variograms of 2D projection images, quantifying variation in grey-level texture from one pixel to the adjacent pixels”. TBS is not a tool capable of directly assessing the bone microarchitecture, but it’s

related to bone characteristics such as the trabecular number, the trabecular separation and the connectivity density.

A high value of the Trabecular Bone Score is associated to a subject possessing fracture-resistant microarchitecture, while a low TBS score indicates a fracture-prone microarchitecture. "There's evidence that TBS can differentiate between two 3-dimensional (3D) microarchitectures that exhibit the same bone density, but different trabecular characteristics.[56].

In [55] it was carried out a case-control study for the evaluation of the potential use of TBS as a complement of BMD measurement, in the prediction of osteoporotic fractures and vertebral fractures alone. The study group was composed by 45 patients with osteoporotic fracture (cases) and 90 age matched controls. Subjects with pathology and/or treatment who could interfere with bone status were not included in the sample. Total spine L2-L4 BMD readings were examined by an expert in DXA scan interpretation. The Trabecular Bone Score was evaluated on the same anatomical regions scanned for the measurement of BMD. The TBS at spine was evaluated as mean value of the measurements of the L2, L3 and L4 vertebrae. The diagnostic value of each parameter was evaluated both by odds ratios (ORs) and by area under the receiving operator curve (AUC: Area under the ROC curve).

Results shown that, in the comparison of the fractured subjects vs non-fractured ones the mean values for spine TBS were significantly different ($p = 0.0005$): in addition, TBS was a statistically predictor of a pathological condition, with an OR of fracture vs. no fracture equal to 1.95 (95% CI : 1.31-2.89) and corresponding AUC of 0.685 (0.599-0.762). In the comparison of only vertebral fractured patients vs control, the OR and AUC increased further: values were respectively 2.66 (1.46-4.85) and 0.776 (0.669-0.862).



Graph 13 Visual comparison between ROC curves of TBS in the discrimination of all fractures combined and vertebral fractures alone

Answering to the question: “What evidence do we have today that TBS reflects bone microarchitecture and perhaps bone strength”, [57] reported that TBS texture measurement was initially performed on 3D micro-computed tomography (μ CT) images and then it was subsequently adopted by DXA measurements, which are based on 2D projection. As cited in [28], since trabecular distribution in the femur region is asymmetric and more complicated, no TBS-like evaluation has yet been developed for femoral trabecular structure.

The TBS method was developed using 3D μ CT images of trabecular bone specimen (vertebra, femoral neck and radius) from human cadavers. Each 2D image obtained with the 3D μ CT is binarized by means of global thresholding: among the pixels in the 2D image, those corresponding to bones are assigned a value 1, while those corresponding to intertrabecular space a value of 0. The values of the voxels (1 or 0) along the projection axis (anteroposterior (AP) for the vertebrae) are summed. At the end, this method will produce as output a 2D image, Figure 28, b. The grey-scale variations in pixels located close to one another in multiple random directions constitute the experimental variogram. The TBS score is the slope at the origin of this experimental variogram on a log-log representation, Figure 30.

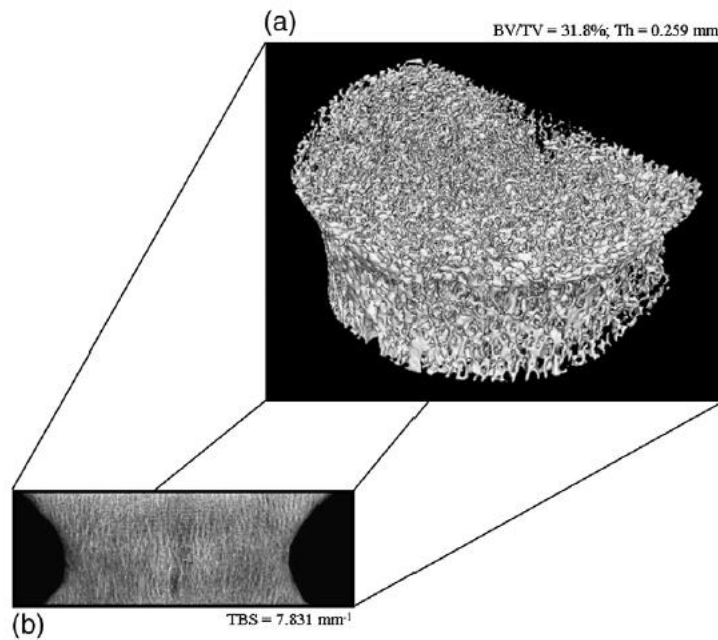


Figure 28: (a) Three-dimensional reconstruction of the trabecular bone microarchitecture in a human cadaver sample. The 2D projection image was obtained by projecting the 3D volume following the AP axis (b)

Coming back to DXA acquisition, the DEXA image, as discussed previously, is generated based on the X-ray absorption at two different energy intensities. The TBS and BMD computations are performed separately and via different methods: for what concern the Bone Mineral Density calculation, Section 2.2.2 describes the principles. The TBS calculation, instead, is computed as described above, so by construction of the slope at the origin of the experimental variogram. As it can be intuitively understood, a 3D image of a compact network at the trabecular level will produce 2D projection images with many grey-level variations of small amplitude and, therefore, a steep slope at the origin of the variogram and consequently a high value of the TBS. variogram, using an algorithm adapted to the characteristics of the DXA images [57]. A low TBS value, in contrast, indicates a poor-quality architecture of the trabecular bone structure, with few grey-level variations of considerable amplitude, therefore a clement slope at the origin of the experimental variogram. As with BMD, the TBS values are calculated for each vertebra and for the overall region of interest. The values possessed by each pixel are shown in coded colours (green, yellow and red) on the final produced report, as shown in Figure 29.

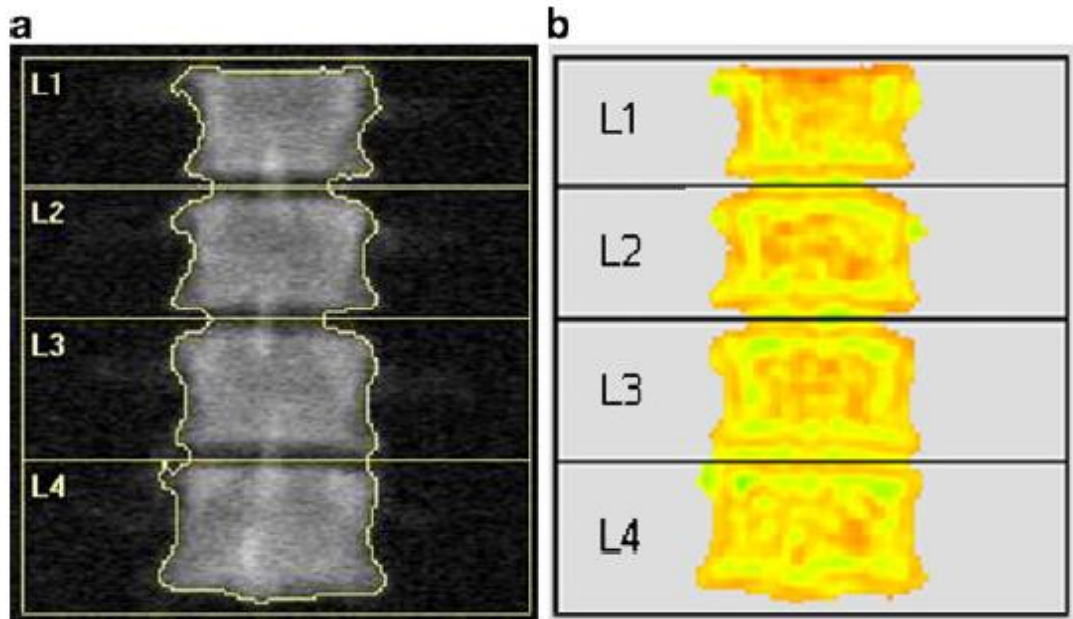


Figure 29: Application of TBS mask on DEXA bone segmentation

A workflow of the algorithm for the calculation of the TBS is provided in figure 30.

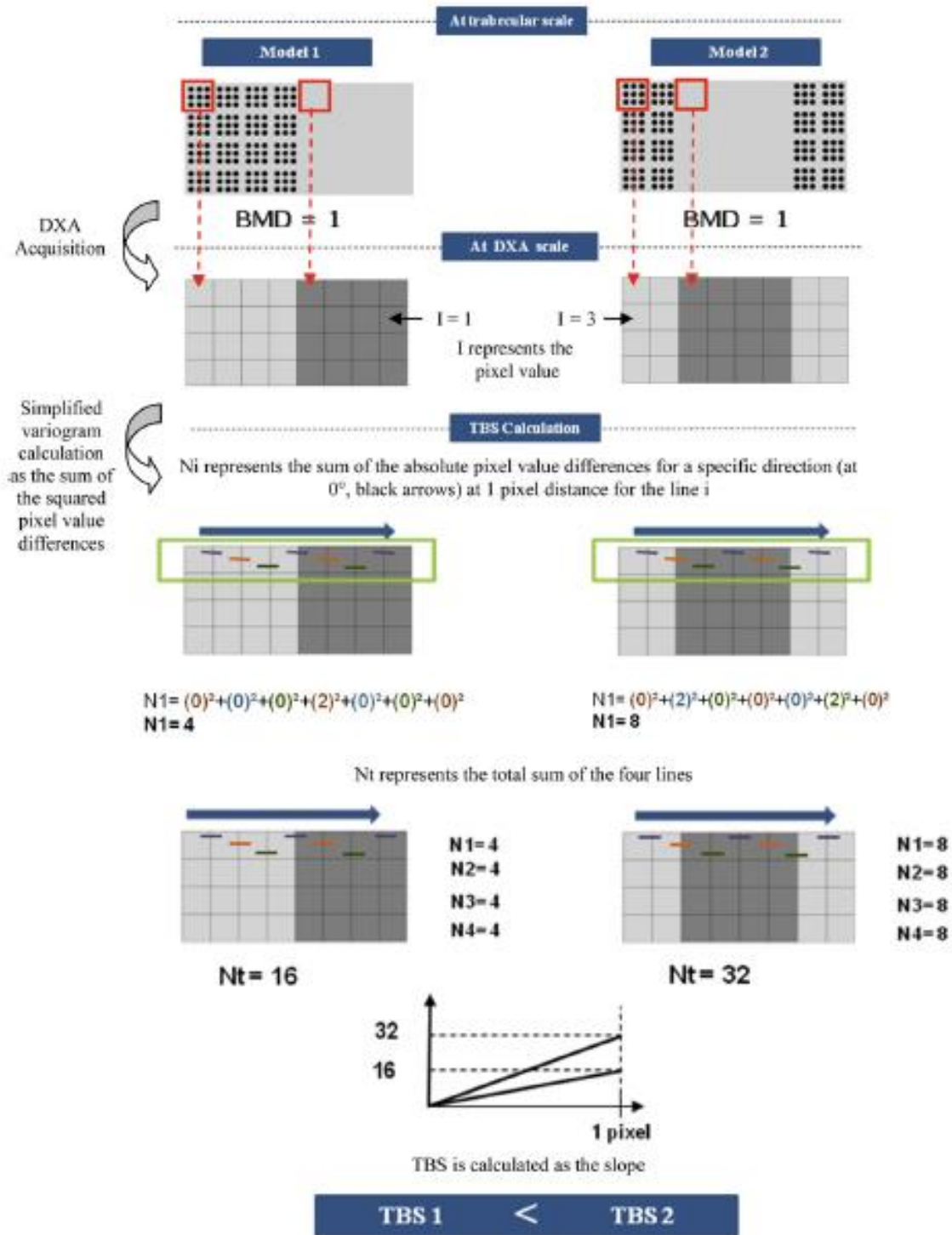


Figure 30: A TBS calculation example using two basic structures, composed of a plate and a set of rods. The two models present the same amount of bone. To simplify the TBS explanation, only one direction is considered, a distance of 1 pixel is used.

2.2.3.1 International Commission Of Clinical Densitometry Iscd: Tbs

As cited in [53] “The International Society for Clinical Densitometry (ISCD) is not-for-profit multidisciplinary professional society with a mission to advance excellence in the assessment of skeletal health”.

With the evolution of the bone densitometry, associated technologies, reference databases etc. it has been necessary to address the issue of a distributed amount of information by a central organ, with the aim to provide and share knowledge among healthcare professionals for the field of the skeletal health. Regarding TBS, the ISCD expressed its Official opinion about the use of the Trabecular Bone Score, but the main concept to be taken into account is the fact that TBS cannot be used alone as a diagnosis instrument for an osteopenic or osteoporotic condition.

The list of observations is reported below:

- TBS is associated with vertebral, hip and major osteoporotic fracture risk in postmenopausal women.
- TBS is associated with hip fracture risk in men over the age of 50 years.
- TBS is associated with major osteoporotic fracture risk in men over the age of 50 years.
- TBS should not be used alone to determine treatment recommendations in clinical practice.
- In patients receiving anti-fracture therapy:
 - The role of TBS in monitoring anti-resorptive therapy is unclear.
 - TBS is potentially useful for monitoring anabolic therapy.
- TBS is associated with major osteoporotic fracture risk in postmenopausal women with type II diabetes.

2.2.4. Bone Strain Index

Although DXA measurements is the most widely adopted technique to provide information about the bone mineral density and bone mineral content, BMD does not take into account for three-dimensional structure of the vertebrae and for the local distribution of the bone mass. [28] declared that the results of this lack of information allows to predict from longitudinal DXA only the 70% of vertebral fractures. The remaining 30% is related to the lack in the information about the

bone strength, being its nature related to the capability to withstand an applied load. Textural parameters such as BMD and TBS provide useful information about bone quantity and bone quality, respectively, but detailed information about geometry and load definition are still missing.

“Considerable effort has been done in order to define a patient-specific structural engineering and Finite Element Models (FEMs) of the proximal femur to estimate femoral strength and to assess hip fracture risk”. [28]

Recently, it has been developed a bone FEM analysis on DXA images named Bone Strain Index (BSI), in order to take into account bone strength features in the prediction of a fracture risk. Bone Strain Index automatically calculates strains and stresses in a bone segment, starting from a specific loading condition, defined specifically for each patient. It is based on finite element algorithms usually used in engineering applications[28] It will be described the principle of working of this algorithm in the following.

The automatic FEA algorithm uses constant triangular mesh following the contour of the bone segmented by DXA dedicated software: at each point of the triangle will be defined properties of stress and strain locally applied using a linear elastic model. The choice of a linear elastic model is given by the reduction of the computational time associated for the construction of the FE model. This will allow to have an easy and not time-consuming implementation of the numerical tool into the workstation used for the DXA. To assign a local value of elastic modulus to each element of the mesh [28] used a linear proportion between the values of the greyscale and the values of local stiffness: In case of a high greyscale value associated to a given pixel, its corresponding local stiffness will be proportionally high, as comprehensible in the following formula.

$$\bar{G} = \frac{\sum_{i=1}^N G_i}{N}$$

$$E_i = \frac{E_0 G_i}{\bar{G}}$$

Where:

- \bar{G} is the mean greyscale value of the scanned DXA matrix.
- G_i is the local greyscale value associated to each pixel of the 2D DXA scan
- N it's the total number of pixels that compose the actual image

- i represents the scanning index of rows and columns in the DXA matrix.

E_0 instead represents the initial global elastic modulus measured from experimental compressive tests. With this computation, it is possible to obtain a 2-dimensional matrix containing the scaled values of stiffness E_i according to E_0 and \bar{G} . Here in Figure 31 (a) it is possible to capture a greyscale image obtained from DXA on a porcine bone sample, while on 31 (b) it's possible to visualize a schematic of the FE- model o the cylindrical sample, including the mesh and the boundary condition.

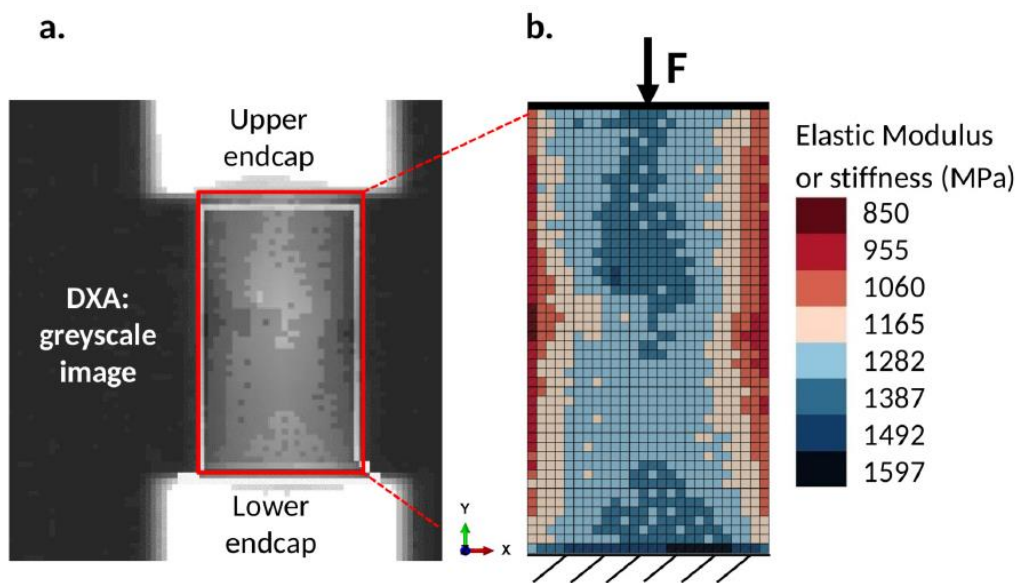


Figure 31: (a) Greyscale image obtained from a DXA on a porcine bone sample (b) Schematic of the FE-model of the cylindrical sample, including the mesh, the loading and boundary conditions

The analysis performed by the Bone Strain Index can be applied both to the vertebral and femoral district. For what concern the vertebral region the analysis starts with building a separate model for each vertebra with the load applied to the upper plate and the constraints applied to the lower plate, according to what described by [28]. a visual representation of this configuration is given in Figure 32.

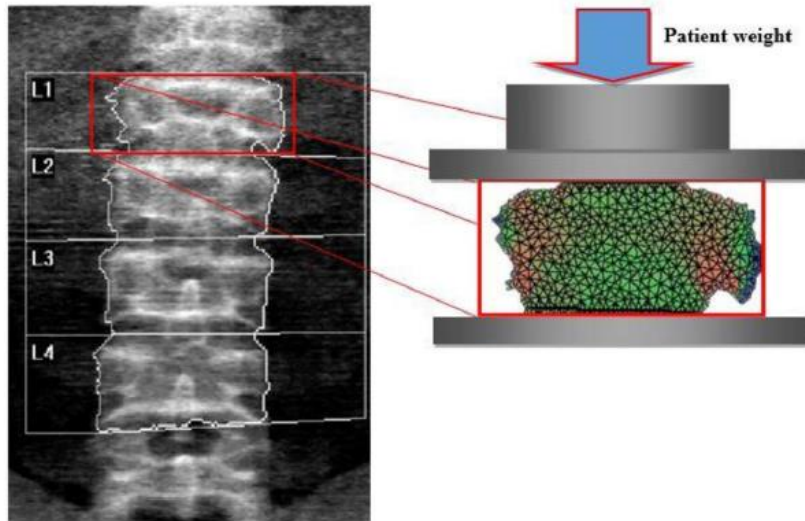


Figure 32: (a) Example of a DXA scan and (b) FEM mask on L1 vertebra obtained with the application of patient weight load

Regarding the femoral region, BSI is instead calculated based on the hypothesis of a “sideways fall” condition with constraints placed on the femoral head and on the lower part of the shaft, and the force applied to the greater trochanteric area, as it was described in [58], also visible in Figure 33 here below.

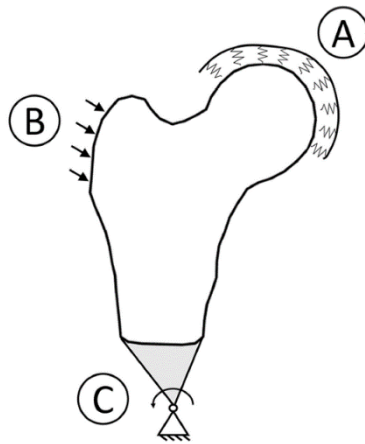


Figure 33: Boundary conditions graphic overview. To simulate a sideways fall condition, the head was bound to the ground using a spring element (B). the impact force was applied on (B), while the distal femur was linked with a hinge (C)

However, in both cases BSI represents a average equivalent strain inside the bone, with the assumption that a high level of strain obtained from the computed mask indicates a bad patient condition, in which the bone is submitted to high load that provoke the generation of high stress value intensities. This result will indicate a propensity to a higher fracture risk condition [28].

The values possessed by each value of the mesh are shown in coded colours on the final produced report Being BSI a strain, this parameter will be unitless, since it's referred to the variation of a dimension referred to the original dimension., mostly express in percentage. In figure 34 and 35 there'll be provided DEXA ROI at the vertebral and femoral district, respectively, with their corresponding calculated strain meshes.

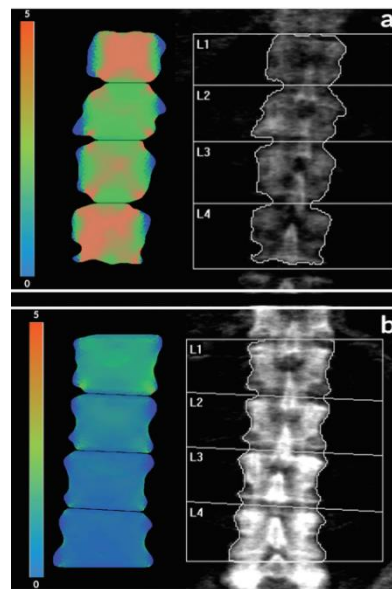


Figure 35: Example of 2 DXA scan vertebral ROIs with their corresponding BSI meshes. As it can be noted, the upper figure (a) is associated to a patient with a higher fracture risk with respect the lower figure (b).

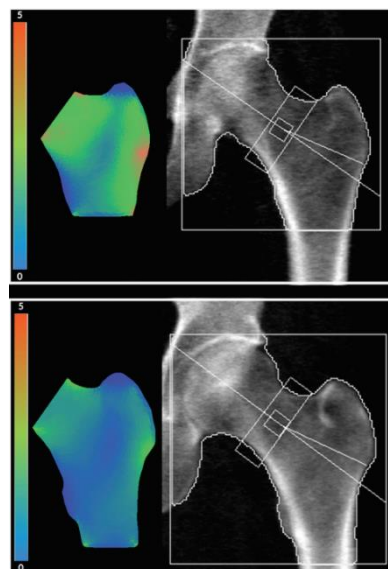


Figure 34: Example of 2 DXA scan femoral ROIs with their corresponding BSI meshes. As it can be noted, the upper figure (a) is associated to a patient with a higher fracture risk with respect the lower figure (b).

3. Mini Health Technology Assessment: multidisciplinary evaluation of consequences after replacement

3.1. Technology Benchmarking

Dual X-ray absorptiometry, nowadays, can be exploited by several image analysis methods to evaluate bone mass and density, bone microarchitecture and bone segments subjected to higher loadings. From 2016, as declared in Section 1.4, it was installed GE-Bravo DEXA scanner in “Repubblica” centre: the machine has been the gold standard technology for the diagnosis of skeletal pathological conditions, as outlined by a panel of experts of the World Health Organization (WHO)[51].

However, reasons related to the obsolescence of the machine with others related to the possibility to exploit useful innovation present at the state of the art, brought to the establishment of this project: the replacement with an innovation technology is an idea that was born as a proof of a multidisciplinary involvement in sharing knowledge and experience, with the aim to generate additional value for the patient experience in CMS and for the support to the clinical evaluation diagnosis. This allows to place the CMS “technological leadership” in an advantageous position: the possibility to adopt healthcare technologies that allow the health clinic to be the one of first adopters of the equipment grant to enrol and attract both physicians and patients.

For this reason, after the consultation of the medical opinion about their necessities in using the most advanced technology, it has been decided to carry out a Mini Health Technology Assessment (mini-HTA) to acquire information about the technical characteristics and current use of the technology. This has been done in order to generate the ideal target in the choice of the new machinery. The reason why it’s called mini-HTA and not simply HTA is related to two main aspects, which are presented below:

- the organizational complexity of the figures that are working on the development of the project.
- The Focus of Action, which is referred to the centre of attention, which

		Focus of Action	
		Clinical Practice	Managerial decision making
Organizational Complexity	High (Team-group-unit)	(Q3) 'Internal Committee' Model	(Q4) 'HTA Unit' Model
	Low (Individual)	(Q1) 'Ambassador' Model	(Q2) 'Mini-HTA' Model

could be limited, as in this case, to effectiveness and safety of the process.

Table 3 : Different organizational arrangements for HTA report realization

The organizational complexity considers how many people are working on the realization of the HTA: in this case, the project has been carried out by a single person. Moreover, the Focus of Action can be differentiated into two categories: the centre of attention can be limited to the analysis of the Clinical Practice, which considers only effectiveness and safety, or it can be extended to a Managerial Decision Making, which means covering all the nine domains of the Core Model, constructing a comprehensive HTA. In the previous table the project will be positioned in the Q2 quadrant. The differentiation using these two main aspects is indicated in [59].

The aiming target of the technology was shaped according to clinical, technical and structural specification and constraints: for what concern the clinical part, the targeting technology was projected to perform normal DXA 2D image acquisitions at different skeletal sites, such as anteroposterior (AP) spine, dual femur, femur and forearm. Moreover, the clinical requirement to be satisfied were about the introduction of innovative software for the execution of textural

measurements, in order to acquire information not only about bone quantity, but also regarding bone quality microarchitecture. For this way TBS integration was required, at least. Further, the system was required to be compliant with orthopaedic and paediatric patients: the first ones refer to the possibility to perform the examination also on patients that present an orthopaedic prosthesis [60] whose inner materials, being high-attenuation materials, could generate streak artifacts around the implantation zone. Concerning technical requirements, instead, the machine was required to be equipped with DICOM 3.0 standard [61] and to be HL7 compatible in order to permit a standardized, precise and error-free sharing of a so sensitive category of data. From the structural point of view, as it will be discussed in the following, structural requirements were to be satisfied due to facility constraints related to the room dimension that is going to host the machine: for this way, different DXA model brand were evaluated before the decision-making implementation. In the following it will be presented the description of all the competitors' specification that were taken into account into this multidisciplinary evaluation.

The European network for Health Technology Assessment (EUnetHTA) is the preferred facilitator of high-quality HTA collaboration in Europe, that has the aim to connect public national/regional HTA agencies, research institutions and health ministers, enabling a standardized realization of HTA reports, based on fundamental criteria. Moreover, it supports an effective exchange of information to support policy decisions by Member States. [62]. At the beginning of 2016 it was released the HTA Core Model Version 3.0 [63], that is a methodological framework for the production of such standardized HTA report. The Core Model, for the realization of a comprehensive HTA document, includes nine different domains that answer to the question related to the impacts in the adoption of a new technology:

- Health problem and current use of technology (CUR).
- Description and technical characteristics of technology (TEC).
- Safety (SAF).
- Clinical effectiveness (EFF).
- Costs and economic evaluation (ECO).
- Ethical analysis (ETH).
- Organisational aspects (ORG).
- Patients and Social aspects (SOC).

- Legal aspects (LEG).

It's of our interest since a subgroup of the domains included in the Core Model was taken into account for the realization of this Mini-HTA report: in particular Description and technical characteristics of technology (TEC), Clinical effectiveness (EFF), Organizational aspects (ORG) and Costs and economic evaluation (ECO) domains were analysed to order to produce indications for the final decision-making process. The reason why to produce a HTA report using these fields is justified by the use of the adopted model, presented here below.

In order to answer to all the possible doubts related to the domains under analysis, "Mini-HTA will be therefore defined as a checklist with several questions about the prerequisites and consequences of using the health technology"[64]. "The Mini-HTA forms used in Denmark typically include twenty to thirty questions grouped according to the four HTA perspectives: technology patient, organization and economy"[64]. It was decided to use the Denmark Mini-HTA model since it can be easily alienable with the necessities of the CMS: being a complete private reality that is experiencing a swift growth, it was necessary to undertake a short timeframe and a limited resources analysis. Of course, this won't ensure the same comprehensivity and quality as an HTA, but at its best it represents a systematic account of the knowledge that the organization itself will be to deliver within a very limited timeframe. [65]. The description of such domains, trying to answer to all their relative aspects, will be reported in the following Sections.

3.2. Description and technical characteristics of the technologies (TEC)

In the following it will be presented the description of the innovation technologies that were taken into examination: it will be provided a description of the technical, clinical and structural specification. In Section 4.4, then, it will be presented the Multi Criteria Decision Analysis (MCDA) framework through which it has been arrived to the final choice in the adoption of the new technology.

3.2.1. FDX Visionary DR, 3D DXA Scan

Being already installed in “Via Larga” and “Nembro Esselunga” centres a Fujifilm DEXA model brand, it has been convenient, thanks to already established communication among the potential supplier, the consultation of an offer coming from this line. The model that was considered names FDX Visionary DR: its specifications were analyzed from the technical, clinical and structural point of view, trying to respect the constraints that were described in Section 3.1. From the clinical point of view the technology was realized with the possibility to execute:

- Anteroposterior (AP), Dual Femur, Femur and Forearm skeletal sites DXA acquisitions.
- Bone Mineral Density (BMD) computation.
- Orthopedic and pediatric applications.
- Total Body BMD. This modality allows to have a ROI consisting of the entire body including the head.[66]



Figure 36: FDX Visionary DR scanner

Fractural risk assessment (FRAX[®]) [23] was included in the collection of included software packages, allowing for the possibility to estimate 10-year fracture probability from obtained clinical risk factors (CRFs)[67].

Moreover, in order to fulfill the clinical requirement requested by specialists in endocrinology with the support of the health director, about the introduction of an innovative software for the execution of textural measurements of bone quality and microarchitecture, the machine under analysis was equipped with a

software algorithm called 3D-DXA, that assesses the proximal femur, only, from a standard hip DXA scan, providing to clinicians an advanced characterization of the cortical and trabecular structures.

As referenced by [68], a statistical shape and appearance model together with 2D-3D registration approach are used to model the femoral shape and bone density distribution in 3D from an anteroposterior DXA projection. Measurements characterizing the geometry and density distribution were computed in both cortical and trabecular compartments.

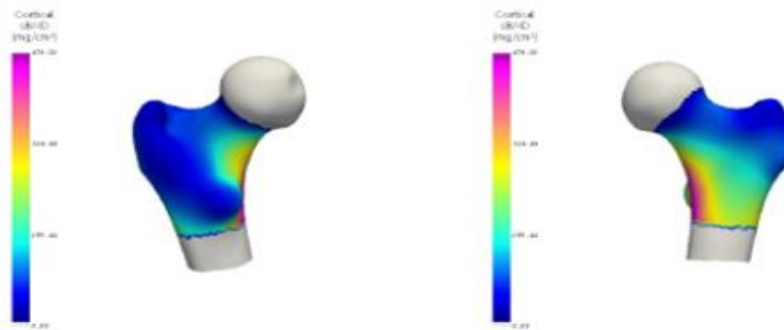
A framework of the algorithm consists into a generation of a 2D mask of the DXA scan, that defines the region of interest to be used in the 3D-2D registration algorithm, and that will be used to initialize the statistical model: the latter will provide a subject-specific femoral shapes and density volumes from anteroposterior DXA projections. The parameters of the model are optimized in an iterative process, in order to maximize the similarity between the projection of the model in AP direction and the DXA image [68]. At the end of the iterations, the statistical model will provide as a result the values of Cortical Surface Bone Mineral Density (Cortical sBMD, expressed in mg/cm^2), Trabecular Volumetric Bone Mineral Density (Trabecular vBMD, expressed in mg/cm^3) and the Integral Volumetric Bone Mineral Density (Integral vBMD, expressed in mg/cm^3): the latter one represents the union of cortical and trabecular compartment. Moreover, the results related to the cortical and trabecular bone density are then used to compute the T and Z score, respectively from a young normal reference population and an age-matched normal reference population, as indicated in Section 2.2.2. The 3D-DXA will automatically generate a report indicating all the aforementioned measurements, providing also a graph containing the punctual position of the patient, dependent on BMD, age and T/Z scores, with respect to the threshold for the identification of an osteoporotic condition. Also, a 2D-half representation of the proximal femoral site, that will be painted using a coded color scale ranging from violet to blue, respectively indicating a high or low cortical, trabecular or integral bone density.

Here below, the automatic report generated by the 3D-DXA, that can be associated with the global BMD report.

Patient : 000 000 Ethnic : 000 000 Height : 000 000 Weight : 000 000 Operator :
 Patient's ID : Sex : 000 000 Prescribing doctor :
 Birth Date : 000 000 Current Age : 000 000 Menopause age : Physician :
 *Effective/DAP/Input dose: 0.4 µSv/4.4 mGy/cm/21 µCy BMR: 0.4 µSv/4.4 mGy/cm/21 µCy

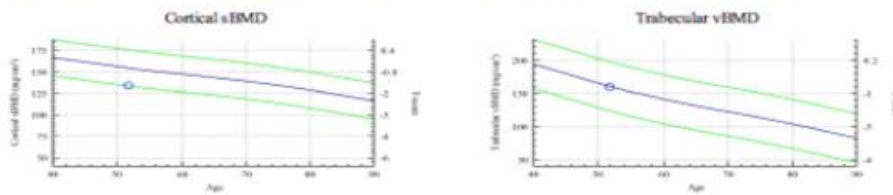
Left Femur 3D-DXA Results

Exam made on the 10-19-2011 at 16:38:55



Results			
Parameter	Result	T-score	Zscore
Cortical sBMD (mg/cm ³)	134	-1.5	-1.0
Trabecular sBMD (mg/cm ³)	160	-0.9	-0.0
Integral sBMD (mg/cm ³)	292	-1.4	-0.5

*Denotes significance at 95% confidence level, LSC for is 11,795 ug/cm³ for Cortical results, 14,104 ug/cm³ for Trabecular results and 16,26 ug/cm³ for Integral results



3D Fan Beam DXA Printing date/time: 03-27-2020 10:37:16 High Energy: 70 keV, Low Energy: 43 keV Ver V4.1.12.0 demo 07-31-2019 / HD 0 - SN: 900 OT 100
 Reference data: Spanish, Caucasian women
 T-score: Computed considering the peak value at 40 years

Figure 37: Main 3D-DXA report

From the technical point of view the technology was provided with:

- X-ray beam with 2D fan-beam geometry.
- Multichannel detector, composed by four elements of 64 arrayed detectors.
- Complete scanning time of 15 seconds for a single anatomical site.
- DICOM 3.0 standard and HL7 compatibility.

From the structural point of view, the machine dimensions were 2.39 m in length and 1.35 m in width, being larger with respect to compact models as a cause of the inclusion of the Total Body BMD modality, that allows to have a ROI consisting of the entire body: it's thus necessary to have greater boundaries of the scan field, and so a larger machine dimension.

3.2.2. Lunar Prodigy PRO, TBS

Contacts have been established with Caresmed, one of the official distributors of General Electric (GE) technologies in Italy: their proposed model for the requirements presented was Lunar Prodigy PRO, one of their most innovative technologies for bone densitometry measurements. In terms of clinical performances, the system was able to perform:

- Anteroposterior (AP), Dual Femur, Femur and Forearm skeletal sites DXA acquisitions.
- Bone Mineral Density (BMD) computation.
- Pediatric applications.
- Regarding the Orthopedic application, instead, it was presented as an optional choice, that, if considered, should have been purchased separately.
- Total Body BMD. This modality allows to have a ROI consisting of the entire body including the head.[66]



Figure 38: GE Lunar prodigy with PRO software package

In terms of included software packages, Lunar Prodigy PRO, as included in the Visionary DR model previously described, is equipped with Fractal risk assessment (FRAX®) for the estimation of the 10-year fracture probability.

In comparison with Fujifilm brand, that proposed a software inclusion based on the measurement of the cortical and trabecular density from a statistical shape and appearance model, GE brand included in the offering the Trabecular Bone Score (TBS) analysis, that instead provides as output an indication not on the trabecular density, but it allows to obtain an indication of the 3D distribution of the internal trabecular microstructure. The system, as deeply described in Section 2.2.4 permits to identify variations of the bone microarchitecture density using experimental variograms of the 2D projection images, quantifying variation in grey-level texture from one pixel to the adjacent pixels [56].

TBS iNsight® is a software package distributed by Medimaps Group, a leading global medical software analytics company founded by a group of clinician practitioners and researchers, based in Switzerland. The Trabecular Bone Score method will retrieve the 2D DXA acquisition and will construct a textural measurement based on greyscale intensity level, producing an experimental variogram, whose slope amplitude will create the indication for the assessment of the trabecular microarchitecture. As discussed in Section 2.2.3, a low TBS value indicates a poor-quality architecture, while a high TBS value will ensure a compact network at the trabecular level.

The TBS software, after the acquisition of the vertebral DXA scan, will produce as output a report including a picture showing the normal DXA scan superimposed with a colorimetric mask indicating the zones more fracture-prone, going toward the red color, and fracture-resistant zones, going toward the green color. Moreover, it will provide a graph containing colored zones as indication of a normal, osteopenic or osteoporotic condition with the punctual position of the patient under analysis in terms of TBS and TBS T and Z-scores, calculated as it was discussed in Section 2.2.2. Lastly, it will be available also a table containing the information about the single vertebra and a series of all the possible results obtained combining different vertebrae together.

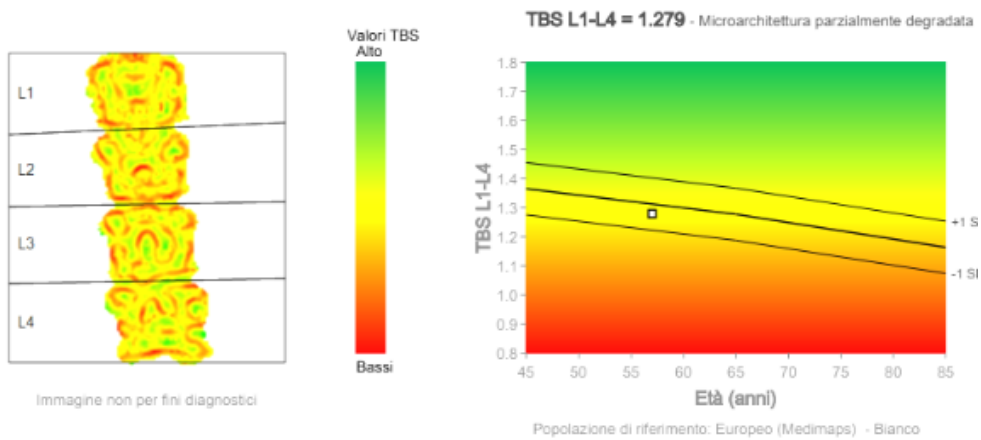


Figure 39: TBS mask applied on the segmented ROI combined with a graphical representation of the patient status with respect to bone microarchitecture distribution

Regione	TBS	TBS Z-score	BMD (g/cm ³)	T-score della BMD
L1	1.284	-	0.803	-1.7
L2	1.212	-	0.798	-2.1
L3	1.290	-	0.819	-2.4
L4	1.331	-	0.751	-2.8
L1-L4	1.279	-0.4	0.792	-2.3
L1-L3	1.262	-0.1	0.807	-1.9
L1-L4(L3)	1.276	-0.2	0.783	-2.3
L1-L4(L2)	1.301	-0.3	0.790	-2.4
L2-L4	1.278	-0.6	0.788	-2.6
L1-L2	1.248	0.3	0.801	-1.6
L1-L3(L2)	1.287	0.0	0.811	-1.8
L1-L4(L2L3)	1.307	0.0	0.776	-2.4
L2-L3	1.251	-0.6	0.809	-2.3
L2-L4(L3)	1.271	-0.5	0.773	-2.8
L3-L4	1.310	-0.8	0.783	-2.9

Table 4: Informative table containing values of TBS, the Z-score of the TBS, BMD and BMD T-score for single or a combination of vertebrae

The Trabecular Bone Score is an index that will furnish indications to the clinicians about the internal bone microarchitecture, but it's necessary to provide guidelines for distinguishing among different physio-pathological conditions on the basis of the value in output of the TBS package. As referenced by [69], determining thresholds for the identification of three different physio-pathological conditions are listed in the table below:

Condition	Threshold
Normal	$TBS > 1.31$
Partially deteriorated trabecular structure	$1.31 \geq TBS > 1.23$
Degraded trabecular structure	$TBS \leq 1.23$

Table 5: Thresholds that discriminate among different trabecular structure distributions.

From the technical point of view the technology was provided with:

- X-ray beam with 2D fan-beam geometry.
- Multichannel detector, composed by two elements of 64 arrayed detectors.
- Complete scanning time of not more than 20 seconds for a single anatomical site.
- DICOM 3.0 standard and HL7 compatibility.

From the structural point of view, Caresmed distributor proposed two different product solutions to be examined:

- Lunar Prodigy with software package PRO, compact size.
- Lunar Prodigy with software package PRO, full size.

As visible in Figure 40, the two models presented different dimensions: the reason why it's worthy to mention the presence of two solutions is based on the fact that GE allow the final user to choose among the two on the basis of its necessities: with Lunar Prodigy PRO in the full size version it's possible to acquire Total Body BMD measurements, while with the compact size it's not possible due to the reduced boundaries of the scanning field of view. Machine dimension for the Full and Compact size were respectively 2.63 m * 1.28m and 2.01m *1.09 m.

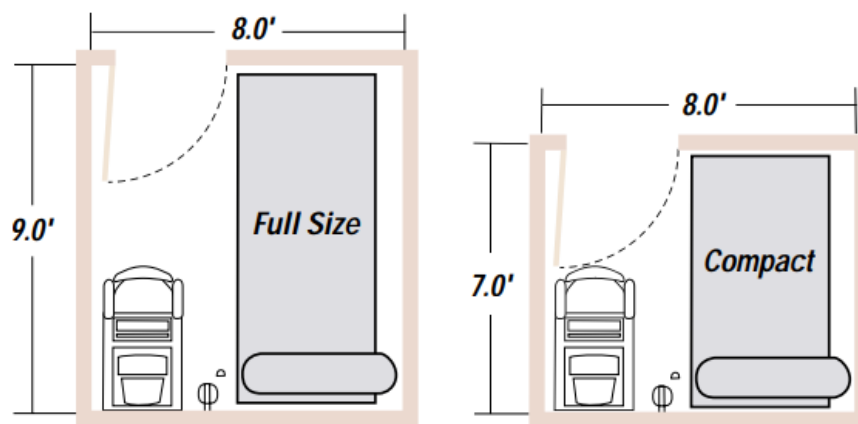


Figure 40: Schematic of Full and Compact sizes of Lunar Prodigy PRO

3.2.3. Horizon Ci, TBS & BSI

The third and last proposal examined came from Technologic, one of the official distributors of Hologic technologies in Italy: the proposed model for the requirements presented was QDR Horizon Ci, a bone densitometer belonging to the last generation DXA scanners produced by Hologic. Available scanning areas are:

- AP lumbar spine, Proximal Femur, Dual Femur, Forearm, with different scanning velocities:
 - Turbo Mode, scanning time 10 of seconds.
 - Fast Array mode, scanning time 30 of seconds.
 - Array mode, scanning time of 60 seconds.
- Bone Mineral Density (BMD) computation.
- Orthopedic and pediatric applications.

- Fractural Risk Assessment (FRAX®) for the estimation of the 10-year fracture probability from obtained clinical risk factors (CRFs)



Figure 41: GE Lunar prodigy with PRO software package

For what concern the clinical point of view, in terms of software innovation, Hologic included in the proposal different software application, as what has been done in the previous offerings:

- One Time Auto Analysis software, that automatically analyses, in real time, spine and femur acquisitions in less than 1 second. Thanks to this software, the read-out time is reduced of about the 85%; moreover, it has been reduced the operator intervention for the boundaries condition, with a consequent reduction in the precision error.
- Medimaps Group distributed TBS iNsiight® also to Hologic group. The description of the technology, together with guidelines for the result interpretation and following diagnosis are provided in Section 2.2.4 and 3.2.2.

BMD, as described in Section 2.2.2, can be defined as an evaluation of the bone quantity, TBS software, instead, permits to obtain an evaluation of the bone quality: with the objective to complete the clinical offer, Technologic company proposed another optional software tool named Bone Strain Index (BSI). The technology was distributed by Tecnologie Avanzate, in collaboration with Technologic company on the Italian landscape. The Bone Strain Index, as described in Section 2.2.4, allows to obtain the strain distribution inside the

scanned object, in order to get detailed information about geometry and load definition. An example of the information level produced by the BMD, TBS and BSI is the following: Bone Mineral Density shows the density characteristics of a given material, such as wood and concrete materials densities (Fig 42.A, B). The TBS, instead, allows to relate the internal structure design showing a difference among a dense or a sparse structure (Fig 42.C, D). The Bone Strain Index allows to complete a diagnostic analysis on a body structure that is daily submitted to a given load (Fig 42. E. F). Moreover, the trabecular distribution in the femur region, being asymmetric and more complicated with respect to the vertebral region, cannot be taken under analysis for a TBS-like evaluation: in fact, any upgrades have been developed yet for the femoral trabecular structure. Conversely, BSI evaluation of the for femoral region follows the same criteria used for the lumbar region[28]

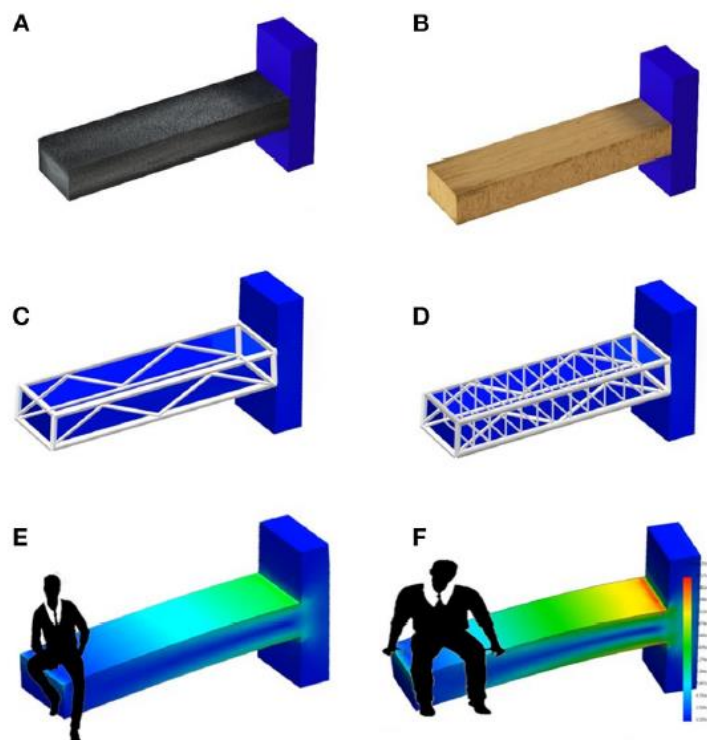


Figure 42: Different information levels provided by BMD, T and BSI.

The BSI software, after the acquisition of vertebral and femoral DXA scans, will produce as output a report including a picture showing the nominal DXA scan superimposed with a colorimetric mask indicating the zones more subjected to higher loads and so to higher strains, going toward the red color, and zones

subjected to lower loads, going toward the blue color. Moreover, it will be provided a graph containing the punctual position of the vertebrae (or neck, troch and inter areas in case of a femoral scan) under analysis in terms of BSI and BMD T-score, previously measured with the normal DXA acquisition. Also, a comparative plot is present in case of previously acquired scans on the same patient, in order to provide a visual representation on how the patient condition changed across time. Lastly, a table containing the information about the single zones analyzed, with their relative BMD, T and Z-scores, and BSI measurements is provided. Here below a dummy report referred to the lumbar and femoral sites is given.

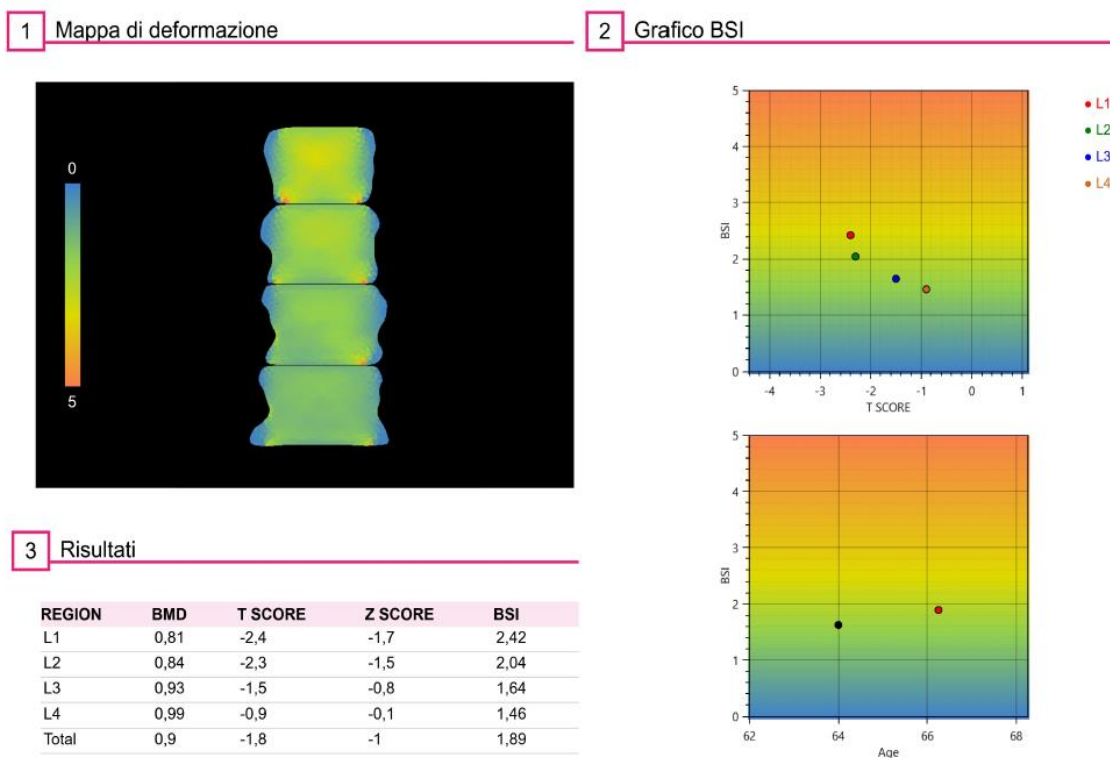


Figure 43: Main BSI report for the lumbar site

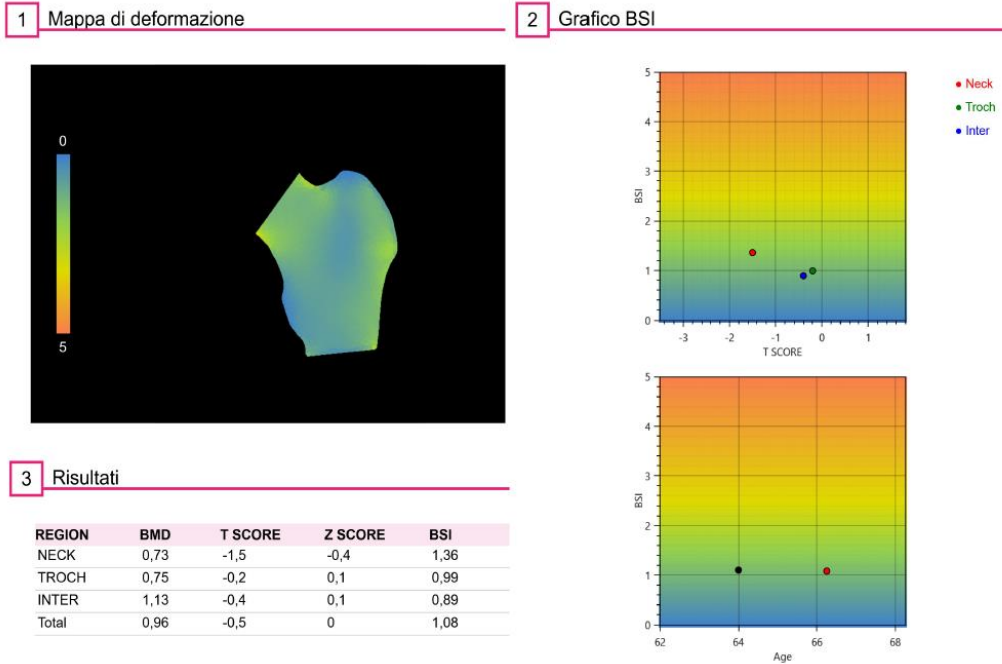


Figure 44: main BSI report for the femoral site

The Bone Strain Index is a parameter that will allow the clinician to have indications about the internal distribution of the loading forces applied on the scanned regions: it will provide as output a unitless measurement about the average strain, being a deformation a ratio among the variation of a dimension referred to the original dimension, expressed in percentage. For this way, it will be necessary to provide guidelines for the correct discrimination among different bone resistance conditions: a bone resistance value ≤ 1.68 will identify a normal structure, while a bone resistance > 1.68 and $<$ than 2.40 will indicate a condition of partial reduction in the capability to withstand to external loads. A reduced bone resistance is present in case of a strain ≥ 2.40 . The aforementioned thresholds are listed in the table below:

Condition	Threshold
Normal	$BSI \leq 1.68$
Partially reduced bone resistance	$1.68 < BSI < 2.40$
Reduced bone resistance	$BSI \geq 2.40$

Table 6: Thresholds that discriminate among different bone resistance conditions, with respect to BSI output

From the technical point of view the technology was provided with:

- A Tube Voltage tuneable range from 70 to 160 KeV.
- X-ray beam with 2D fan-beam geometry.
- Multichannel detector, composed by 2 elements of 64 arrayed detectors.
- Complete scanning time of not more than 20 seconds for a single anatomical site.
- DICOM 3.0 standard and HL7 compatibility.

From the structural point of view, Technologic distributor proposed a machine model with extreme extension in the axial and width directions of 1.92*1.06 m, as visible in Figure 45 reporting a typical installation disposition of the machine, provided by Technologic during the presentation of the proposal.

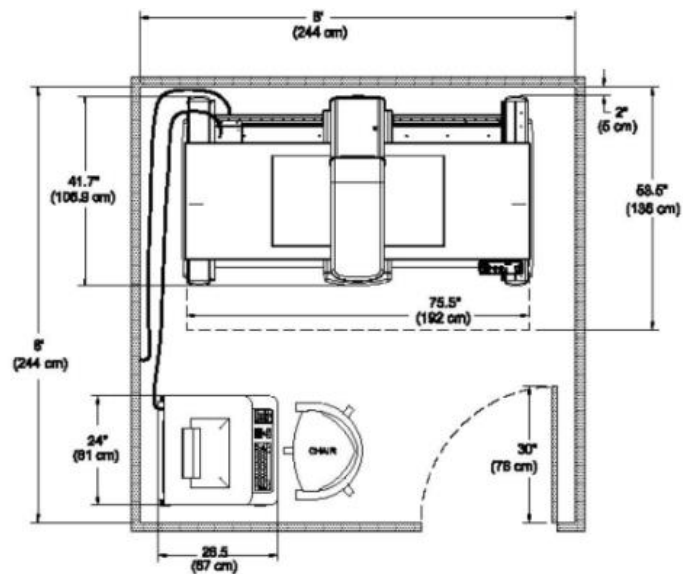


Figure 45: Schematic of a typical installation site, with reported dimensions

3.3. Clinical effectiveness (EFF)

Osteoporosis is a common bone disease characterized by low bone mass and altered bone microarchitecture, resulting in decreased bone strength with an increased risk of fractures. The diagnosis of osteoporosis, currently based on bone mineral density (BMD) which considers only the density of the bone, doesn't provide a measure of bone microarchitecture. However, over 50% of fractures occur in patients non osteoporotic, which can be explained by microarchitecture defects that were not detected by the BMD alone.[70].

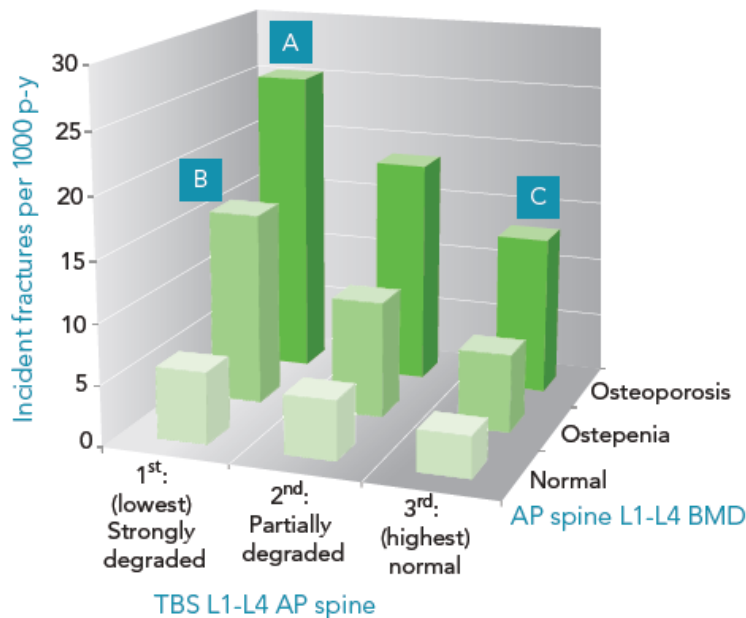


Figure 46: Matrix distribution of combined TBS and BMD incidence fracture values, per 1000 person-years

From Figure 46 it's possible to establish that the incidence fracture built with a combination of TBS and BMD measurements, the greatest TBS utility relies on individuals whose BMS levels are close to the intervention level: up to 25% of patients will then be impacted.[71].

In endocrinology:

- Diabetic patients with poor glycaemic control present an elevated risk of fracture but paradoxically their BMD is higher than in healthy patients (Ulivieri et al., no date). Poor glycaemic control has been associated with

high fracture risk and lower TBS values. TBS has been shown to be a predictor of fracture risk in diabetic patients, independent of the BMD.[73].

- Primary hyperparathyroidism (PHPT) is a common endocrinopathy often accompanied by bone fragility and elevated risk of fracture which is not fully captured by the BMD [74]. TBS is lower in PHPT patients and associated with vertebral fractures: it helps to identify the PHPT patients that are under a higher risk of fracture, to improve the osteoporosis management as such it has been included in the guidelines for the management of Osteoporosis and PHPT.[6]. Not only TBS can provide an improvement of the fracture risk: in the case-control study carried out by [75], it was demonstrated that there was association among BSI with vertebral fractures in PHPT. The assessment was computed on lumbar spine (LS), femoral neck (FN), and total hip (TH). The study enrolled 50 PHPT patients and 100 age- and sex- matched control subjects from an outpatient clinic. BSI was significantly higher at LS (2.28 ± 0.59 vs 2.02 ± 0.43 , $P = 0.009$), FN (1.72 ± 0.41 vs 1.49 ± 0.35 , $P = 0.001$), and TH (1.51 ± 0.33 vs 1.36 ± 0.25 , $P = 0.002$) in PHPT patients.
- Glucocorticoids (GCs) are therapeutically used to suppress various allergic, inflammatory and autoimmune disorders and it is one of the most common causes of secondary osteoporosis. GCs treatment increases fracture risk, which is not entirely captured by the BMD. TBS is lower in GCs-treated patients, especially in those with osteoporotic fractures. The added value of TBS in these patients is to help to identify the GCs-treated patients that are under risk of fracture.[76].
- Patients under advanced stages of chronic kidney diseases have an increased risk of fragility fractures due to alterations on bone strength, involving both bone mass and bone microarchitecture deterioration.[77]. TBS has found to be lower in these patients and it was shown to be a good and independent predictor of fragility fractures in patients with CKD or who underwent kidney transplantation.[77].
- Patients with Rheumatoid Arthritis (RA) are especially prone to develop osteoporosis and fractures, however, most of them occur in patients with bone density above the osteoporotic threshold. This discrepancy may be related to alterations of bone, which are not captured by BMD, that is,

changes in bone quality. TBS has been shown to be lower in patients with RA and a good predictor of vertebral fractures. [78].

- The presence of Osteophytes, a common disorder in older patients and those with Osteoarthritis, can falsely elevate the BMD measurements leading to misdiagnosis[79]. Unlike BMD, TBS results has been demonstrated to be minimally affected by the presence of osteophytes, providing a more accurate fracture risk assessment.

3.4. Organization (ORG)

The development of the New Clinical offer is, however, related to projects that are operationally feasible and economically sustainable. Therefore, a proper prior analysis of all these conditions, that make the project worthwhile, must be done. The process of annual projects authorization consists in the approval of a budgetary request that will be allocated on a given project development. Obviously, the actualization of a given project will depend further on other factors: as an example, the availability of the clinicians during the current year with respect to the previous year in which it has been conducted the analysis. In this case, the allocated budget for the procurement of a new bone densitometer was 75.000 €. All the proposals that were taken into account respected this economic constraint, but of course a purchase negotiation with the final chosen brand has been carried out.

The GANTT chart has been constructed in order to provide a visual representation of the main activities duration, from the Health Technology Assessment phase up to the activation of this new medical service: BMD with TBS/BSI Clinical Insight. The GANTT chart is divided into three main temporal windows:

- Mini-Health Technology Assessment. During this period, it has been conducted an analysis onto the clinical and technical specifications, according to the initial requirements. A draft of the Mini-HTA report, including EFF and TEC domain has been produced, with the aim to outline this evaluation to CMS specialists in radiology and endocrinology. Physicians, by reading this document, have contributed to the identification of the most effective solution to be adopted.

- Multi Criteria Decision Analysis & Operative Plan. In this step the main activities concerned the identification of the most cost-effective solution to be adopted, with a bidirectional communication between the final supplier and the DCE department for modifications of some contract items, such as the Inclusion of AntiX screen for shielding, clarifications on suitability installation, schedule for the installation, configuration and final testing with the Qualified Expert of Radiation Protection. Moreover, a coordination with the CMS Operative Department has been carried out, in order to close Densitometry examination Agendas for a time window needed for the replacement, the installation of the new machine with subsequent configuration and Technical&Medical personnel training
- Installation, Configuration & Testing. In this final part it has been actualized all the operative plan previously scheduled. Program included the On-site installation of the new health technology, BMD and TBS calibration. Also, as it was previously planned with OPS department, a daily agenda was opened in order to allow Technical personnel training.

Here below it has been depicted the GANTT chart, with a complete duration ranging from the 1-st April until to 11-th July 2022.

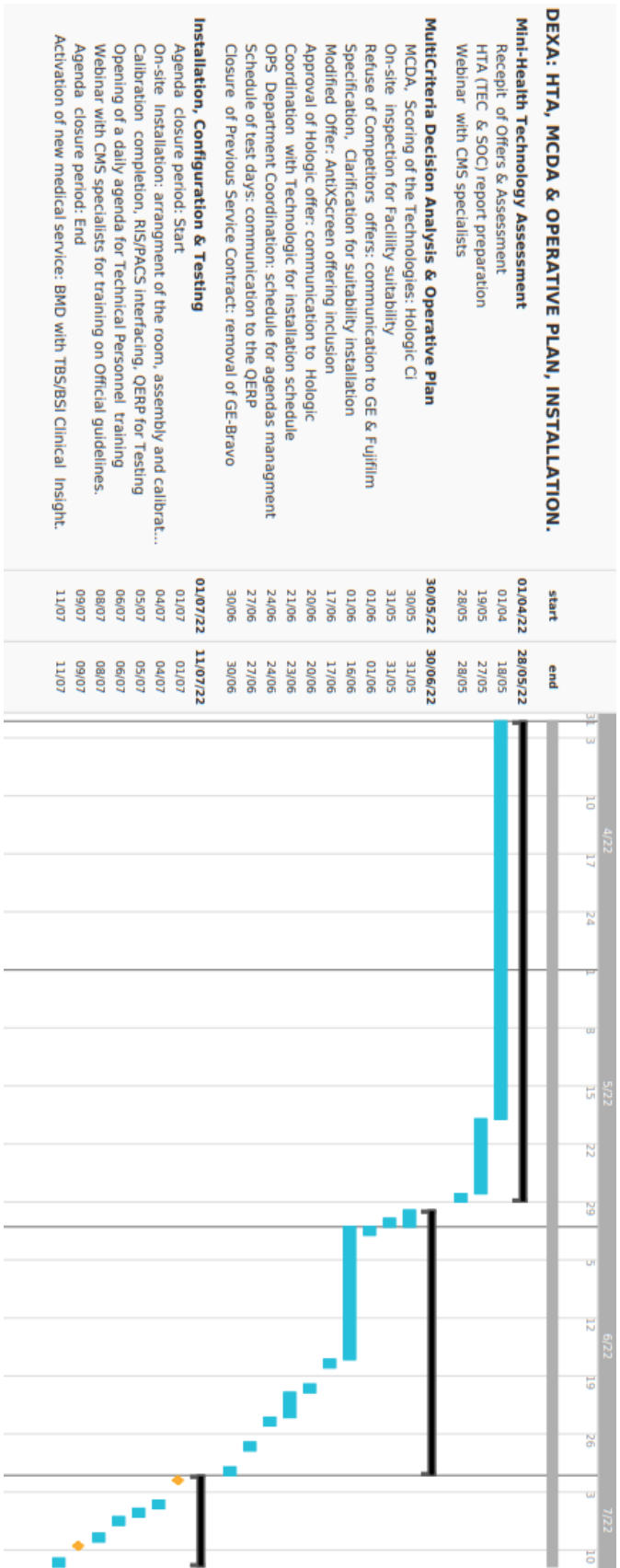


Figure 47: GANTT chart. From HTA phase up to DEXA installation

3.5. Economic analysis (ECO)

Thanks to the possibility of having an internal System Applications and Products in Data Processing (SAP) architecture, it's possible for CMS to use data as a source of added value. In this case, being different DEXA technologies installed in the various health clinics, a comparative analysis of the patient demand for DEXA examination can be done. The total medical equipment of CMS on bone densitometry consists of:

- A FDX Visionary A model, installed in "Nembro Esselunga" centre, currently ongoing.
- A FDX Visionary A model, installed in "Via Larga" centre, currently ongoing.
- A Hologic Discovery model, installed in "Cervetto B" centre, dismissed in June 2022.

From the graph present below (Fig. 48) it's evident the displacement between the amount of requests for DEXA examination in "Repubblica" centre with respect to all other health clinics. Reasons that can be attributed to this effect are related to the strategic position of Panfilo Castaldi centre, located in Repubblica district, one of the most central areas of the city centre. Secondly, this health clinic was one of the first historical clinics opened in Milan as Centro Medico Santagostino: thus, the interest coming from all the participants for the execution of a medical service has increased over the years: specialists of different branches and a large catchment area of patients that believe in CMS value since its opening in "Repubblica" centre.

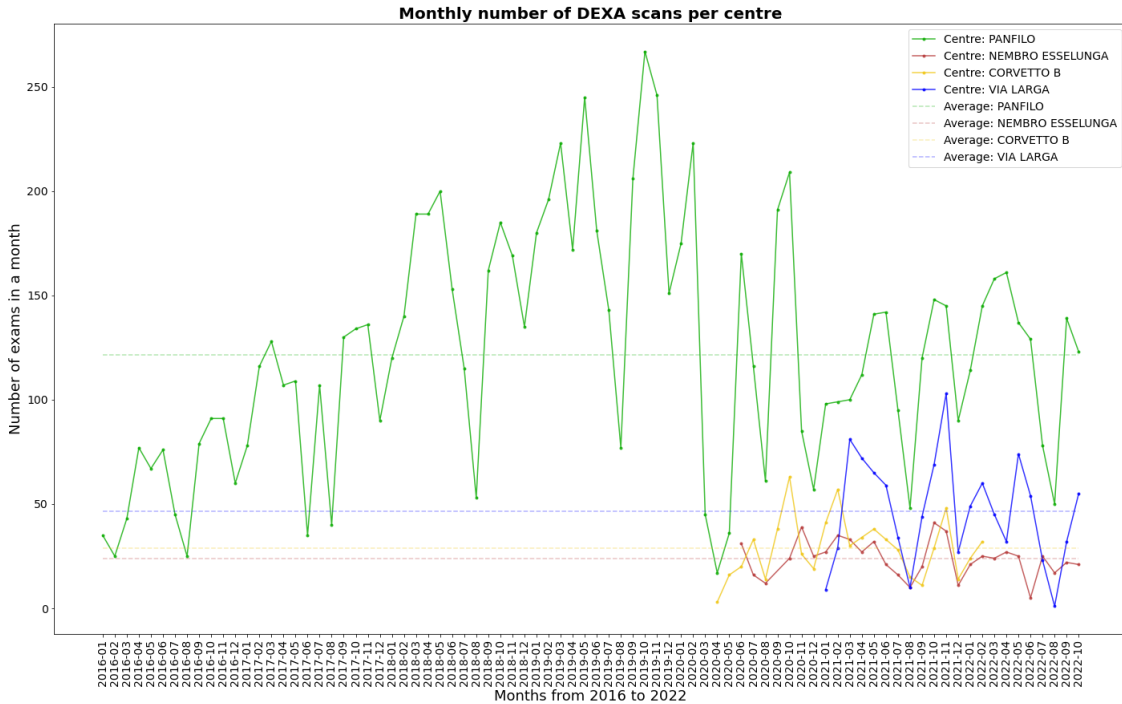


Figure 48: Monthly number of DEXA scans divided per centre from 2016.

As it can be visualized from the plot, the average monthly number of DEXA scans performed in “Repubblica” from January 2016 to October 2022 is 121.68 exams, with respect to:

- “Nembro Esselunga” centre, with 23.8 exams per month.
- “Via Larga” centre, with 46.6 exams per month.
- “Corvetto B” centre, with 28.9 exams per month performed until February 2022.

From the considerations done previously, based on the strategic position and history of “Panfilo Castaldi” centre, and from the punctual information about the average number of DEXA scans in each centre provided with DEXA technology, it is clear that the replacement with an innovation technology has been strategically accounted for “Panfilo Castaldi” centre.

The Operative Department, on the basis of the historical data related to the monthly average patient demand for DEXA examination requests in “Panfilo Castaldi” centre, established a cost associated to the examination request for a

Computerized Bone Mineralometry with TBS insight (**DENSITOMETRIA OSSEA COMPUTERIZZATA (MOC) CON APPROFONDIMENTO CLINICO TBS**) at 60 € / examination.

On the basis of the allocated annual budget for the procurement of a new bone densitometer, and on the basis of the associated price for the delivery of a BMD examination, a Time To Break Even (TBE) measure, expressed in months, can be determined as:

$$TBE (t) = \frac{\text{Budget Allocation}}{\text{Average monthly number} * \text{Cost}}$$

Where:

- TBE(t) = time required in months before to reach the BE point.
- Budget Allocation = Initial Annual Budget allocation, expressed in euro.
- Average monthly number = Average number of monthly DXA scans, in absolute units.
- Cost = Unit Cost of the examination, expressed in euro.

The result will indicate the interval of time needed before to reach the Break-Even point, so the temporal window required before generated cash flows equalize the initial cost for the introduction of the innovation. Taking into account a Budget Allocation for DEXA of 75.000 €, a Unit Cost of Examination of 60 € and an Average number of monthly DXA scans of 121.68 acquisitions for Panfilo Castaldi centre, as showed previously, the TBE will correspond to 10.27 months, so less than one year. Of course, a purchase negotiation with the final chosen brand has been carried out, so the value of TBE has been reduced from the one reported above.

4. Multi criteria decision analysis

4.1. Receipt of offers & assessment: HTA (EFF, TEC) report preparation

Any HTA process, for the evaluation of a given innovation with respect to a standard in care, is developed starting from the research for the best alternatives to be selected. In this case, contacts were already established between CMS and several different competitors of DEXA technology, that also presented the inclusion of different solutions for software innovation, being the one of final targets of the project for the improvement of the clinical quality in diagnosis. Therefore, the baseline from which the project started took place from the analysis of the proposals presented by three main competitors already known in the landscape of CMS growth, for a variety of other technologies, such as CT installation, mammographer or ultrasound applications.

Contacts were taken with the different competitors as a first modality to obtain information about technical, economic specifications on the products for which the company was interested in. Clinical valuable features instead, were internally analysed from scientific literature: PubMed® and Google Scholar were used as a source for state-of-the-art documentation. After a proper consultation of inherent publications, an official communication was sent to all the distributors, that were invited to arrange a meeting for the presentation of their technology. A formal email followed the convocation, including a more detailed description of what was taken into account during the reunion, from the technical and economic points of view. Meetings were arranged in the CMS Head Office, with a schedule that included one reunion per-week, in order to have time to define a literature research workflow for the proposed features included in each DEXA technology.

By comparing the three hardware, no significant difference was found in order to attribute a major importance on a technology with respect to another one. From the point of view of the software packages included, this factor was one of the major determinants in the choice of the final offer to be accepted. 3D-DXA software provided an assessment of only the proximal femur area, thus any upgrade for the analysis of the lumbar spine was provided. Moreover, the analysis for obtaining a more informative description of the bone trabecular

microstructure was computed with the use of a statistical shape and appearance model, providing information on the Trabecular Volumetric Bone Mineral Density (Trabecular vBMD, expressed in mg/cm^3). However, this measure was not providing the target information requested by internal CMS specialists, such as a measurement that was able to provide a textural analysis of the bone quality. Trabecular Bone Score (TBS) analysis, instead, provides as output an indication not on the trabecular density, rather it allows to obtain an indication of the 3D distribution of the internal trabecular microstructure. Medimaps Group distributed TBS iNsight® to both the last two competitors (GE and Hologic), so the competition among the two participants in terms of this software package included was nullified. However, the TBS technology, as cited in [28], cannot be applied to the femoral site since the trabecular distribution in the femur region is asymmetric and more complicated. Hologic allowed to compensate for this restriction by introducing the Bone Strain Index, produced by Tecnologie Avanzate brand. The Bone Strain Index allows to complete a diagnostic analysis on a body structure that is daily submitted to a given load since it permits to obtain a local strain distribution of the scanned object with the use of a FEA model. Moreover, instead of TBS technology, currently applied only on the lumbar spine site, BSI evaluation for the femoral region follows the same criteria used for the lumbar region.

By gathering all these information, a webinar with specialists in endocrinology, supported by the clinical opinion of the CMS radiology health director was scheduled, in order to collect an opinion on the evidence-based information retrieved during the research period. The meeting was scheduled for the 28-th of May, 2022. A presentation containing a description of the clinical effectiveness (EFF) and technical (TEC) domains was prepared. The objective of this presentation was to validate the clinical valuable features that were internally analyzed from scientific literature.

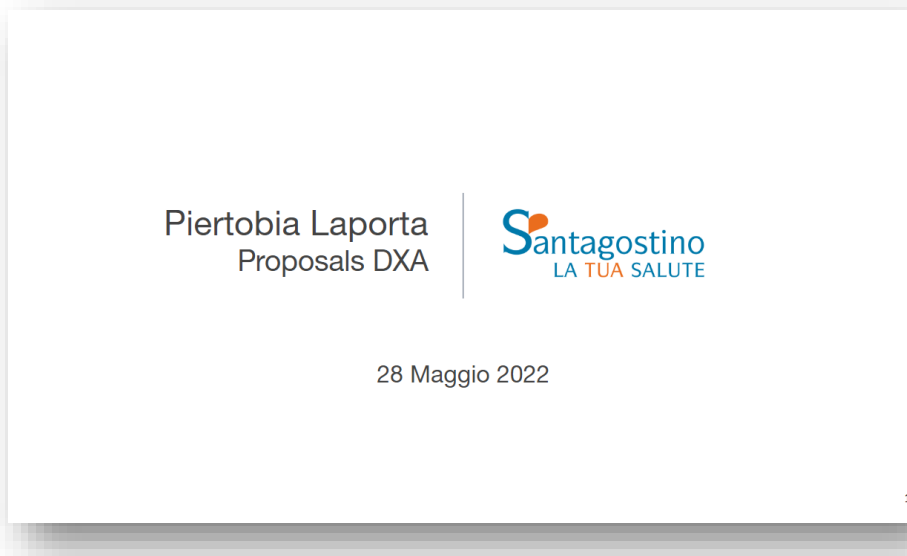


Figure 49: Proposals DXA, cover of the presentation to CMS endocrinologists and radiologists.

There were faced contents related to the technical specifications, concerning which brand possessed the requirements needed to satisfy the project specifications, such as the intention to introduce bone quality measurement technologies. Not only, it was provided the evidence for a beneficial effect for the specialties under analysis. In endocrinology a variety of different case studies can experience the improvement in the diagnostic capability of this instrumentation: it has been demonstrated that, except of osteoporosis, in which DEXA examination was established as a standard technology, many other pathologies, such as diabetes, PHPT, rheumatoid arthritis and osteoarthritis can benefit from the improvement in the fracture risk assessment provided by the software that were proposed.

4.2. Multi criteria decision analysis: internal offer acceptance

Nowadays, Health Technology Assessment (HTA) is mainly conducted based on clinical effectiveness and safety studies and medico-economic studies. The description of other aspects, such as organizational aspects are rarely considered. In addition, healthcare organizations are characterized by a high level of complexity and a very dynamic environment [80]: that's why it's of fundamental

importance to take in charge trade-offs between multiple, often conflicting objectives.

Cost-effectiveness/ cost-utility analyses (CEA, CUA) are some of the main types of economic evaluations used for healthcare [81]. They are a comparative analysis of the relative costs and outcomes of two or more alternatives. Cost-effectiveness analysis measure the health consequences of an intervention in a single natural unit (such as cases averted, or life-years saved). However, a limitation of this is that it's difficult to compare studies investigating interventions targeting different diseases or outcomes, since their health consequences will be expressed in different units, limiting its potential for informing policymakers. To address this, a specific form of cost-effectiveness known as cost-utility analysis was developed. CUA measure the health consequences with a generic measure of health status, which can account for benefits on reduced morbidity and mortality, such as DALYs (Daily Adjusted life-years) and QALYs (Quality Adjusted life-years). As these metrics can be used for a wide range of diseases, the cost-effectiveness can be directly compared to each other. The use of DALYs or QALYs as outcomes within cost-utility analyses has been a notable improvement compared to only measuring the intervention's effect in terms of diseases cases or deaths averted. However, this generic measure of health status has limitations: for the aims of this project, generic summary measures on only the clinical improvement with respect to a standard technology may be overly simplistic and reductionist and may not be capturing all of the benefits of this intervention, since other aspects related to TEC and ORG domains should be taken into account.

That's why multi-criteria decision analysis (MCDA) methods aim to facilitate the identification of the best possible solution to a given problem that requires considering a set of aspects or criteria, which are often heterogeneous. Core components of any MCDA method are:

- The alternatives in competition with one another.
- The criteria by which alternatives are assessed.
- The level of performance of each alternative for each criterion.
- The relative weight of each criterion.

MCDA approaches include many techniques. Table 6 summarizes different typologies of scoring and weighting method. This covers the stated preference approaches used by most of the MCDAs undertaken in health care.

Criterion	Method	Scoring task	Weighting task
Choice based	DCE/conjoint analysis	Which alternative is preferred, given the performance of each on all criteria	
	PAPRIKA	Which alternative is preferred, given the performance of each on two criteria	
Ranking Direct rating	Best-worst scaling	Which is the worst and best alternative from three or more choices, given the performance of each on all criteria	
	SMARTER Scales	Not usually used for scoring The importance of alternatives on each criterion is considered on a scale, such as a visual analogue scale (VAS)	Rank order of criteria Importance of each criterion considered separately on a scale
	Point allocation, e.g., SMART	Points are allocated to alternatives in proportion to their relative importance on a criterion	Allocation of points between criteria in proportion to their relative importance
Pairwise	AHP	Alternatives are compared pairwise on each criterion and their "intensity of importance" relative to each other is usually expressed on a 1-9 ratio scale	Pairwise comparison of the "intensity of importance" of criteria on a 1-9 ratio scale
	MACBETH	Pairwise comparison of alternatives on each criterion to assess their relative importance using semantic categories	Pairwise comparison of the "intensity of importance" using seven qualitative (semantic) categories of importance
Swing weighting	SMARTS	Not used for scoring	Relative importance of ranges of performance on each criteria (the "swing")
Scoring functions	Bisection and difference methods	The range of performance on a criterion defines the 0 and 100 points on the scoring function. The shape of the function is determined by 1) bisection: identify the performance level that is worth 50 and 2) difference: identify the score on the 0-100 scale for the midpoint on the range of performance. These steps are then repeated for the subscales to define the shape of the scoring function	Not used for weighting

Table 7: Main scoring and weighting methods for MCDA. [84]

A pseudo Best-Worst Scaling method [82], as indicated in Table 6, was used for our purposes. In particular, it was evaluated the possibility to introduce scoring measurements, with relative weights, for the identification of the best possible alternative. The criteria included in the decision analysis were the ones taken into account for the production of the HTA report that was presented to CMS specialists, unified with ECO and ORG domains: thus, the MCDA was carried out on EFF, TEC, ECO and ORG domains.

In order to provide the same importance level to the domains under analysis, during the development of this phase it was decided to attribute equal weights to all the four domains.

The most commonly applied aggregation formula for combining the individual scores is the additive model, whose formulation is presented below:

$$V_j = \sum_{i=1}^N s_{ij}w_i$$

where V_j is the overall value of technology j , s_{ij} is the score for technology j on criterion i , and w_i is the weight attached to criterion i . A list containing specifications on how to attribute a score to each criterium taken into account for our purposes is presented below:

Clinical Effectiveness (EFF):

- Software packages included.
 - A score = 0 was attributed in case of failure to meet the minimal requirement in providing a measurement of the bone quality.
 - A score = 1 was attributed in case solutions with only TBS software included.
 - A score = 3 was attributed in case solutions with both TBS and BSI software included.

Description and technical characteristics of technology (TEC):

- Paediatric application.
 - A score = 1 was attributed in case of inclusion of paediatric modality, that allows for the possibility to perform examination onto paediatric patients, aged more than 3 years.
 - A score = 0 was attributed in case of absence of paediatric modality.
- Orthopaedic application.
 - A score = 1 was attributed in case of inclusion of orthopaedic modality.
 - A score = 0 was attributed in case of absence of orthopaedic modality.
- Beam geometry.
 - A score = 1 was attributed in case of fan beam geometry.
 - A score = 0 was attributed in case of pencil beam geometry.
- DICOM 3.0 and HL7 compatibility.

- A score = 1 in case of compatibility with RIS/PACS architectures.
- A score = 0 otherwise.

Costs and economic evaluation (ECO):

- Price of the machine at first economic offer receipt.
 - A score = 1 in case of a purchasing price lower than the budget allocation for a new bone densitometer.
 - A score = 0 otherwise.
- Warranty period.
 - A score = 1 was attributed in case of a contract with a warranty period whose duration higher or equal than twelve months.
 - A score = 0 otherwise.
- RX-tube replacement.
 - A score = 0 was attributed in case of a contract without any provision indicating for a RX-tube replacement, in case of damage, for free, during the warranty period.
 - A score = 1 was attributed in case of a contract provision indicating for a single unit X-ray replacement, in case of damage, for free.
 - A score = 2 was attributed in case of a contract provision indicating for more than one unit X-ray replacement, in case of damage, for free.

Organizational aspects (ORG):

- Technical Service response time, in case of technical issues.
 - A score = 1 was attributed in case a response time lower than eight hours, in order to compare an efficient assistance during a current working day.
 - A score = 0 otherwise.
- Number of ordinary repairs in a year.
 - A score = 1 was attributed in case of a number of ordinary repairs in a year higher or equal to one.
 - A score = 0 otherwise.
- In stock availability of the target technology.

- A score = 1 was attributed in case of presence of in stock units of the target technology, in order to allow to a priori schedule the installation days according mainly for our purposes. In fact, during August 2022, in “Repubblica” centre, the Engineering and Technical (ET) Department planned for activities of structural restyling and medical imaging devices installation, such as an MRI O-Scan, placed in the R6 ambulatory. In a preliminary phase of the installation project for the MRI, technical maintenances and replacement were done in order to prepare the site for the in-house installation. Thus, installation and configuration days for the DEXA apparatus were planned in the same period, so during the first decade of July, 2022.
- A score = 0 was attributed otherwise.

Starting from the EFF domain, it was considered as a first requirement the inclusion of a textural analysis, generated by a given software package, that was able to provide a description of the trabecular bone distribution as an indication of the bone quality, with respect only to a bone quantity description. 3D-DXA software provided an assessment of only the proximal femur area, thus any upgrade for the analysis of the lumbar spine was provided. Moreover, the analysis for obtaining a more informative description of the bone trabecular microstructure was computed with the use of a statistical shape and appearance model, providing information on the Trabecular Volumetric Bone Mineral Density (Trabecular vBMD, expressed in mg/cm^3). However, this measure was not providing the target information requested by internal CMS specialists, such as a measurement that was able to provide a textural analysis of the bone quality. It's therefore necessary to specify that the evaluation for FDX Visionary DR model wasn't carried out furthermore. Trabecular Bone Score (TBS) analysis, instead, provides as output an indication not on the trabecular density, rather it allows to obtain an indication of the 3D distribution of the internal trabecular microstructure. Medimaps Group distributed TBS iNsight® to both the last two competitors (GE and Hologic), so the competition among the two participants in terms of this software package included was nullified. However the TBS technology, as cited in [28], cannot be applied to the femoral site since the trabecular distribution in the femur region is asymmetric and more complicated.

Hologic allowed to compensate for this restriction by introducing the Bone Strain Index, produced by Tecnologie Avanzate brand. The Bone Strain Index allows to complete a diagnostic analysis on a body structure that is daily submitted to a given load since it permits to obtain a local strain distribution of the scanned object with the use of a FEA model. Moreover, instead of TBS technology, currently applied only on the lumbar spine site, BSI evaluation for the femoral region follows the same criteria used for the lumbar region. After having gathered all these information, during the webinar scheduled with internal specialist in endocrinology and the health director for radiology it was attributed a point = 2 for Hologic, 1 instead for GE and 0 for Fujifilm. The latter proposal was not analysed furthermore after the consultation with internal physicians.

In terms of the technology characteristic (TEC), the last two competitors showed several differences. The paediatric module was included in both the technologies, but only Hologic provided for free also the orthopaedic application, with the possibility to allow scans on orthopaedic patients with prosthesis: General Electric instead proposed this module as an optional choice that, if considered, should have been purchased separately. Beam geometry, DICOM 3.0 and HL7 compatibility were both included in the two technologies.

Costs and economic evaluation (ECO) taken into account the purchasing price of the two technologies. Both of them respected the constrain of the annual budget allocation dedicated to new bone densitometer. Obviously, a negotiation was carried out with both the suppliers, but in this description, it will be taken into account only the initial budget allocation as a threshold to be accepted: the final purchasing price is considered as a confidential business information. A warranty period with a duration higher or equal than twelve months was considered as an acceptable threshold for assigning a score equal to one to this specific criterium. GE included in the contract a warranty period of twelve months, however Hologic proposed instead for two years of warranty period duration: therefore, although it was attributed one to both of them, it was taken into account the temporal elongation provided by the Hologic brand. For what concern the RX- tube replacement, General Electric included in the contract a single unit for free in case of damages, while Hologic proposed an unlimited number of units, during the warranty period. Therefore, also this further displacement was considered.

By considering the Organizational domain (ORG), a Technical Service response time, in case of issues, was considered. In order to compare an efficient assistance

during a current working day it was established that eight hours of latency were the threshold to be considered. GE included for a response time lower or equal than 24 hours, compared to Hologic brand that proposed for eight hours of time window. Therefore, it was assigned 1 to Hologic brand, 0 to GE competitor. The number of ordinary repairs included was equal for the two proposals, so 1 point was assigned to both the participants. The stock availability of the target technology has been a core theme to be analysed in this evaluation: Hologic brand specified in its offer that the technology would have been delivered in a few days, since it was already present as a stock product. General Electric, instead, proposed a different option for satisfying the requirement of an almost immediate availability: it came up with the Lunar Prodigy PRO model in the full-size version. With the full-size version was possible to acquire Total Body BMD measurements. The machine was deemed unsuitable for two main reasons:

- The low incidence rate of Total Body BMD requests in the Lombardy region.
- A structural constraint related to the reduced dimension of the final installation site: the R7 ambulatory of “Panfilo Castaldi” centred was composed of 8 m^2 of walkable floor. Therefore, a machine whose length was of 2.63 meters wasn’t suitable for the installation, as visible in Figure 50, if we consider the dimension of the longitudinal side of the ambulatory and the occupancy given by the opening of the door.

At the end, point 1 was assigned only to Hologic brand, for reasons listed above. This multi criteria evaluation allowed to attribute an overall value V_1 to GE group proposal equal to 2, while an overall value V_2 to Hologic proposal equal to 3.5. Therefore, the target solution was in this way identified as the Hologic proposal, with its Horizon Ci technology.

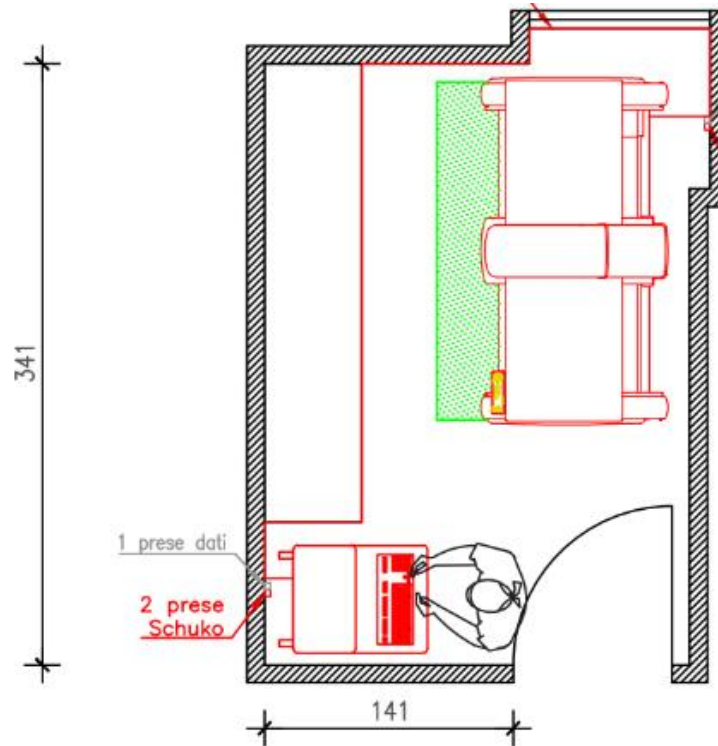


Figure 50: Planimetry of the R7 ambulatory.

GE and Fujifilm brands play an active role inside the market segment of Technologies in Medical Imaging: therefore, a formal communication was given as indication of refuse for their economic offer. Of course, being CMS a reality in perpetual growth it was advanced the indication that future new health clinic openings could become potential new target for the introduction of DEXA technologies. These distributors provide a variety of different Technologies for medical imaging: therefore, it is considered as a good practice to keep forward relations with these potential final suppliers.

Initially, the economic offer presented by Hologic brand included the a bone densitometer DEXA with Fan Beam geometry, a TBS and a BSI module. Although these requirements already satisfied the clinical standard suggested by the CMS endocrinologists in association with the health director, there was the necessity to also request the inclusion of an X-ray radiation shielding screen, commonly named as AntiX screen. This medical equipment was present in the R7 ambulatory before GE-Lunar Bravo was dismissed, in order to ensure the correct

radioprotection requirements, on the basis of a more frequent dose exposition of the technical personnel in charge for the use of the technology. However, with the closure of the service contract with the supplier of the GE-Bravo technology, the old distributor provided also the AntiX screen: therefore it was necessary to find a solution for ensuring the activation of the clinical examination in the scheduled timeline. After a negotiation with Technologic distributor, it was possible to obtain the inclusion of a moving shielding X-ray barrier in the economic offer at the same purchasing price with respect to the final offer without AntiX.

5. Installation, configuration & training

5.1. Operating plan

With the objective to permit an optimization of wasting time and associated costs related to the company, it was scheduled an operating plan before the installation of the new DEXA technology. The various steps towards the final goal were represented in Figure 47 with the use of the GANTT chart.

5.1.1. On-site inspection for facility suitability

On the 31-th of May it was conducted an on-site inspection with the Building Manager of the ET Department. The aim was to assess the suitability of the R7 ambulatory of “Panfilo Castaldi” centre for the new installation. The requirements to be respected were in terms of structural, electric and radioprotection suitability.

Structural suitability: it's worthy to specify that the predisposition of the ambulatory was already prepared for being suitable to a DEXA installation, since GE-Lunar Bravo was installed in that position from 2016 up to the 31-th of June. However, a long utilization of the ambulatory combined with the necessity to perform preventive maintenance brought to the necessity to perform an on-site inspection for the verification of the functionality of the ambulatory. The total longitudinal side of the ambulatory was 3.41 m: if we consider the opening of the door of 0.9 m, the available space to be occupied was of 2.51 m. Technologic distributor proposed a machine model with extreme extension in the axial and width directions of 1.92*1.06 m, therefore a disposition of the technology in the longitudinal side, placed beside the right wall of the ambulatory would have been allowed. A DEXA machine does not present a considerable weight, as it could be a MRI installation: the densitometer weight was of 318 kg, therefore there was done any feasibility study for the floor of the ambulatory. A washbasin was already present in the ambulatory as a prerequisite for the suitability of the space under examination. A climate system at 21 °C was already installed in the ambulatory: with the aid of the Building Manager, it was performed a control of the system in order to ensure a correct and beneficial temperature for both the operators and patients.

Electric suitability: for the power supply of the densitometer, it was required an electric socket of type Shucko with input voltage supply powered with 220 V, with a differential magnetothermal switch for reason of safety and prevention in case of a direct contact with the electric apparatus of the machine. The technology was also equipped with a workstation, used by the technical personnel for the exam execution: for ensuring a communication with the CMS PACS it was required to have in the ambulatory a data socket for a correct data transmission towards the RIS/PACS architecture. For the console power supply, it wasn't necessary a dedicated electric socket, since the scanner itself was able to furnish 120VAC 6A, with the use of connecting electric cable. Both the requirements were already satisfied: however it was performed a control of the functioning and connectivity in order to avoid complications during the installation and configuration days. When medical facilities operate X-ray, MRI, Laser and CT scanners in their day-to-day operations they are required to post in use warning signs above room doors. The technology provided by Hologic was equipped with the possibility to provide in output 120VAC 3A to the warning lamp placed above the room door. The warning lamp is composed by 2 main parts: the upper part has the role to signal with a white colour the fact that the machine is turned on, while the lower part will be turned on only in case of X-ray emission. A schematic of the link between the machine and the lamp, combined with a representation of the lamp itself, are provided in Figure 51.

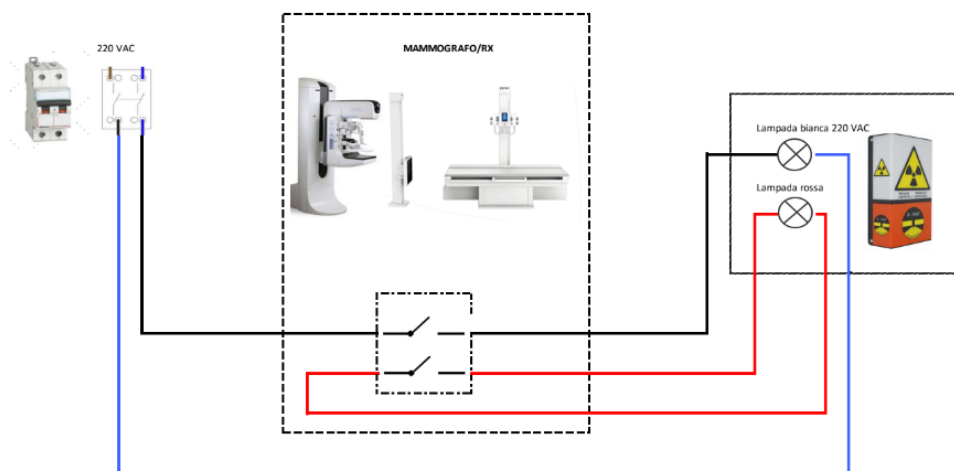


Figure 51: schematic of the link between the machine, the warning lamp and the power supply

Radioprotection: at first, it's worthy to mention that any ambulatory that present an in-room technology for performing X-ray exposition is equipped with a Pb shielding whose thickness is linearly dependent on the X-ray tube peak voltage. In this case, a 1mm Pb shielding that was surrounding the lateral walls of the ambulatory was already present, in order to prevent for useless exposition the surrounding ambulatory that daily house operators, physicians and patients. In order to ensure a correct source to operator distance, a predisposition of the console placement was established, according to the specification provided by the distributor, as visible in Figure 52: solid perimeter line indicates $8.8 \mu\text{Gy}/\text{h}$.

The workstation was required to be located at a radial distance from the C-arm of at least 0.74 m. After the on-inspection, it was proved that the source to operator distance, according to the workstation placement, would have been of 1.60 m, so more than double with respect to the requirements.

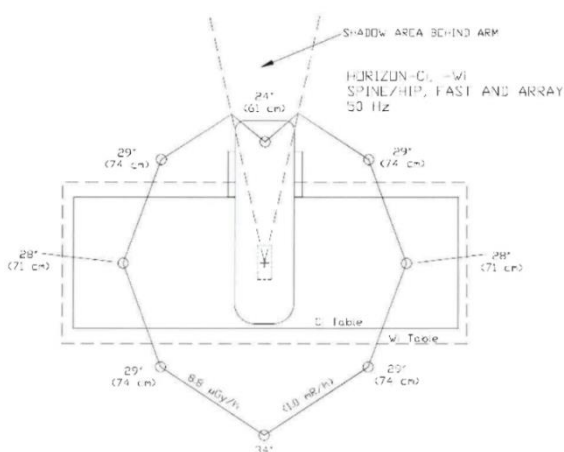


Figure 52: Isodose curves of DEXA Horizon Wi/Ci.

Finally, as already expressed in Section 4.2, the economic offer accepted by CMS for the Horizon Ci model also included a moving shielding X-ray barrier: during the on-site inspection it was predisposed also the placement of the moving barrier in the ambulatory. A picture of the shielding barrier is provided in Figure 53.



Figure 53: X-ray radiation shielding screen.

5.1.2. Coordination before installation

A formal communication was sent to Technologic company: after the acceptance of the modified economic offer, with AntiX screen inclusion, it was requested a schedule for the on-site installation, configuration and training of the technical personnel days. The Project Manager (PM) of Technologic provided a schedule of the working days divided into three sessions:

- Monday 04/07. It was specified the arrival of the in-charge carrier for the technology, set for half past twelve, pm. The positioning of the technology in the installation site would have been followed also by an internal engineer of Technologic company, who would have dedicated the rest of the working days for ambulatory arrangement, machine assembly and phantom calibration.
- Tuesday 05/07. Calibration completion, RIS/PACS interfacing and testing of the machine would have been performed during this working day. The schedule of the days was received on the 21-th of June 2022: the possibility to identify earlier the working day in which it would have been necessary the presence of the Qualified Expert of Radiation Protection (QEPR) for testing the machine, allowed for the production of a formal request to the

QEPR for the date specified at this point, that was sent on the 27-th of June 2022.

- Wednesday 06/07. Training of technical personnel would have been performed during this current day. That's why, on the 24-th of June 2022, it was sent a formal communication to the Operative Department (OPS) of CMS, whose major employment is devoted to the management of physicians' agendas. The presented request regarded the closure of agendas from the 1-st of July until to the 11-th of July, in order to have the time window required for performing the aforementioned points. Moreover, a request for the opening of a daily agenda in the date specified at this point was done, in order to perform training of technical personnel with real case studies. The specification of the request included to have at least more than four patients in the agenda for that date: the OPS confirmed the opening of the agenda for six patients, with a duration for single examination doubled with respect to the current practice, established so for 30 minutes. A confirmation about the feasibility of this program was received by the Project Manager of Technologic. Also, the daily examinations would have been performed with the guidance of an internal engineer of Technologic company, who would have followed the operativity of the operator during the execution of the exam.

5.2. Installation

As it was announced in the schedule presented by the PM of Technologic, the machine was delivered on the 4-th of July 2022. The transported arrived to "Panfilo Castaldi" centre during the morning. The R7 ambulatory was emptied by the old technology on the 31-th of June, where the old distributor withdrew the GE-Bravo machine. During the phase of entry in the ambulatory, the machine was positioned vertically on a system provided with special wheels for transportation, as visible in Figure 54.



Figure 54: Vertical positioning of the machine with wheels for transportation (a). In room machine positioning (b).

Once the technology was placed, the rest of the working day was dedicated to machine assembly of the C-arm and phantom calibration. It's worthy to mention that the phantom used for the initial calibration would have been used also for the daily Quality Check (QC) of the machine, performed by the technical personnel at the beginning of each daily agenda: Horizon, in fact, possess a system of Quality Check that makes the use of a anthropomorphic phantom of the lumbar spine (L1-L4). Every morning, the machine automatically will perform a QC after the positioning of the phantom in a specified position given by laser beams. The result of the daily QC would be stored in a plot showing the obtained data. The admitted field of variation goes from +1.5% up to -1.5%.



Figure 55: C-arm mounting on DEXA apparatus (a). Phantom Calibration (b).

5.3. Configuration & testing

During the following day, an internal engineer of Technologic was employed for the configuration of the workstation with the installed technology. In fact, Horizon Ci was equipped with a console directly powered by the machine itself. The workstation contained the software implementation produced by Hologic, the so-called APEX software, through which it's possible to:

- Perform the daily Quality Check. The system will automatically produce laser beams in an orthogonal direction for guiding the correct positioning of the phantom.
- Execute an exam.
- Analyse a scan stored in the local archive.
- Produce a standardized report of the BMD measurement.
- Execute a backup of the patient data, with associated scan and BMD measurements.

- Store patient data in a local archive.



Figure 56: Workstation with APEX software.

After the workstation setup, a configuration of the machine with the internal RIS/PACS architecture was performed. In particular:

- Worklist. Query parameters were tuned with an OT modality, whose AETitle was MOCCASTALDI.
- Storage. The destination for DICOM storage was set for an IP address that was reserved for the machine under analysis, with REPUBBLICAFEED as AeTitle.
- Query Retrieve. The IP address and AETitle were initialized as the ones used for Storage modality, since the retrieve of historical information would have been performed from the same PACS IP address.

After the RIS/PACS configuration setup, it was performed a test acquisition on the lumbar spine phantom, whose BMD report was sent to the internal storage network in order to verify the correct functioning of the configuration.

During the 5-th of July not only machine configuration with RIS/PACS architecture was performed: to validate the correct functionality of the DEXA apparatus the Qualified Expert in Radiation Protection was also enrolled, in order to perform the testing of the technology. As a result, the machine fulfilled the criteria of correct functioning, safety and radioprotection, in order to ensure a correct day-by-day operativity.

5.4. Training

The 6-th of July 2022 was devoted to training of the Technical Personnel for the correct use of the technology. In particular, an internal engineer of Technologic company trained the Technical Personnel for:

- The procedure of daily Quality Check, that would have been performed at the beginning of each daily agenda.
- Patient positioning.
- A correct use of the APEX software. The interface, after a lumbar spine of femoral scan, would allow for selecting:
 - Global ROI, in order to exclude from the BMD analysis lumbar or femoral regions that are out of interest for the clinical evaluation.
 - Bone Map, that allow for a correction of the automatically segmented bone structure. Thus, this procedure allows for a semi-automatic segmentation of ROIs.
 - Vertebral Lines, representing horizontal lines that divide a region containing one single vertebra. The displacement of the Vertebral Lines can be modified according to the experience of the Technical Personnel, with the aim to include in a single vertebral segment the whole content related to this anatomical site.
 - Include/exclude vertebrae from the BMD analysis, in case of more than 1 SD T-score difference between two adjacent vertebrae, as indicated in [53]: the excluded vertebra will be the one presenting the highest BMD T-score among the two.

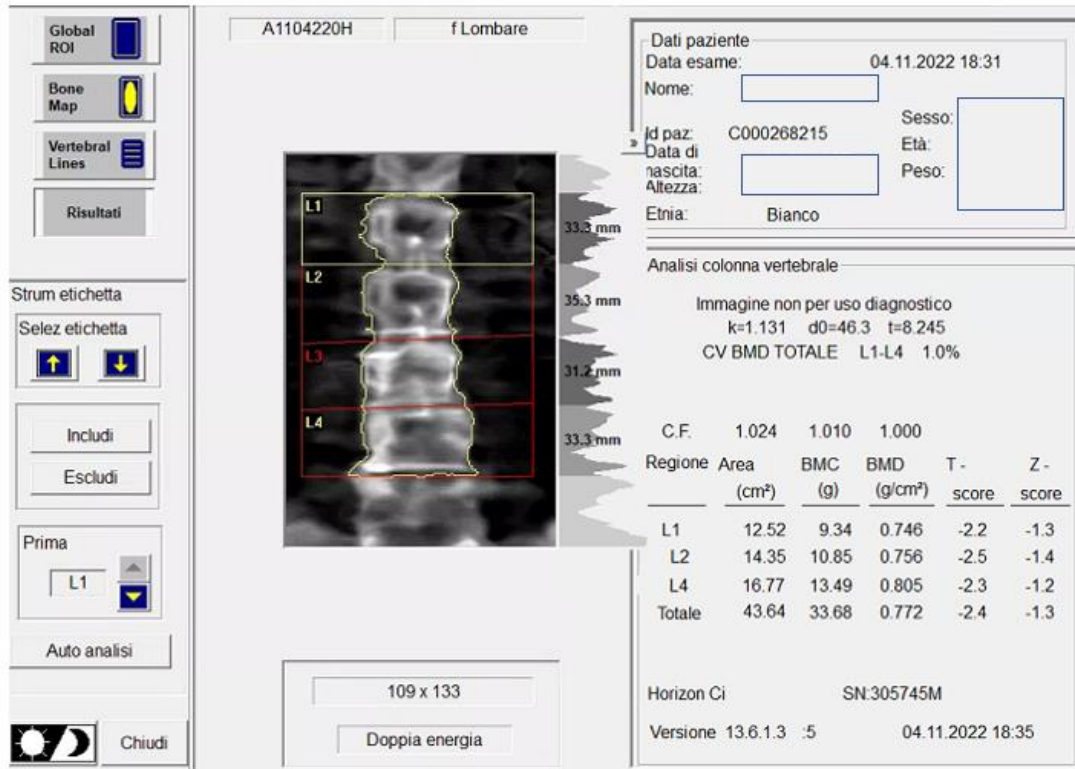
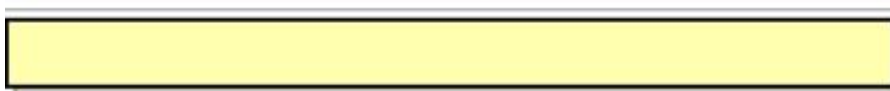


Figure 57: APEX User Interface.

Once completed the post-processing, the Technical Personnel was trained to conclude the examination and send to the RIS/PACS architecture the report produced by the scanner, as visible in Figure 58, in order to allow the medical personnel to compile the medical report associated to the medical images acquired.

Santagostino
Via Panfilo Castaldi, 6
Milano, Italia 20124



Medico di riferimento:

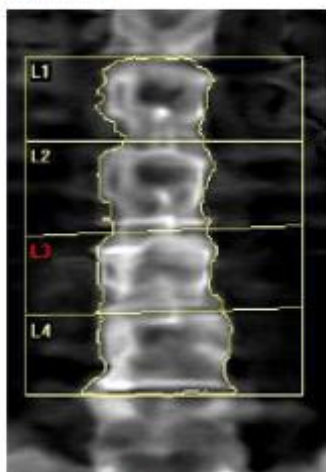


Immagine non per uso diagnostico
k = 1.131, ø2 = 46.3
109 x 133
DAP: 2.0 cGy/cm²

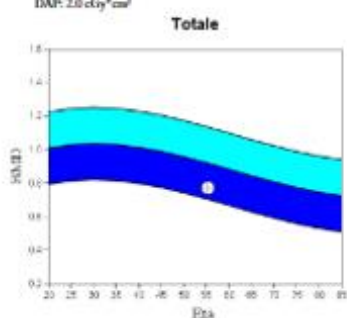
Informazioni sulla scansione:

Data scansione: 04 Novembre 2022 ID: A110422011
Tipo di scansione: f Lombare
Analisi: 04 Novembre 2022 18:35 Versione 13.6.1.3:5
Col: T
Operatore:
Modello: Horizon Ci (S/N 305745M)
Commento:

Riepilogo risultati DXA:

Regione	Area (cm²)	BMC (g)	BMD (g/cm³)	T-score	Z-score
L1	12.52	9.34	0.746	-2.2	-1.3
L2	14.35	10.85	0.756	-2.5	-1.4
L4	16.77	13.49	0.805	-2.3	-1.2
Totale	43.64	33.68	0.772	-2.4	-1.3

Totale BMD CV 1.09%, ACI = 1.05%, BCP = 1.010, TI = 8.05
Classificazione WHO: Osteopenia
Rischio frattura: Aumentato



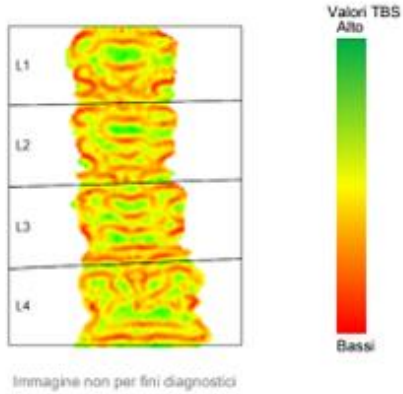
Commento:

Figure 58: Hologic BMD report.

For what concern the TBS and BSI report production, once the BMD scan was completed, the system was configured in order to send directly the 2D acquired image to the two software, for the computation of the Trabecular Bone Score and the Bone Strain Index with their corresponding reports. The three documents will be sent together to the RIS/PACS architecture with the formula of encapsulated PDF. A representation of TBS and BSI report is visible respectively in Figure 59 and Figure 60.

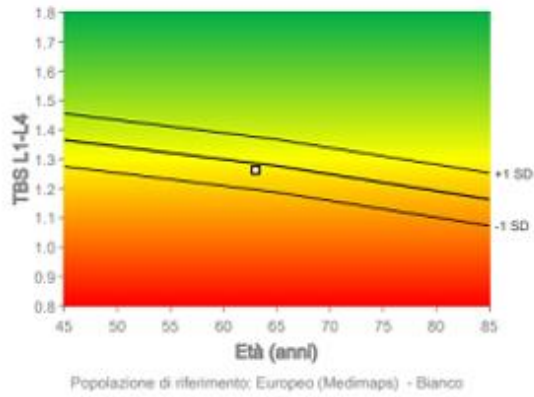
REPORT DI SALUTE OSSEA

1 Mappatura TBS



2 Risultato TBS del rachide lombare

TBS L1-L4 = 1,263 - Microarchitettura parzialmente degradata



3 Valutazione dello stato scheletrico

L'osteoporosi è una malattia scheletrica sistemica caratterizzata da una bassa massa ossea ed un deterioramento microarchitettonico del tessuto osseo, con conseguente aumento della fragilità ossea e suscettibilità alla frattura.¹

Il TBS deriva dalla struttura dell'immagine DXA e ha dimostrato di essere correlato alla microarchitettura ossea e al rischio di fratture. Fornisce informazioni indipendenti dalla BMD.

Per chiarezza, il "Bone Resilience Index" è definito come la combinazione delle categorie del T-score della BMD e del TBS. Le zone del Bone Resilience Index sono stabilite in base al livello di rischio di frattura.²

		BMD T-score*		
		Normale	Osteopenia	Osteoporosi
TBS	Normale	Normale	Moderata	Bassa
	Parzialmente deteriorato	Moderata	Bassa	Estremamente bassa
	Deteriorato	Bassa	Estremamente bassa	Estremamente bassa

* Il T-score della BMD corrisponde al valore minimo di colonna vertebrale, femore totale e collo femorale

** TBS L1-L4 Microarchitettura normale > 1.31; Degradata ≤ 1.23



4 Strumenti di decisione terapeutica

BMD T-score:

Sito Osseo	T-score della BMD	T-score della BMD corretto con TBS*
Colonna vertebrale	-5.0	-5.5
Collo femorale <-	-3.2	-3.5
Femore Totale <-	-2.9	-3.1

*Convalidato solo per le donne caucasiche. La cellula grigia corrisponde al valore minimo. La freccia visualizzata accanto al sito osseo dell femore rappresenta il lato del femore preso in considerazione nell'esame: <- per femore di sinistra, >- per femore di destra.

5 Risultati dettagliati del rachide lombare

Regione	TBS	TBS Z-score	BMD (g/cm ³)	T-score della BMD
L1	1.237	-	0.465	-4.8
L2	1.238	-	0.553	-4.3
L3	1.235	-	0.536	-5.0
L4	1.342	-	0.435	-5.7
L1-L4	1.263	-0.3	0.494	-5.0
L1-L3	1.237	0.1	0.518	-4.5
L1-L4(L3)	1.272	-0.1	0.480	-5.0
L1-L4(L2)	1.271	-0.2	0.476	-5.2
L2-L4	1.271	-0.5	0.502	-5.2
L1-L2	1.238	0.4	0.508	-4.3
L1-L3(L2)	1.236	0.1	0.502	-4.6
L1-L4(L2L3)	1.290	0.2	0.448	-5.4
L2-L3	1.236	-0.5	0.544	-4.7
L2-L4(L3)	1.290	-0.3	0.486	-5.4
L3-L4	1.288	-0.7	0.481	-5.6

6 Note & Riferimenti Bibliografici

Data di generazione del report: 11/06/2022 4:33:40 PM
Data dell'analisi: 10/26/2022 - Versione TBS iNsign: 3.1.2
DXA: Horizon CI #305745M - File: PA22A26A.P0J

1. Consensus Development Conference, Am J Med 94, 646-650 (1994)
2. Tratto da J. Bone Miner. Res. 26, 2762-2769 (2011)
3. Calcif Tissue Int. 96, 500-509 (2015)
4. Tratto da Osteoporos Int. 29, 751-758 (2018)

Figure 59: TBS iNsign® report.

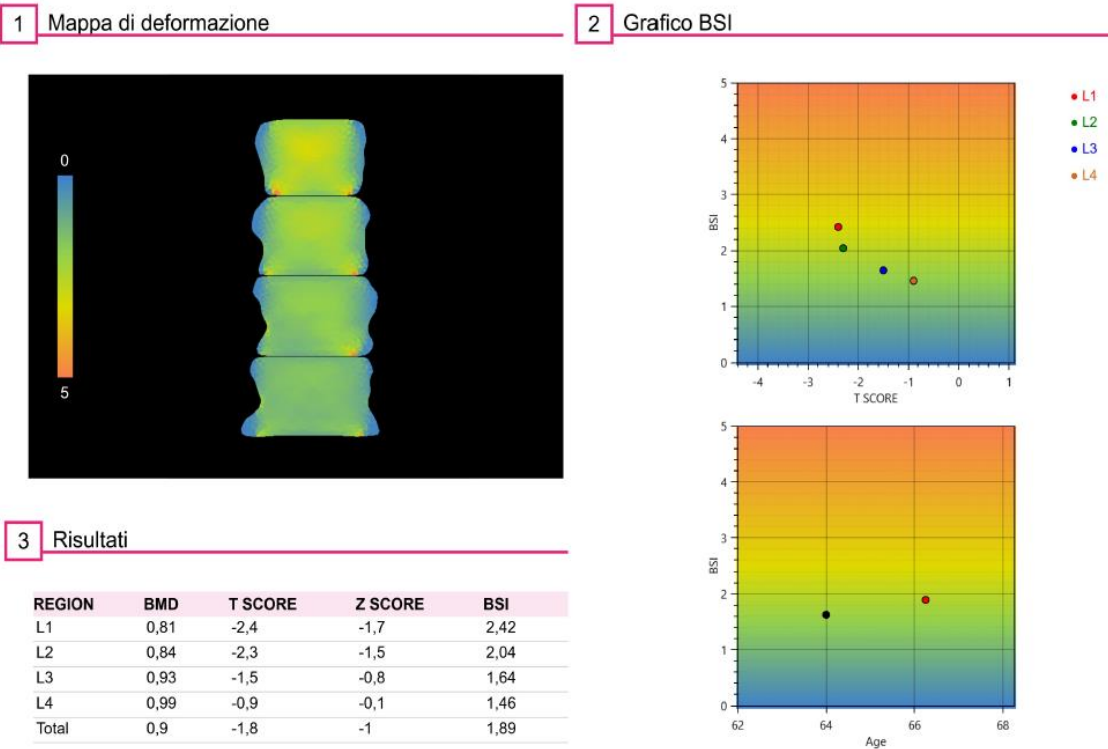


Figure 60: BSI report for the lumbar spine site.

As declared in the GANTT chart described in Section 3.4, on the 8-th of July it was scheduled a webinar with CMS specialists in the field of radiology and endocrinology, with the aim to inform them about the correct use of BMD, TBS and BSI threshold according to guidelines, in order to interpret in a standardized manner any real case study. As specified in Sections 2.3.2, 3.3.2 and 3.3.3 thresholds are listed below:

- Bone Mineral Density
 - *Normal*. A BMD value within 1 SD of the young adult reference mean (T-score ≥ -1).
 - *Low bone mass (osteopenia)*. A BMD whose value is between -1 SD and -2.5 SD with respect to the young adult mean.
 - *Osteoporosis*. A BMD value lower or equal to -2.5 SD with respect to the young adult mean.
 - *Severe osteoporosis (established osteoporosis)*. A BMD value lower or equal to -2.5 SD with respect to the young adult mean, but in this case in presence of one or more fragility fractures.

- Trabecular Bone Score
 - *Normal*. A TBS value higher than 1.31.
 - *Partially deteriorated trabecular structure*. A TBS value comprised between 1.31 (included) and 1.23.
 - *Degraded trabecular structure*. A TBS value lower or equal than 1.23.
- Bone Strain Index.
 - *Normal*. A BSI value lower or equal than 1.68.
 - *Partially reduced bone resistance*. A BSI value comprised between 1.68 and 2.40.
 - *Reduced bone resistance*. A BSI value higher or equal than 2.40.

5.5. General feedbacks

After the introduction of the new bone densitometer, technicians and physicians experienced a positive reaction with its use in the current practice. Of course, this has been possible thanks a preoperative training on the correct use of all the features that the machine provided. Technical personnel showed a particular interest in the functionalities provided by the APEX software: with respect to the previous technology, Horizon Ci provided additional tools for the post-processing of the image, such as the Bone Map feature, that allows for a manual refinement of the automatic segmentation performed by the DEXA scan. Furthermore, the possibility of performing a manual modification of the Vertebral Lines, with the additional feature of changing the angular displacement of the separator among two adjacent vertebrae, provided an increase of the accuracy of the output, which is the BMD value. Physicians felt the introduction of the TBS and BSI software modules since their first examination to be reported: for what concern patients with endocrinologic diseases, it was possible to obtain a measurement related to the bone quality of the segment under analysis, in order to provide the most accurate indication to patients under examination. As reported in Section 3.3, with diabetic patients, whose health status is previously determined with a protocol anamnesis, it has been possible to attribute a higher fracture risk thanks to the analysis of the trabecular microstructure: in fact, in the case of this category of patients, the reported BMD value is paradoxically higher with respect to healthy patients, while a measurement of the TB score can provide an indication of the 3D distribution of a deteriorated bone architecture. BSI empowered software

applications with the possibility to expand the analysis related to the bone quality also at the femoral site, that with TBS it isn't still possible. The process of internalization of this new technology was conducted by a single project owner, but many actors were included in the workflow for the schedule, operation, and training of the new technology. The proof to have the possibility to report an improvement of the diagnosis effectiveness is considered one of the pillars for CMS growth: for this way, thanks to the accommodation provided by the company after a first positive impression, it will be possible to consider this innovation in healthcare also in surrounding health clinics, in order to increase the impact of the generated value, for both the company and the society [1].

6. Conclusion and future developments

6.1. Conclusion

The whole process of assessment, decision-making and configuration for the introduction of Horizon Ci technology has been only one of the many activities carried out during my internship in Santagostino medical centre. The personal effort in the good realization of any internal process has been the aspect that advanced the most for my professional experience. The Department of Clinical Engineering allowed me for having this opportunity: there were many projects that were proposed, but consequentially to my academic background I decided to choose the project for the introduction of this innovation. This opportunity allowed me for the application of concepts and notions that were learnt during my personal course of study at Politecnico di Milano. Technical background in understanding the technical concepts related to imaging in diagnostics permitted to differentiate among the proposed alternatives with a rational comprehension, mostly related to the process to the generation of the image as first output of the DEXA scan. A particular interest with respect to the medical diagnostic field was provided firstly by personal experiences, and the subsequent confidence was then developed with the attendance to the academy: courses taken at Politecnico, such as Electronic Design, Methods for Biomedical Imaging and Computer Aided Surgery, and Medical Applications of Radiation Fields allowed me to develop a full comprehension of the variety of mechanisms of high energy radiation generation, tissue-material interaction and image formation. The possibility to directly apply all this knowledge was rewarding for all the effort done to understand the physics of this complicated science field. Not only, apart from the technical aspects, the skills that were needed to actualize this project from the managerial, operative and economic point of view were aspects that were never encountered before in my professional experience. Being the owner of a project means to have the responsibility to guide the entire workflow towards an effective, efficient and valuable management of subsequent tasks: the description of the clinical and technical features, to be presented then to the clinical audience, has been only one of the responsibilities for a global satisfaction. In fact, a precise time-based schedule of all the activities has been

necessary in order then to combine all the actors take took part in this process: the preventive communication with internal and external figures of CMS allowed not only to actualize the project without many bottlenecks, prone to happen in case of an incorrect management of the preoperative activities to be prepared, but also allowed a personal growth in attributing a main importance to the planification of the activities, even if the timing conditions in the future won't be fully respected. The economic part was then considered as one of the most important opportunities for an improvement of my personal skills: the possibility to take part in a private health clinics showed its main advantages for this domain, since a correct negotiation with the final supplier, taken out personally, before the acceptance of the economic offer, allowed to generate value for all the participants: it was possible to generate value in understating how an economic mediation take place, but most importantly it was possible to allocate the saved budget in further projects considered for the current year.

6.2. Limitations

The introduction of new software tools for the improvement of the clinical diagnosis required an additional effort in terms of integration among the different measurement quantities. The presence of three separated software for the analysis of a single case study requires a non-indifferent labour in understating the correct functioning of the operative procedure to produce a valent report to be delivered to the physicians that will examine the reported documentation. The lack of the combination of the information in a more condense way could be considered as a first drawback of this implementation. Moreover, a reduced possibility in the customization of the report could bring to an initial confusion for the physician that will have to visualize and report using the available information coming from the DXA scanning. In addition, from the applicative point of view it has been possible to activate only a portion of the available typologies of scanning for patients: as an example, spinal morphometry is a typology of DEXA scanning that is present as a module in the Horizon Ci model, but it's an application that, for the moment, hasn't been considered yet for the opening of a dedicated medical service, since for timing reasoning it has been considered more effective to concentrate on the activation of a medical performance that presents a higher catchment area of patients.

6.3. Outlooks

From the examinations carried out with the Horizon Ci scanner, and thanks to an efficient data storage archive it has been possible to understand that most of patients coming to CMS with a request for a bone densitometry with TBS/BSI module were external patients. Apparently, it could be imagined that most probably an internal patient coming to CMS with the intention to perform a first endocrinological examination would be addressed for a bone densitometry with TBS/BSI integration. Instead, it has been possible to ascertain that there's interest coming from outer realities that allows to bring patients to experience the technologic leadership and clinical excellence of Santagostino medical centre.

With the objective to expand the innovation to generate additional value it has been already considered the possibility to introduce the technology installed in "Panfilo Castaldi" centre also in other health clinics. As a proof of that, as mentioned in Section 1.1, there's a growing interest on new apertures in Rome, with a particular attention in the verticalization of the radiologic field: that's why, innovation in medical technologies must be taken into account. Positive feedback coming from the analysis of the trend for requests of a bone densitometry exam could ensure the inclusion of new DEXA scanners in the radiological equipment together with Computerized Tomography, Mammography, US and MRI machines.

6.4. Acknowledgments

I would dedicate these few words to all people that permeated this period with words of courage and perseverance, included myself.

I would express gratitude toward to all my Department: every people composing the CMS Engineering and Technical Department gave its contribution. Every word was hugely appreciated: any encouragement, support and caress provided me a bit more to continue, to keep up. Thank you.

Special thanks to Mirco Baroni, my company tutor, head of the CE Department, and now colleague and confidant, that supported me in periods in which things became heavy to sustain. Every word spent with you allowed me to mature from a professional and personal point of view. Thank you.

My colleagues of the CE Department, part of the ET Department: Giacomo Cattaneo, Marco Gucciardi, Giulia Bainsi. I would like to thank you for all the days spent together. It has been an excellent experience to work with you: a team composed by people that all together try to keep care to all the huge medical equipment of CMS. 4777 medical devices, 5 guys. Thank you.

My other colleagues of the ET Department: Andrea Codini, Silvia Sau, Alice Brusa, Andrea Filippi, Juan Vargas. Everyone left something to me. Andrea Codini, head of the ET Department: every moment contains energies that aim to generate ideas, projects, sometimes dreams. Thank you. Silvia Sau, PM of the new openings: many times you permitted me to open the eyes, or simply to change their direction, with the aim to observe things from other points of view, focusing to reach a final goal for my professional and personal growth. Thank you. Andrea Filippi, Building Manager of the ET Department, thank you for all the support you gave to me: I've always been excited to share ideas and opinions with you, even more after a night full of study. Thank you.

Apart from work, there're many people that gave their contribution for allowing me to be as I am today. Sebastian, you've always been present, from the first days here at the university: we became friends, we are friends, and I'm sure we'll be as we are for all the rest. Thank you so much.

Karim, Paolo, I'm sure we'll keep going. Thank you for this travel towards the unknown, Polaris. The importance it to stick together, keep going, and try our best to realize the impossible. No words, no things, only proves.

Mam, Dad, sister: you always believed in me, sometimes more than I believed in myself. Please, continue to do so, continue to give me your energy and trust. I won't disappoint you.

I promise.

7. Bibliography

- [1] 'Annual Report', 2021. https://salute.santagostino.it/annual-report-2021?_ga=2.60378223.392574938.1663764562-1634980332.1663764562&_gl=1*fpyz8n*_ga*MTYzNDk4MDMzMzMi4xNjYzNzY0NTYy*_ga_CEMWP8JGSY*MTY2Mzc2NzUwNy4yLjEuMTY2Mzc2ODcxNS42MC4wLjA. (accessed Sep. 21, 2022).
- [2] O. N. Hoffmann Sara, 'View of Different But Still The Same? How Public And Private Sector Organisations Deal with New Digital Competences', Oct. 01, 2018. <https://academic-publishing.org/index.php/ejeg/article/view/657/620> (accessed Oct. 04, 2022).
- [3] Regione Lombardia, 'Legge Regionale 11 agosto 2015 , n. 23', Aug. 2015.
- [4] A. B. Polistena and F. Spandonaro, "'Le Performance Regionali'", 2022.
- [5] 'CREA Sanità'. <https://www.creasanita.it/index.php/it/> (accessed Oct. 04, 2022).
- [6] 'WHO Technical Report Series 921 PREVENTION AND MANAGEMENT OF OSTEOPOROSIS Report of a WHO Scientific Group'.
- [7] 'Regolamento UE 2016 679. Arricchito con riferimenti ai Considerando... - Garante Privacy'. <https://www.garanteprivacy.it/web/guest/home/docweb/-/docweb-display/docweb/6264597> (accessed Oct. 08, 2022).
- [8] 'Decreto Legislativo del Governo n. 187 del 26 maggio 2000 Attuazione della direttiva 97/43/Euratom in materia di protezione sanitaria delle persone contro i pericoli delle radiazioni ionizzanti connesse ad esposizioni mediche.» Associazione Italiana di Radioterapia ed Oncologia Clinica'. <https://www.radioterapiaitalia.it/aggiornamento-legislativa/documenti-it-aggiornamento-legislativa/normativa-radiazioni-ionizzanti/decreto-legislativo-del-governo-n-187-del-26-maggio-2000-attuazione-della-direttiva-9743euratom-materia-protezione-sanitaria-delle-persone-pericoli-delle-radiazioni-ionizzanti-conn/> (accessed Oct. 08, 2022).

- [9] 'Ricerca: I tempi di attesa per le prestazioni ambulatoriali in Lombardia'.
<https://www.polis.lombardia.it/wps/portal/site/polis/DettaglioRedazionale/pubblicazioni/studi-e-documenti/tempi-di-attesa-ambulatorio> (accessed Oct. 10, 2022).
- [10] 'Esenzione dal pagamento del ticket per eta' e per reddito'.
<https://www.ats-brianza.it/it/ticket/168-le-esenzioni-per-reddito.html> (accessed Oct. 10, 2022).
- [11] Y. David *et al.*, 'VII Clinical Engineering 74 Clinical Engineering', 2006.
- [12] I. L. Presidente and D. Repubblica, 'ATTUAZIONE DELLA DIRETTIVA 93/42/CEE CONCERNENTE I DISPOSITIVI MEDICI', vol. 47, 2007.
- [13] 'EUR-Lex - 32007L0047 - EN - EUR-Lex'. <https://eur-lex.europa.eu/legal-content/IT/TXT/?uri=celex%3A32007L0047> (accessed Oct. 10, 2022).
- [14] 'EUR-Lex - 31990L0385 - EN - EUR-Lex'. <https://eur-lex.europa.eu/legal-content/it/ALL/?uri=CELEX:31990L0385> (accessed Oct. 10, 2022).
- [15] 'EUR-Lex - 31998L0079 - EN - EUR-Lex'. <https://eur-lex.europa.eu/legal-content/IT/TXT/?uri=celex%3A31998L0079> (accessed Oct. 10, 2022).
- [16] 'Il ruolo dell' ingegnere clinico nel SSN'.
<https://www.aiic.it/materiale-informativo/> (accessed Oct. 10, 2022).
- [17] 'Overview - FHIR v4.3.0'. <https://www.hl7.org/fhir/overview.html> (accessed Oct. 11, 2022).
- [18] 'About Health Level Seven International | HL7 International'.
<http://www.hl7.org/about/index.cfm?ref=nav> (accessed Oct. 11, 2022).
- [19] 'HTA 101: Introduction to Health Technology Assessment'.
<https://www.nlm.nih.gov/nichsr/hta101/ta10103.html#HTAi> (accessed Oct. 13, 2022).
- [20] 'What Is Optical Coherence Tomography? - American Academy of Ophthalmology'. <https://www.aao.org/eye-health/treatments/what-is-optical-coherence-tomography> (accessed Oct. 15, 2022).
- [21] F. Lacarrubba, V. D'Amico, M. R. Nasca, F. Dinotta, and G. Micali, 'Use of dermatoscopy and videodermatoscopy in therapeutic follow-

- up: A review', *Int J Dermatol*, vol. 49, no. 8, pp. 866–873, Aug. 2010, doi: 10.1111/J.1365-4632.2010.04581.X.
- [22] H. Kröger, P. Vainio, J. Nieminen, and A. Kotaniemi, 'Comparison of different models for interpreting bone mineral density measurements using DXA and MRI technology', *Bone*, vol. 17, no. 2, pp. 157–159, 1995, doi: 10.1016/S8756-3282(95)00162-X.
- [23] J. A. Kanis, A. Oden, H. Johansson, F. Borgström, O. Ström, and E. McCloskey, 'FRAX® and its applications to clinical practice', *Bone*, vol. 44, no. 5, pp. 734–743, May 2009, doi: 10.1016/J.BONE.2009.01.373.
- [24] K. J. Chun, 'Bone densitometry', *Semin Nucl Med*, vol. 41, no. 3, pp. 220–228, 2011, doi: 10.1053/J.SEMNUCLMED.2010.12.002.
- [25] V. Bousson *et al.*, 'Trabecular bone score (TBS): available knowledge, clinical relevance, and future prospects', *Osteoporos Int*, vol. 23, pp. 1489–1501, 2012, doi: 10.1007/s00198-011-1824-6.
- [26] M. S. Tabatabaei, M. Langarizadeh, and K. Tavakol, 'An Evaluation Protocol for Picture Archiving and Communication System: a Systematic Review', *Acta Informatica Medica*, vol. 25, no. 4, p. 250, 2017, doi: 10.5455/AIM.2017.25.250-253.
- [27] L. Pothuaud, N. Barthe, M. A. Krieg, N. Mehsen, P. Carceller, and D. Hans, 'Evaluation of the Potential Use of Trabecular Bone Score to Complement Bone Mineral Density in the Diagnosis of Osteoporosis: A Preliminary Spine BMD-Matched, Case-Control Study', *Journal of Clinical Densitometry*, vol. 12, no. 2, pp. 170–176, Apr. 2009, doi: 10.1016/J.JOCD.2008.11.006.
- [28] F. M. Ulivieri and L. Rinaudo, 'Beyond Bone Mineral Density: A New Dual X-Ray Absorptiometry Index of Bone Strength to Predict Fragility Fractures, the Bone Strain Index', *Front Med (Lausanne)*, vol. 7, p. 1096, Jan. 2021, doi: 10.3389/FMED.2020.590139/BIBTEX.
- [29] R. E. Faw and J. K. Shultis, 'Radiation Sources', *Encyclopedia of Physical Science and Technology*, pp. 613–631, 2003, doi: 10.1016/B0-12-227410-5/00636-0.
- [30] R. Behling and F. Grüner, 'Diagnostic X-ray sources—present and future', *Nucl Instrum Methods Phys Res A*, vol. 878, pp. 50–57, Jan. 2018, doi: 10.1016/J.NIMA.2017.05.034.
- [31] 'CODATA Value: electron volt'. <https://physics.nist.gov/cgi-bin/cuu/Value?evj> (accessed Oct. 17, 2022).

- [32] 'Interaction of Radiation with Matter'. <http://www.sprawls.org/ppmi2/INTERACT/> (accessed Nov. 13, 2022).
- [33] M. Berger, Q. Yang, and A. Maier, 'X-ray Imaging', *Lecture Notes in Computer Science (including subseries Lecture Notes in Artificial Intelligence and Lecture Notes in Bioinformatics)*, vol. 11111 LNCS, pp. 119–145, Aug. 2018, doi: 10.1007/978-3-319-96520-8_7.
- [34] D. Oborska-Kumaszyńska and S. Wiśniewska-Kubka, 'Analog and digital systems of imaging in roentgenodiagnosics', *Pol J Radiol*, vol. 75, no. 2, p. 73, 2010, doi: 10.5772/19847.
- [35] 'Chapter 5: Solid-state diodes and diode characteristics [Analog Devices Wiki]'. <https://wiki.analog.com/university/courses/electronics/text/chapter-5> (accessed Oct. 20, 2022).
- [36] A. H. Khan and R. A. Chaudhuri, 'Fan-beam geometry based inversion algorithm in computed tomography (CT) for imaging of composite materials', *Compos Struct*, vol. 110, no. 1, pp. 297–304, Apr. 2014, doi: 10.1016/J.COMPSTRUCT.2013.11.019.
- [37] M. v. DeVita and S. H. Stall, 'Dual-energy X-ray absorptiometry: a review', *J Ren Nutr*, vol. 9, no. 4, pp. 178–181, Oct. 1999, doi: 10.1016/S1051-2276(99)90030-4.
- [38] 'United States Patent 19 Ohtsuchi et al. 54) K-EDGE FILTER AND AN X-RAY'.
- [39] Maciej Serda *et al.*, 'Synteza i aktywność biologiczna nowych analogów tiosemikarbazonowych chelatorów żelaza', *Uniwersytet śląski*, vol. 7, no. 1, pp. 343–354, 2013, doi: 10.2/JQUERY.MIN.JS.
- [40] D. Generale Della Programmazione Sanitaria, 'MINISTERO DELLA SALUTE DIPARTIMENTO DELLA QUALITA' Individuazione dei criteri di Accesso alla Densitometria Ossea'.
- [41] T. D. Rachner, S. Khosla, and L. C. Hofbauer, 'Osteoporosis: now and the future', *The Lancet*, vol. 377, no. 9773, pp. 1276–1287, Apr. 2011, doi: 10.1016/S0140-6736(10)62349-5.
- [42] G. Karaguzel and M. F. Holick, 'Diagnosis and treatment of osteopenia', doi: 10.1007/s11154-010-9154-0.
- [43] N. Salari *et al.*, 'Global prevalence of osteoporosis among the world older adults: a comprehensive systematic review and meta-analysis', *J Orthop Surg Res*, vol. 16, no. 1, pp. 1–13, Dec. 2021, doi: 10.1186/S13018-021-02821-8/TABLES/3.

- [44] M. A. Clynes, N. C. Harvey, E. M. Curtis, N. R. Fuggle, E. M. Dennison, and C. Cooper, 'The epidemiology of osteoporosis', *Br Med Bull*, vol. 133, no. 1, pp. 105–117, Apr. 2020, doi: 10.1093/BMB/LDAA005.
- [45] D. C. Welten, H. C. G. Kemper, G. B. Post, and W. A. van Staveren, 'A Meta-Analysis of the Effect of Calcium Intake on Bone Mass in Young and Middle Aged Females and Males', *J Nutr*, vol. 125, no. 11, pp. 2802–2813, Nov. 1995, doi: 10.1093/JN/125.11.2802.
- [46] M. Khan, A. Jose, and S. Sharma, 'Physiology, Parathyroid Hormone', *StatPearls*, Jun. 2022, Accessed: Oct. 22, 2022. [Online]. Available: <https://www.ncbi.nlm.nih.gov/books/NBK499940/>
- [47] P. Egger, S. Duggleby, R. Hobbs, C. Fall, and C. Cooper, 'Cigarette smoking and bone mineral density in the elderly.', *J Epidemiol Community Health (1978)*, vol. 50, no. 1, pp. 47–50, Feb. 1996, doi: 10.1136/JECH.50.1.47.
- [48] D. L. Kendler *et al.*, 'Vertebral Fractures: Clinical Importance and Management', *Am J Med*, vol. 129, 2016, doi: 10.1016/j.amjmed.2015.09.020.
- [49] B. Stanghelle, H. Bentzen, L. Giangregorio, A. H. Pripp, and A. Bergland, 'Effect of a resistance and balance exercise programme for women with osteoporosis and vertebral fracture: Study protocol for a randomized controlled trial', *BMC Musculoskelet Disord*, vol. 19, no. 1, pp. 1–9, Apr. 2018, doi: 10.1186/S12891-018-2021-Y/TABLES/1.
- [50] 'Vertebral fractures. a The Genant semiquantitative method is a visual... | Download Scientific Diagram'. https://www.researchgate.net/figure/Vertebral-fractures-a-The-Genant-semiquantitative-method-is-a-visual-grading-system-for_fig2_343947239 (accessed Oct. 22, 2022).
- [51] H. P. Dimai, 'Use of dual-energy X-ray absorptiometry (DXA) for diagnosis and fracture risk assessment; WHO-criteria, T- and Z-score, and reference databases', *Bone*, vol. 104, pp. 39–43, Nov. 2017, doi: 10.1016/J.BONE.2016.12.016.
- [52] H. Kröger, P. Vainio, J. Nieminen, and A. Kotaniemi, 'Comparison of different models for interpreting bone mineral density measurements using DXA and MRI technology', *Bone*, vol. 17, no. 2, pp. 157–159, Aug. 1995, doi: 10.1016/S8756-3282(95)00162-X.
- [53] 'Adult Positions - ISCD'. <https://iscd.org/learn/official-positions/adult-positions/> (accessed Oct. 23, 2022).

- [54] S. M. Nazia Fathima, R. Tamilselvi, and M. Parisa Beham, 'A Survey on Osteoporosis Detection Methods with a Focus on X-ray and DEXA Images', *IETE J Res*, 2020, doi: 10.1080/03772063.2020.1803771.
- [55] L. Pothuaud, P. Carceller, and D. Hans, 'Correlations between grey-level variations in 2D projection images (TBS) and 3D microarchitecture: Applications in the study of human trabecular bone microarchitecture', *Bone*, vol. 42, no. 4, pp. 775–787, Apr. 2008, doi: 10.1016/J.BONE.2007.11.018.
- [56] N. C. Harvey *et al.*, 'Trabecular bone score (TBS) as a new complementary approach for osteoporosis evaluation in clinical practice', *Bone*, vol. 78, pp. 216–224, Sep. 2015, doi: 10.1016/J.BONE.2015.05.016.
- [57] V. Bousson, C. Bergot, B. Sutter, P. Levitz, and B. Cortet, 'Trabecular bone score (TBS): Available knowledge, clinical relevance, and future prospects', *Osteoporosis International*, vol. 23, no. 5, pp. 1489–1501, May 2012, doi: 10.1007/S00198-011-1824-6/FIGURES/5.
- [58] M. Terzini, A. Aldieri, L. Rinaudo, G. Osella, A. L. Audenino, and C. Bignardi, 'Improving the hip fracture risk prediction through 2D finite element models from DXA images: Validation against 3D models', *Front Bioeng Biotechnol*, vol. 7, no. SEP, p. 220, 2019, doi: 10.3389/FBIOE.2019.00220/BIBTEX.
- [59] N. Martelli *et al.*, '[Hospital-based health technology assessment in France: how to proceed to evaluate innovative medical devices?]', *Ann Pharm Fr*, vol. 72, no. 1, pp. 3–14, Jan. 2014, doi: 10.1016/J.PHARMA.2013.09.002.
- [60] P. D. Parchi *et al.*, 'Biomechanics of Interspinous Devices', 2014, doi: 10.1155/2014/839325.
- [61] 'DICOM'. <https://www.dicomstandard.org/> (accessed Oct. 25, 2022).
- [62] 'Vision, Mission, and Values - EUnetHTA'. <https://www.eunethta.eu/about-eunethta/mission-vision-and-values/> (accessed Oct. 25, 2022).
- [63] 'HTA Core Model® - EUnetHTA'. <https://www.eunethta.eu/hta-core-model/> (accessed Oct. 25, 2022).
- [64] K. Kidholm, L. Ehlers, L. Korsbek, R. Kjærby, and M. Beck, 'Assessment of the quality of mini-HTA', *Int J Technol Assess Health Care*, vol. 25, no. 1, pp. 42–48, Jan. 2009, doi: 10.1017/S0266462309090060.

- [65] 'INTRODUCTION TO MINI-HTA-a management and decision support tool for the hospital service The Danish Centre for Evaluation and Health Technology Assessment Introduction to mini-HTA 3 Introduction to mini-HTA-a management and decision support tool for the hospital service', Accessed: Oct. 26, 2022. [Online]. Available: <http://www.dacehta.dk/>
- [66] A. Bazzocchi, F. Ponti, U. Albisinni, G. Battista, and G. Guglielmi, 'DXA: Technical aspects and application', *Eur J Radiol*, vol. 85, no. 8, pp. 1481–1492, Aug. 2016, doi: 10.1016/J.EJRAD.2016.04.004.
- [67] J. A. Kanis, A. Oden, H. Johansson, F. Borgström, O. Ström, and E. McCloskey, 'FRAX® and its applications to clinical practice', *Bone*, vol. 44, no. 5, pp. 734–743, May 2009, doi: 10.1016/J.BONE.2009.01.373.
- [68] L. Humbert *et al.*, '3D-DXA: Assessing the Femoral Shape, the Trabecular Macrostructure and the Cortex in 3D from DXA images', *IEEE Trans Med Imaging*, vol. 36, no. 1, pp. 27–39, Jan. 2017, doi: 10.1109/TMI.2016.2593346.
- [69] D. Hans, A. L. Goertzen, M. A. Krieg, and W. D. Leslie, 'Bone microarchitecture assessed by TBS predicts osteoporotic fractures independent of bone density: the Manitoba study', *J Bone Miner Res*, vol. 26, no. 11, pp. 2762–2769, Nov. 2011, doi: 10.1002/JBMR.499.
- [70] E. S. Siris *et al.*, 'Bone Mineral Density Thresholds for Pharmacological Intervention to Prevent Fractures', *Arch Intern Med*, vol. 164, no. 10, pp. 1108–1112, May 2004, doi: 10.1001/ARCHINTE.164.10.1108.
- [71] E. v. McCloskey *et al.*, 'A Meta-Analysis of Trabecular Bone Score in Fracture Risk Prediction and Its Relationship to FRAX', *Journal of Bone and Mineral Research*, vol. 31, no. 5, pp. 940–948, May 2016, doi: 10.1002/JBMR.2734.
- [72] F. M. Ulivieri *et al.*, 'Utility of the trabecular bone score (TBS) in secondary osteoporosis', doi: 10.1007/s12020-014-0280-4.
- [73] F. P. Chen, S. F. Kuo, Y. C. Lin, C. M. Fan, and J. F. Chen, 'Status of bone strength and factors associated with vertebral fracture in postmenopausal women with type 2 diabetes.', *Menopause*, vol. 26, no. 2, pp. 182–188, Feb. 2019, doi: 10.1097/GME.0000000000001185.
- [74] E. Romagnoli *et al.*, '"Trabecular Bone Score" (TBS): an indirect measure of bone micro-architecture in postmenopausal patients with primary hyperparathyroidism', *Bone*, vol. 53, no. 1, pp. 154–159, Mar. 2013, doi: 10.1016/J.BONE.2012.11.041.

- [75] G. Tabacco *et al.*, 'Evaluation of bone quality by dxa-based bone strain index in primary hyperparathyroidism', *Endocrine Abstracts*, vol. 73, May 2021, doi: 10.1530/ENDOABS.73.AEP104.
- [76] E. S. Leib and R. Winzenrieth, 'Bone status in glucocorticoid-treated men and women', *Osteoporosis International*, vol. 27, no. 1, pp. 39–48, Jan. 2016, doi: 10.1007/S00198-015-3211-1.
- [77] E. Shevroja, O. Lamy, and D. Hans, 'Review on the Utility of Trabecular Bone Score, a Surrogate of Bone Micro-architecture, in the Chronic Kidney Disease Spectrum and in Kidney Transplant Recipients', *Front Endocrinol (Lausanne)*, vol. 9, no. SEP, p. 561, Sep. 2018, doi: 10.3389/FENDO.2018.00561.
- [78] S. Bréban *et al.*, 'Identification of Rheumatoid Arthritis Patients With Vertebral Fractures Using Bone Mineral Density and Trabecular Bone Score', *Journal of Clinical Densitometry*, vol. 15, no. 3, pp. 260–266, Jul. 2012, doi: 10.1016/J.JOCD.2012.01.007.
- [79] S. Kolta *et al.*, 'TBS result is not affected by lumbar spine osteoarthritis', *Osteoporosis International*, vol. 25, no. 6, pp. 1759–1764, 2014, doi: 10.1007/S00198-014-2685-6.
- [80] A. Dubromel and M.-A. Duvinage-Vonesch, 'Loïc Geffroy & Claude Dussart (2020) Organizational aspect in healthcare decision-making: a literature review', *J Mark Access Health Policy*, vol. 8, no. 1, p. 1810905, 2020, doi: 10.1080/20016689.2020.1810905.
- [81] H. C. Turner *et al.*, 'An Introduction to the Main Types of Economic Evaluations Used for Informing Priority Setting and Resource Allocation in Healthcare: Key Features, Uses, and Limitations', *Front Public Health*, vol. 9, Aug. 2021, doi: 10.3389/FPUBH.2021.722927.
- [82] I. L. Hollin, J. Paskett, A. L. R Schuster, N. L. Crossnohere, J. F. P Bridges, and J. F. P Bridges JohnBridges, 'Best-Worst Scaling and the Prioritization of Objects in Health: A Systematic Review', *Pharmacoeconomics*, vol. 40, pp. 883–899, 123AD, doi: 10.1007/s40273-022-01167-1.

List of Figures

Figure 1: Distribution of CMS centres in the Lombardy region [1]	3
Figure 2: Distribution of CMS centres in Italy [1].....	3
Figure 3: Ranking of regional performance [5]	4
Figure 4: CMS's mission [1].	5
Figure 5: Diathermocoagulator equipped with RFID technology	9
Figure 6: R7 ambulatory in "Panfilo Castaldi", GE-Bravo positioning.....	11
Figure 7: The Electromagnetic (EM) Spectrum	14
Figure 8: Cut view of an X-ray tube assembly	16
Figure 9: Simplified X-ray tube with a rotating anode and a heated filament	16
Figure 10: Schematic of the X-ray pathway crossing the patient, towards the detector	17
Figure 11: X-ray from source to detector	18
Figure 12: Schematic view of the photoelectric effect	20
Figure 13: Schematic view of the Compton effect	20
Figure 14: Cross-sectional diagram of the X-ray film.....	22
Figure 15: Simplified schematic diagram of a cross-sectional structure of two pixels of a-Se X-ray image detector.....	23
Figure 16: Energy levels of an organic scintillation molecule.....	24
Figure 17: Electronic potential in forward and reverse bias mode	25
Figure 18: Functioning of a reverse biased photodiode.....	26
Figure 19: Two sets of linear projections, whose final intensity correspond to value pL.....	27
Figure 20: A single set of linear projections acquired in the transversal plane	27
Figure 21: Parameters of a projection ray: angular and linear displacement θ and t	28
Figure 22: Fan beam geometry representation.....	28
Figure 23 Single slice acquired with fan-beam geometry.....	29
Figure 24: Hip fracture rates for men and women combined in different countries of the world, categorized by risk. Countries are coded red (annual incidence >250/100 000), orange (150–250/100 000) or green (<150/100 000) where estimates are available	34
Figure 25: Classification of vertebral fractures by the Genant semiquantitative method	41

Figure 26: DEXA scan image (a) spine with vertebrae numbering (b) right femur (c) left femur (d) forearm.....	41
Figure 27: Model for the calculation of volumetric bone mineral density (BMDvol) using DXA data.....	42
Figure 28: (a) Three-dimensional reconstruction of the trabecular bone microarchitecture in a human cadaver sample. The 2D projection image was obtained by projecting the 3D volume following the AP axis (b).....	48
Figure 29: Application of TBS mask on DEXA bone segmentation.....	49
Figure 30: A TBS calculation example using two basic structures, composed of a plate and a set of rods. The two models present the same amount of bone. To simplify the TBS explanation, only one direction is considered, a distance of 1 pixel is used.....	50
Figure 31: (a) Greyscale image obtained from a DXA on a porcine bone sample (b) Schematic of the FE-model of the cylindrical sample, including the mesh, the loading and boundary conditions	53
Figure 32: (a) Example of a DXA scan and(b) FEM mask on L1 vertebra obtained with the application of patient weight load.....	54
Figure 33: Boundary conditions graphic overview. To simulate a sideways fall condition, the head was bound to the ground using a spring element (B). the impact force was applied on (B), while the distal femur was linked with a hinge (C)	54
Figure 34: Example of 2 DXA scan vertebral ROIs with their corresponding BSI meshes. As it can be noted, the upper figure (a) is associated to a patient with a higher fracture risk with respect the lower figure (b).....	55
Figure 35: Example of 2 DXA scan femoral ROIs with their corresponding BSI meshes. As it can be noted, the upper figure (a) is associated to a patient with a higher fracture risk with respect the lower figure (b).....	55
Figure 36: FDX Visionary DR scanner.....	61
Figure 37: Main 3D-DXA report.....	63
Figure 38: GE Lunar prodigy with PRO software package	65
Figure 39: TBS mask applied on the segmented ROI combined with a graphical representation of the patient status with respect to bone microarchitecture distribution	66
Figure 40: Schematic of Full and Compact sizes of Lunar Prodigy PRO.....	68
Figure 41: GE Lunar prodigy with PRO software package	69
Figure 42: Different information levels provided by BMD, T and BSI.....	70
Figure 43: Main BSI report for the lumbar site	71
Figure 44: main BSI report for the femoral site.....	72
Figure 45: Schematic of a typical installation site, with reported dimensions	73

Figure 46: Matrix distribution of combined TBS and BMD incidence fracture values, per 1000 person-years.....	74
Figure 47: GANTT chart. From HTA phase up to DEXA installation.....	78
Figure 48: Monthly number of DEXA scans divided per centre from 2016....	80
Figure 49: Proposals DXA, cover of the presentation to CMS endocrinologists and radiologists.	84
Figure 50: Planimetry of the R7 ambulatory.	92
Figure 51: schematic of the link between the machine, the warning lamp and the power supply.....	96
Figure 52: Isodose curves of DEXA Horizon Wi/Ci.	97
Figure 53: X-ray radiation shielding screen.....	98
Figure 54: Vertical positioning of the machine with wheels for transportation (a). In room machine positioning (b).	100
Figure 55: C-arm mounting on DEXA apparatus (a). Phantom Calibration (b).	101
Figure 56: Workstation with APEX software.	102
Figure 57: APEX User Interface.	104
Figure 58: Hologic BMD report.	105
Figure 59: TBS iNsight® report.	106
Figure 60: BSI report for the lumbar spine site.	107

List of Graphs

Graph 1: X-ray spectrum using a tungsten anode. Low-energy X-rays are absorbed by the components of the X-ray tube itself. Characteristic radiation lines from anode occur at approximately at 60 and 70 KeV.	15
Graph 2: Graph of the Beer-Lambert law as a function of t variable.....	19
Graph 3: Attenuation coefficient variation as a function of energy and tissue type.....	19
Graph 4: Schematic view of the Compton effect.....	21
Graph 5: Spectrum of X-rays after gadolinium K-edge filter.....	30
Graph 6: Mass attenuation coefficient of a soft and cortical tissue	31
Graph 7: Estimates of the number of hip fractures between 1950 and 2025 by gender and region	35
Graph 8: Number of men and women at high fracture risk in 2040 relative to 2010, by world region	36
Graph 9: Bone Mineral Content (BMC) as a function of age in men and women.....	36
Graph 10: Age-specific incidence rates of hip, vertebral and forearm fracture	40
Graph 11: Distribution of BMD in young healthy women aged 30-40 years .	44
Graph 12: Increasing prevalence of osteoporosis with increasing age when using WHO criteria for diagnosis of osteoporosis	44
Graph 13 Visual comparison between ROC curves of TBS in the discrimination of all fractures combined and vertebral fractures alone	47

List of Tables

Table 1 : Impact of osteoporosis-related fracture across Europe.....	37
Table 2: WHO diagnostic categories for osteoporosis.	45
Table 3 : Different organizational arrangements for HTA report realization	58
Table 4: Informative table containing values of TBS, the Z-score of the TBS, BMD and BMD T-score for single or a combination of vertebrae.....	66
Table 5: Thresholds that discriminate among different trabecular structure distributions.	67
Table 6: Thresholds that discriminate among different bone resistance conditions, with respect to BSI output	72
Table 7: Main scoring and weighting methods for MCDA. [84]	86

